

no.2 / June 2010

ISSN 1453 - 7303

Hidraulica

Revista de

HIDRAULICA, PNEUMATICA, UNGERE CENTRALIZATA, SENZORICA, MECATRONICA

CONTENTS

1. EDITORIAL

Phd.Eng. Petrin DRUMEA (Hydraulics & Pneumatics Research Institute, Bucharest – Romania) pp.5 – 6

2. DESIGN OF THE SELF-ENERGISING ELECTRO-HYDRAULIC BRAKE (SEHB)

Dipl.Ing. Julian Ewald (RWTH Aachen Univ. Inst. for Fluid Power Drives and Controls), Dr.Ing. Matthias Liermann (American Univ. of Beirut, Lebanon), Univ.Prof. Dr.Ing. H. Murrenhoff (RWTH Aachen Univ. Institute for Fluid Power Drives and Controls) pp. 7 - 22

3. INFLUENCE OF AIR CONTENT ENTRAINED IN FLUID OF OPERATING PARAMETERS OF VANE PUMP WITH DOUBLE EFFECT

Radovan S. Petrovic- (Center for automatic control and fluid technics Faculty of Mechanical Engineering Kraljevo University of Kragujevac, Serbia), Wang Zheng Rong - (Dept. of Fluid power and control, LAN Zhou University of technology, LAN Zhou, China), Andrzej Banaszek - (Technical University of Szczecin, Faculty of Maritime Technology Poland) pp. 23 – 32

4. DETERMINATION OF THE ACTUATION FORCE OF SPOOL VALVES WITH ZERO COVERAGE (1st Report, Theoretical Analysis)

Ph.D.eng. Dragos Ion Guta, Ph.D.eng. Teodor Costinel Popescu, Ph.D.stud.eng. Catalin Dumitrescu - (Hydraulics & Pneumatics Research Institute, Bucharest – Romania) pp. 33 - 38

5. CONTRIBUTIONS CONCERNING RHEOLOGICAL METHODS FOR EVALUATING THE DURABILITY OF INDUSTRIAL LUBRICANTS

Irina RADULESCU (S.C. I.C.T.C.M. S.A. Bucharest, ROMANIA), Alexandru RADULESCU (University POLITEHNICA Bucharest, RO.) pp. 39 – 44

6. ORIGINAL CONSTRUCTION AND MATHEMATICAL MODEL OF A PNEUMO-HYDRAULIC POSITIONING UNIT

Prof. Phd.Eng.Mihai AVRAM, Lect.PhD.Eng. Despina DUMINICĂ, Prof.PhD.Eng.Constantin Bucşan, Eng. Victor CONSTANTIN- ("POLITEHNICA" University of Bucharest) pp.45 – 52

7. ASSISTED RESEARCH OF THE ELEMENTS AND THE SYSTEMS BY USING THE ELEMENTAR TRANSFER FUNCTIONS AND VIRTUAL INSTRUMENTATION

Prof.univ.Ph.D.Eng.Adrian Olaru (University Politehnica of Bucharest Romania) and Ph.D.Eng.Serban Olaru (RomSYS Mechatronics Company) pp. 53 - 70

8. STATIC DIMENSIONING OF COMPONENT PARTS OF TWO-STAGE SERVO VALVES

Stud.PhD.Eng. Dutu I., Stud.PhD.Eng. Lupu B., Stud.PhD.Eng. Lepadatu I. - (Hydraulics & Pneumatics Research Institute, Bucharest - ROMANIA) pp. 71 - 74

Manager of magazine:
PhD. eng. Petrin DRUMEA
e-mail: ihp@fluidas.ro

Chief editor:
PhD. eng. Gabriela MATACHE
e-mail: fluidas@fluidas.ro

Specialized reviewers:
PhD. eng. Adrian MIREA
(ROMFLUID S.A. Bucharest)
Math. eng. Gabriel RĂDULESCU
(INOE 2000 -IHP Bucharest)
Prof. PhD.eng. Guido BELFORTE
(Politecnico di Torino, Italia)
PhD. eng. Heinrich Theissen
(Institute for Fluid Power Drives and Controls - IFAS, Germany)
Prof. PhD. eng. Pavel MACH
(Czech Technical University in Prague, Czech Republic)

Editorial Board:
Prof. PhD. eng. Nicolae ALEXANDRESCU
Prof. PhD. eng. Nicolae VASILIU
Prof. PhD. eng. Paul SVASTA
Prof. PhD. eng. Alexandru MARIN
PhD. eng. Daniel MARIN
PhD. eng. Gabriela MATACHE
PhD. eng. Petrin DRUMEA
PhD. eng. Corneliu CRISTESCU
PhD. eng. Ion PIRNA
PhD. eng. Dragos ION GUTA

Executive editors:
Valentin MIROIU
e-mail: vmiroiu.ihp@fluidas.ro
Ana-Maria Carla POPESCU
e-mail: hidraulica@fluidas.ro

Graphics & DTP:
Valentin MIROIU
e-mail: vmiroiu.ihp@fluidas.ro

Published by:

**Hydraulics & Pneumatics Research Institute
INOE 2000 - IHP Bucharest-Romania**

Address:
14 Cuşitul de Argint,
district 4, Bucharest, cod 040557
ROMANIA
Phone: +40 21 336 39 90; +40 21 336 39 91
Fax: +40 21 337 30 40
E-mail: ihp@fluidas.ro
Web: www.ihp.ro
Web: www.ihp.ro/hidraulica

with support of:

**National Professional Association of Hydraulics and
Pneumatics in Romania - FLUIDAS**
E-mail: fluidas@fluidas.ro
Web: www.fluidas.ro

CONDITIONS FOR SUBMISSION OF PAPERS FOR "HIDRAULICA" MAGAZINE

1. Page format is A4 (210 x 297)
2. The text of an article, drawings included, shall not exceed 8 conventional pages.
3. The article shall be draft in two columns, using MS Office Word 97 to 2007, preferably with fonts Arial CE or Times Roman R, font size 12, at 1 (one) line in page; diacritical marks shall be used. Also, formulas shall be written in Arial CE too; Microsoft Equation is recommended.
4. Since no. 1 / 2008 issue of "HIDRAULICA" articles submitted for publishing shall be written in English.
5. Together with article shall be presented also an abstract of the paper in 10 rows and keywords; abstract and keywords shall be written in Romanian and English.
6. All figures and tables included in articles must be mentioned in text; figures and captions must have titles.
7. When authors belong to several institutions, each author is marked with a number of asterisks. Each number of asterisks will be associated with an institution. Caption of asterisks will be presented at bottom of page. For the first author or corresponding author is an e-mail address shall be provided.
8. Tables and figures will be presented in the following formats: .bmp, .jpeg, .tiff, .eps, .ai, .cdr;
9. Papers must be original contributions of the author, not remakes or translations of other papers.
10. Authors retain full responsibility for the accuracy of statements expressed, for calculations and results displayed.
11. Not allowed for publishing papers that were published in full or in part in other publications.
12. Review committee reserves the right to make recommendations for improving the articles or to not publish material regarded as inappropriate. Unpublished manuscripts are not returned.
13. Magazine does not grant copyrights.
14. Paper intended to be published shall be submitted via one of the e-mail addresses : hidraulica@fluidas.ro or fluidas@fluidas.ro.

EDITORIAL

COOPERATION IN RESEARCH

Globalization that showed up in the last decades reached a stage over which would be extremely hard to pass, but from which would probably develop a new form, more convenient and eventually more human than what it is right now. The changes would have taken place even if the global crisis had not affected the whole mankind, because there is a constrain over the limits of what may be acceptable. In this situation the first step Hydraulic Power from Romania made was to affiliate at the international organization from the field. We created the national professional association FLUIDAS and affiliate to the European organization CETOP. The next steps might be to create partnerships between the Romanian companies and the most important European firms, for following the trend of more close approaching between the European countries.

In the field of research and development I think that must be surpassed the first steps, of mobilities and must be approached the solution of collaborating on themes of high economic interest and use at their utmost the technical scientific endowments of the laboratories from the research institutions from Romania, which in many cases are of top. Of course we cannot convince immediately the Europeans that we are capable to work intelligently but if we intensively endeavour to make a good impression, we will be for sure able to accomplish it in due time. If we analyse the technical and scientific capabilities of the research institutions and universities from Romania, we find that there are no major difference from what is in the West. At this moment what makes the difference is the economic system to which we belong and in which we work and just a little the technical endowments or the quality of the staff. The research centres from Bucharest, Cluj, Iasi, Timisoara, Galati or Brasov could establish without any problem partnerships with the research institutions from Aachen, Berlin, Dresda, Brno, Warsaw, Cracow, Wroclaw, Torino, Linz, Poitiers and all the others.



Ph.D.Eng. **Petrin DRUMEA**
MANAGER
Hydraulics & Pneumatics Research Institute

The only real difficulty is represented by the thematic, because anywhere in the world the main problem is the beneficiary of the research activity and the technical level. In the technical fields we should concentrate on industrial research and innovation, cause of the facts generated by the global economic crisis. It is obvious that we cannot found partnerships on the base of tales about technique and we should rather focus on finding interested purchasers for our work results. As much important as the technical level would be the quality of the research results which would make them easily absorbed by the manufacturers who cannot change quickly and entirely their manufacture technologies.

For creating an active international cooperation is needed to be made a radical change in what regards the appreciation of the specialists and of the research institutions, on the groundwork of articles, of organizing professional symposiums, based on quality criteria. We should be much more concerned about the innovation capabilities, the possibilities of technological transfer and the adaptability potential to the real economic situation.

A handwritten signature in black ink, consisting of stylized, overlapping loops and lines.

EDITORIAL

COOPERAREA IN CERCETARE

Globalizarea manifestata in decursul ultimelor decenii a ajuns la un nivel peste care greu se va trece si de la care probabil se va dezvolta o alta forma decat cea de acum traditionala, o varianta mai supla si eventual mai umana. Modificarile ar fi aparut chiar si in conditiile in care criza economico-financiara-sociala nu ar fi afectat intreaga omenire pentru ca exista deja o fortare a limitelor acceptabilului. In aceasta situatie primul pas pe care hidraulica romaneasca l-a facut a fost cel de afiliere la familia europeana a domeniului, prin infiintarea asociatiei profesionale FLUIDAS si afilierea acesteia la organizatia europeana CETOP. Urmatorii pasi vor fi probabil in directia intrarii firmelor cu capital romanesc intr-un parteneriat cu marile firme europene, pentru incadrarea in tendinta actuala de apropiere si mai mare a tarilor batranului continent.

In domeniul cercetarii-dezvoltarii cred ca trebuie depasiti primii pasi, cei ai "mobilitatilor" si trebuie abordata solutia colaborarii pe teme de interes economic si foarte important ar fi sa fie utilizata baza tehnico-stiintifica a laboratoarelor din unitatile de cercetare din Romania, care in multe situatii sunt de un bun nivel. Sigur ca nu vom putea sa convingem imediat pe europeni ca suntem capabili de munca inteligenta, dar cu eforturile de rigoare poate fi depasita imaginea proasta creata in ultimii ani. Daca analizam doar posibilitatile tehnice si stiintifice ale centrelor de cercetare din institutele de cercetare si cele din universitati se constata ca de fapt nu sunt diferente fata de ceea ce exista in occident. La ora actuala diferenta o face sistemul economic in care ne desfasuram activitatea si foarte putin dotarile tehnice sau calitatea personalului. Centrele de cercetare din Bucuresti, Cluj, Iasi, Timisoara, Galati sau Brasov pot intra fara probleme in parteneriate cu marile centre de cercetare din Aachen, Berlin, Dresda, Brno, Varsovia, Cracovia, Wroclaw, Torino, Linz, Poitiers si celelalte. Singura problema este si va fi tematica, intrucat peste tot se pune problema destinatarului activitatii de cercetare si a nivelului tehnic.



Ph.D.Eng. **Petrin DRUMEA**
MANAGER
Hydraulics & Pneumatics Research Institute

In domeniile tehnice va trebui sa ne concentram pe cercetarea industrială si pe inovare data fiind situatia reala aparuta in urma crizei mondiale. Este limpede ca nu vom putea intra in relatii de parteneriat in zona cercetarii cu povesti despre tehnica ci va trebui sa ne preocupe cu precadere lucrarile la care gasim unitatea careia sa ii poata fi transferate rezultatele muncii noastre. La fel de important ca nivelul tehnic va fi si capacitatea lucrarilor de a putea fi absorbite de unitatile de productie care nu isi pot schimba rapid si integral tehnologiile de fabricatie.

Pentru ca aceasta cooperare internationala sa devina activa este nevoie ca la noi in tara sa fie modificate cateva idei de tipul aprecierii principale a specialistilor si a centrelor de cercetare pe baza de articole, pe baza de organizare a unor simpozioane de cele mai multe ori nesemnificative, pe baza mobilitatilor sau pe baza unor relationari in afara tehnicii. Aceste criterii nu trebuie desfiintate numai ca ponderea lor trebuie sa fie depasita de capacitatea inovativa, de posibilitatile transferului tehnologic si de adaptabilitatea la situatia concreta a posibilitatilor tehnologice.



DESIGN OF THE SELF-ENERGISING ELECTRO-HYDRAULIC BRAKE (SEHB)*

Dipl.-Ing. Julian Ewald (1), Dr.-Ing. Matthias Liermann (2), Univ.-Prof. Dr.-Ing. H. Murrenhoff (1)

(1): RWTH Aachen University, Institute for Fluid Power Drives and Controls

(2): American University of Beirut, Lebanon

1 Introduction

The Self energising Electro-Hydraulic Brake (SEHB) is developed at the Institute for Fluid Power Drives and Controls of RWTH Aachen University. The idea was developed during the research project "Intelligent, Integrated Single-Wheel Traction and Brake Module (EABM) /Her08/ and was awarded with the science award of North Rhine-Westphalia /AN07/. In spite of it being originally designed for use in railway vehicles it is also adequate for motor vehicles and industrial applications. This article presents the basics about the dimensioning and design of the SEHB. It also shows the conflicts due to contradictory optimisation aims and how they can be solved by compromises. Moreover, a test facility and test results are presented.

1.1 Hydraulic Brakes

Until the 1930s, in some vehicles even until the 1960s, mechanical brakes were used. Bowden cables, leverages and redirections transferred the force from the brake pedal to the wheel brakes. A disadvantage was the high amount of maintenance. Furthermore the irregular force transmission to the brake callipers caused uneven wear /Bre04/. The first hydraulic wheel brake actuator was patented in 1917 by Malcolm Loughhead, a civil engineer. This invention started the triumph of hydraulic brakes as it doubled the brakes' efficiency. In the beginning drum brakes represented the state of the art.

Their main advantage is the capability of implementing a mechanical boosting of the brake force. Consequently the activating force can be kept on a low level.

The drum brake has disadvantages because of insufficient cooling, and other disadvantages such as difficult dosability, friction variation and squeaking sounds. When higher brake power was needed, the use of disc brakes became common. However, in the beginning disc brakes with a booster were not available. The necessary actuating force for disk brakes was very high compared to drum brakes. Not until the invention of the pneumatic brake booster, disc brakes succeeded on the market. The vacuum reinforcement provided for high brake power, easy dosability and a low pedal force. A central brake booster between brake pedal and main brake cylinder replaced the local intensification at each drum brake. Different reinforcement factors at the wheel brakes were prevented, allowing an equal distribution of brake forces. Soon ideas for self energising disc brakes were developed /Tou64/, but they could not compete with brake booster systems.

1.2 Mechatronic Brake Systems

The requirements for brake systems of motor and railway vehicles are becoming more difficult to fulfil. For both types of vehicles high brake power, low energy demand, good controllability and the ability of brake force feedback are requested.

*This paper is a translation of the German original printed in "O+P Ölhydraulik und Pneumatik" issue 5 year 2009.

In addition, there are specific requirements such as a flexible brake management or a distributed brake system with interfaces for railway applications. Pneumatic brake systems or brake systems with vacuum boosters cannot meet these requirements or can only fulfil them with high effort. This is why the development of mechatronical brake systems is promoted. The wedge brake is an example for a highly developed brake system that works in the region of critical self energisation. The central element of the wedge brake is the wedge bearing. It is located between the moving brake pad and the brake calliper. It allows for the conversion from friction force to clamping force. A control unit influences the position of the wedge by an electric motor with a spindle system /Gom06/.

1.3 Working principle of the SEHB

The principal idea of a self energising brake is to use the kinetic energy of the vehicle to clamp the brake shoes towards the brake disk. The brake calliper is moveable in the direction of the friction force. The brake torque is supported by an hydraulic cylinder. In contrast to other existing brake systems, the SEHB is controlled in the postcritical reinforcement region /Lie08/. Depending on the driving direction one of the two supporting cylinders is pressed in. **figure11** shows the SEHB in top and side view. The functionality of the SEHB will be explained by describing a brake cycle. Initially the brake is released with a gap between the disc and the brake pads. The valves NC V3 and NO V4 are closed, so that a hydraulic force holds back the prestressed spring, integrated into the brake actuator (BA). As soon as the valve NO V4 opens, chamber B of the brake actuator is connected to low pressure.

The spring pushes the brake actuator out and oil is drawn through the check valve into chamber A. The spring force presses the brake pads against the brake disc, building up a low friction force. This force is transferred to the vehicle by one of the supporting cylinders. The other cylinder stays in its position allowing a pressure build-up in both directly connected cylinders. The configuration with two plunger cylinders is considerably simpler than preceding systems /Lie06/.

The hydraulic self energisation is due to the connection of the supporting cylinders with the brake actuator. The oil flows through the high pressure check valve HPCV and the NO V1 valve. The process of self energisation is interrupted as soon as the NO V1 valve closes. The SEHB always needs to be controlled, because of the postcritical self energisation. If it is not controlled, the brake clamps until the pressure limiting valve opens.

The pressure p_{AZ} in the supporting cylinder is the controlled parameter. If the dimensions are known, the retarding force can be directly calculated with this pressure. If the mass of the vehicle is known, the deceleration can be calculated as well.

The four shift valves NO V1, NC V2, NC V3 and NO V4 connect the two chambers of the brake actuator either with high or low pressure. By choosing normally open (NO) and normally closed (NC) valves, a fail-closed behaviour is guaranteed, so that the brake clamps in case of a failure of the electric power supply.

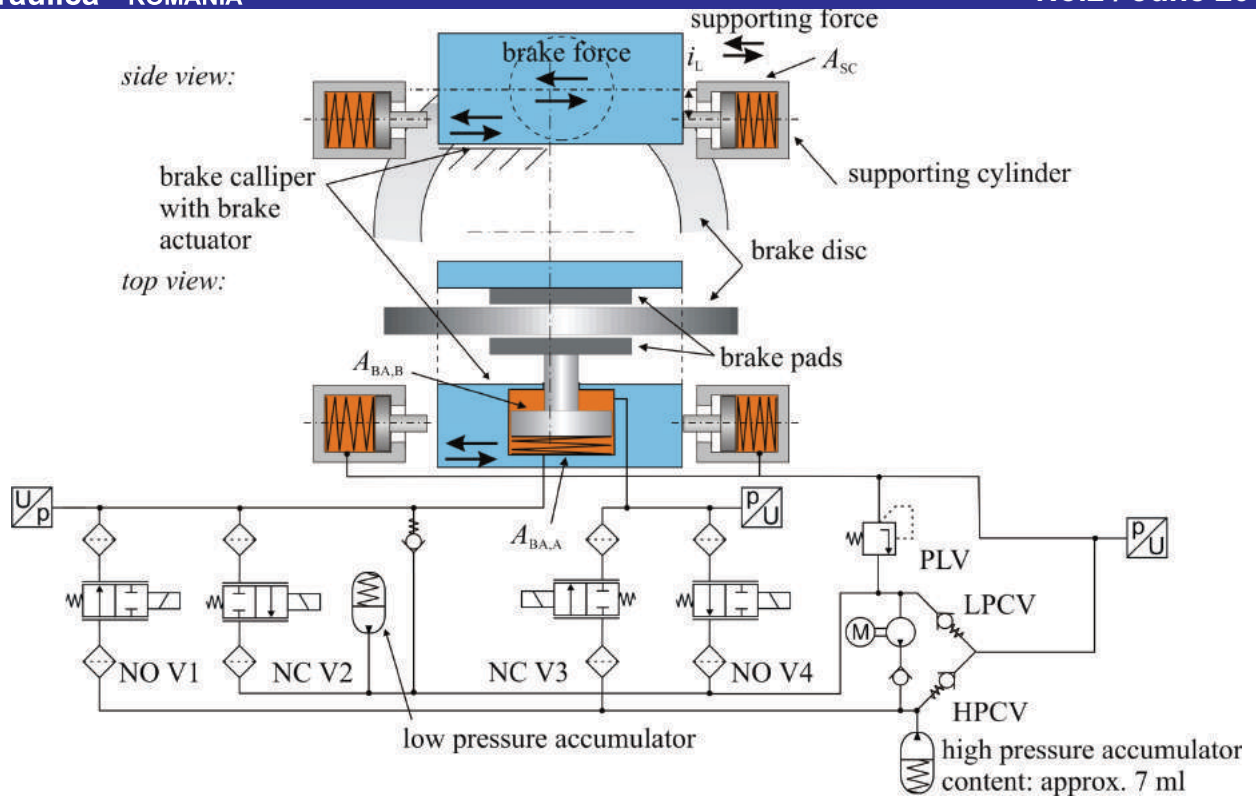


figure 1-1: Working principle of the SEHB with simplified support

The low pressure is kept on a low value by an accumulator. Thus, a higher stiffness of the fluid is achieved [Mur08]. At the same time cavitation in the suction part is prevented.

The high pressure accumulator is needed to release the SEHB completely against the spring force of the brake actuator. While braking, the accumulator is charged automatically as soon as the pressure in the high pressure part rises above the loading pressure of the accumulator. To release the brake, the accumulator's volume of a few millilitres is led into chamber B so that the brake opens completely against the spring force. A gap between the disc and the brake pads is set. If the vehicle is parked and the high pressure accumulator is empty, the vehicle has to be started up against a low braking force from the preloaded spring. Another possibility is to release the brake by the pump shown in - figure1-1.

2 Basics of dimensioning and design

In order to dimension the diameter of the brake actuator (BA) and of the supporting cylinder (SC) the path of self energisation is considered. By choosing the diameters it is ensured that for all friction coefficients which can occur in normal operation, the pressure in the supporting cylinder is always higher than in the brake actuator. Thus, the brake can energise itself when valve NO V1 is open. From this consideration the simplified condition for the relation of the hydraulic surfaces can be deduced, as presented in [Lie06].

$$A_{BA,A} > \frac{1}{2 \cdot \mu \cdot i} \cdot A_{SC} \quad \text{eq. 2-1}$$

$$\mu_{\min} = \frac{1}{2 \cdot i} \cdot \frac{A_{SC}}{A_{BA,A}} \quad \text{eq. 2-2}$$

Certain effects, which restrain the self energisation have not been considered in this calculation. These effects are: friction, spring forces and flow losses at the valves.

Therefore, in the following, - eq.21 will be expanded. The used variables are defined in figure 2-1.

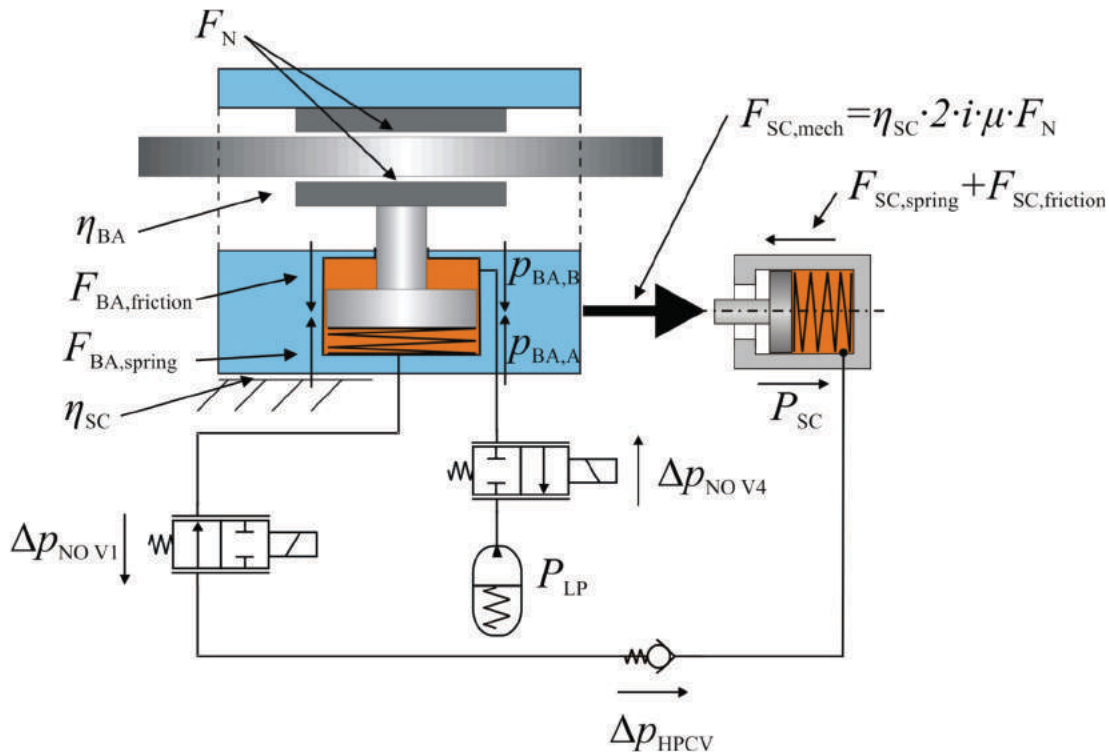


figure 2-1: Definition of hydraulic and mechanic variables

The pressure losses at the high pressure check valve, consisting of the opening pressure and of a part depending on the volume flow, are considered together as the pressure Δp_{HPCV} . The volume flow through the high pressure check valve also flows through the valve NO V1 causing another pressure loss Δp_{NOV1} . The pressure losses depend on the operating point, the surface of the brake actuator $A_{BA,A}$ and on the compliance of the brake calliper.

$$p_{SC} = p_{BA,A} + \Delta p_{HPCV} + \Delta p_{NOV1} \quad \text{eq. 2-3}$$

The mechanical force at the supporting cylinder $F_{SC,mech}$ is balanced to the hydraulic force, the friction forces and to the spring force which presses the piston back to its initial position.

$$\begin{aligned} F_{SC,mech} &= F_{SC,hydr} + F_{SC,Reib} + F_{SC,Feder} = \\ &= p_{SC} \cdot A_{SC} + F_{SC,friction} + F_{SC,spring} \end{aligned} \quad \text{eq. 2-4}$$

The force at the supporting cylinder is also balanced to the friction force actuating in the friction radius. The friction force is calculated with the normal force per brake pad F_N , the friction parameter between brake disc and brake pad μ , the number of friction surfaces (2) and the transmission i . Mass forces are neglected. The conduction of the brake force to the supporting force is considered with an efficiency factor.

$$F_{SC,mech} = \eta_{SC} \cdot 2 \cdot i \cdot \mu \cdot F_N \quad \text{eq. 2-5}$$

The transmission i is defined as the quotient between friction radius and the distance between the centre of the friction radius and the supporting cylinder's force application point.

$$i = \frac{r_B}{r_{SC}} \quad \text{eq. 2-6}$$

The force applied to the brake pad depends on the efficiency of the brake calliper η_{BA} . The efficiency factor describes the quotient of the normal force at the friction pad and the force at the brake actuator. This force results from the hydraulic force in chamber A and the spring force reduced by friction forces and by the hydraulic force in chamber B. The hydraulic chamber B can be used for control or can be connected to low pressure by the valve NO V4. In this case, the pressure in chamber B is equal to the low pressure plus a pressure loss at valve NO V4 caused by the flow.

$$F_{SC,mech} = \eta_{SC} \cdot 2 \cdot i \cdot \mu \cdot \eta_{BA} \cdot (p_{BA,A} \cdot A_{BA,A} - p_{BA,B} \cdot A_{BA,B} - F_{BA,friction} + F_{BA,spring}) \quad \text{eq. 2-7}$$

The minimal friction value is calculated by rearranging eq.2-7 and inserting it into eq.2-1 for the critical case.

$$\mu_{min} = \frac{F_{SC,mech}}{\eta_{SC} \cdot 2 \cdot i \cdot \mu \cdot \eta_{BA} \cdot (p_{BA,A} \cdot A_{BA,A} - p_{BA,B} \cdot A_{BA,B} - F_{BA,friction} + F_{BA,spring})} \quad \text{eq. 2-8}$$

To achieve $F_{SC,mech}$ eq.2-4 and eq.2-3 are inserted into eq.2-8. Furthermore it is assumed that chamber B of the brake actuator is connected to low pressure and that the pressure loss at valve NO V4 is known.

$$\mu_{min} = \frac{(p_{BA,A} + \Delta p_{HPCV} + \Delta p_{SOV1}) A_{SC} + F_{SC,friction} + F_{AZ,spring}}{\eta_{SC} \cdot 2 \cdot i \cdot \eta_{BA} \cdot (p_{BA,A} \cdot A_{BA,A} - (p_{LP} + \Delta p_{EOV4}) \cdot A_{BA,B} - F_{BA,friction} + F_{BA,spring})} \quad \text{eq. 2-9}$$

The minimal friction value depends on the operating point which is expressed by the parameter $p_{BA,A}$ in this context. For the dimensioning it is interesting to know the minimal friction coefficient which still allows self energisation. The pressure $p_{BA,A}$ in chamber A adopts values between low pressure and maximum pressure that are known from the requirements. To start with an example for the dimensioning of the SEHB the idealised minimal friction coefficient is calculated with eq.2-2. The resulting value is 0.097. For the calculation with eq.2-9 the parameters listed in table2-1 are needed as well.

The pressure loss Δp_{HPCV} of each high pressure check valve can be identified from its data sheet. The spring forces in the brake actuator and the supporting cylinder are determined during the design and can be presumed as known.

It is clearly more complex to detect the friction forces at the cylinders and the mechanical efficiency factors. They can be determined from measurements. Since they depend heavily on external factors, they should be estimated to the safe side.

The minimal friction coefficient depending on the pressure in the brake actuator is shown in figure2-2. As shown, the minimal friction coefficient is in most operating points higher when using the extended calculations. Through this, the dimensioning must be done with a calculation based on eq.2-9.

efficiency from friction force to supporting force	η_{SC}	0,95
efficiency of the brake calliper	η_{BA}	0,95
spring force of the brake actuator	$F_{BA, spring}$	3000 N
friction force of the brake actuator	$F_{BA, friction}$	500 N
area of the brake actuator, chamber A	$A_{BA, A}$	5026 mm ²
area of the brake actuator, chamber B	$A_{BA, B}$	3063 mm ²
area of the supporting cylinder	A_{SC}	706,9 mm ²
spring force of the supporting cylinder	$F_{SC, spring}$	150 N
friction force of the supporting cylinder	$F_{SC, friction}$	50 N / 100 N
transmission from friction force to supporting force	i	0,725
pressure difference at the high pressure check valve	Δp_{HPCV}	0,2 bar
pressure difference at valve NO V1	Δp_{EOV1}	0,1 bar
pressure difference at valve NO V4	Δp_{EOV4}	0,1 bar
low pressure	P_{LP}	2,9 bar

table 2-1: Parameters for the dimensioning

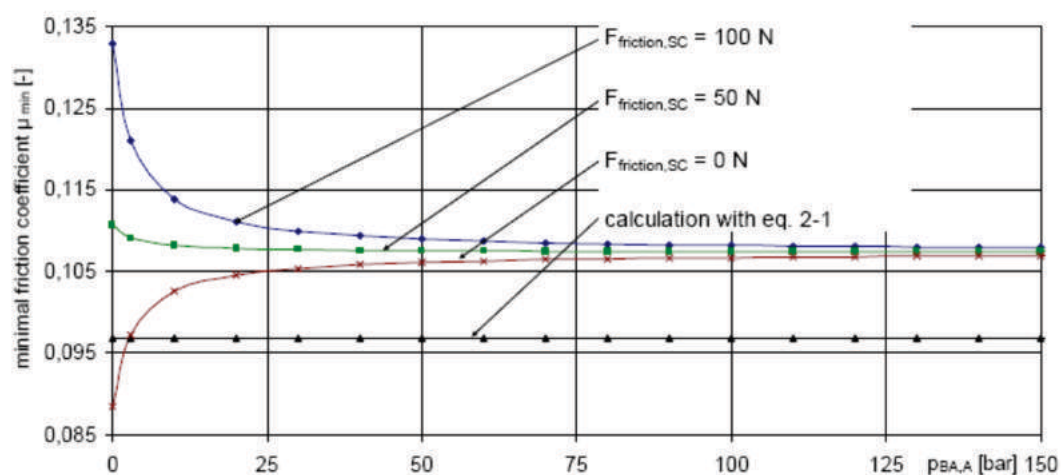


figure 2-2: Minimum friction coefficient in simplified and extended calculation

2.1 Fail-Closed Concept

The SEHB shown in **-figure11** brakes if the electric control fails. The limit is set up by the opening pressure of the relief valve. The brake calliper closes until an adjustable friction force is reached. By opening the pressure limiting valve, the fluid from the supporting cylinder is let to the low pressure part of the SEHB. The pressure in the brake actuator remains or can be limited by another pressure relief at the brake actuator. When the supporting cylinder is empty, the drag force can no longer be increased. For this reason the brake force cannot be readjusted if the friction factor decreases. In this case, the brake force can only be regulated by the pump shown.

Because of the targeted railway application the SEHB incorporates a fail-closed principle. This means that in case of a failure of the power supply it has to brake with a defined brake force. The high force level is achieved by the self energisation.

The initialisation of the braking process can be implemented in different ways. Apart from a mechanical spring, a hydraulic force can be considered. **figure23** shows three other possibilities for the implementation. As an alternative for the spring a hydraulic reservoir could be used. It either actuates the brake directly (1), activates it through an electrically operated valve (2) or actuates a second cylinder (3). The advantage of the hydraulic solution is that it can easily be switched off by a valve. In addition, the hydro accumulator can be positioned separately from the brake actuator to fit into the package. This allows for a very compact brake actuator. All variants have in common that they form a system which is hydraulically separated. No connections between the brakes are necessary, the SEHB can be installed as a module without any exterior hydraulic connections. For service issues the SEHB can be maintained when taken off the vehicle.

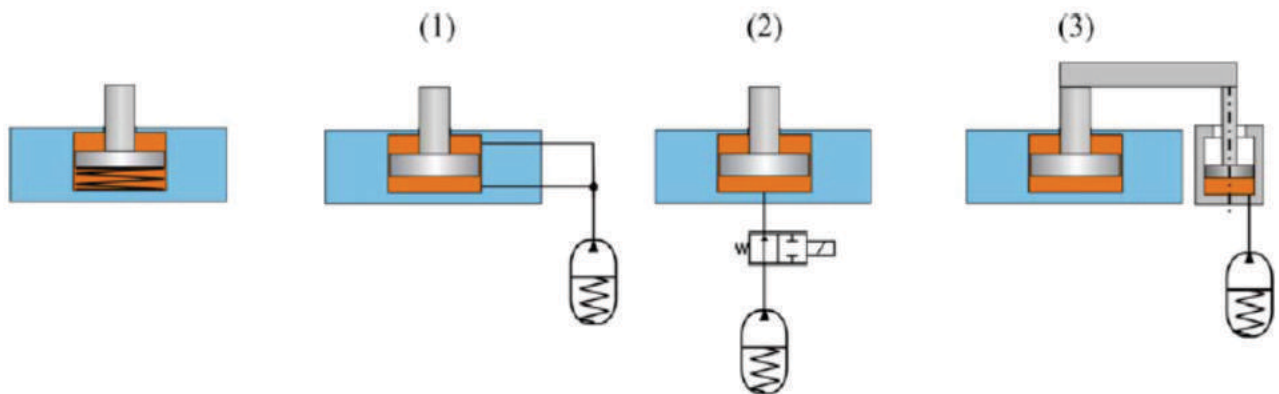


figure 2-3: Possibilities for the hydraulic "spring"-force

Another possibility to start the braking process is to use a pump as shown in **-figure11**. In this case the pump would have to start for every braking process. As an alternative the use of a(n) (electric) magnet is possible /Hof07/. However, these alternatives require a safe energy supply.

2.2 Fail-Open Concept

In contrast to the fail-closed concept there is the fail-open-concept. It is used in other applications, such as passenger cars. If the control unit fails, there must not be a brake intervention as a suddenly blocked wheel can mean a higher risk than the partial fail like of the braking system.

For a fail-open-concept, an unintentional closing of the brake must be prevented. If the electric control fails, any self energisation of the brake must be prohibited. This is why the normally open and the normally closed valves are used interchanged compared to the fail-closed system. In case of a failure in the electric control, the brake actuator is connected with the low pressure. Consequently, the closed brake is released if the electric control fails. For a fail-open application the brake calliper is significantly simplified because, as in conventional automobile brakes, plunger cylinders can be used as actuators.

Instead of providing a calliper independent fallback for the actuator, a direct hydraulic connection to the master brake cylinder can be created, in analogy to automobile brakes when the vacuum booster has failed. Experience shows that this connection can be configured so that the safety requirements are met. **figure2-4** shows a breaking system with four SEHB callipers. Still, they are directly connected to a brake pedal. As in conventional brake callipers the brake release is passive. The elastic deformation of the seals serves for an automatic set up of a gap between brake disc and brake pads.

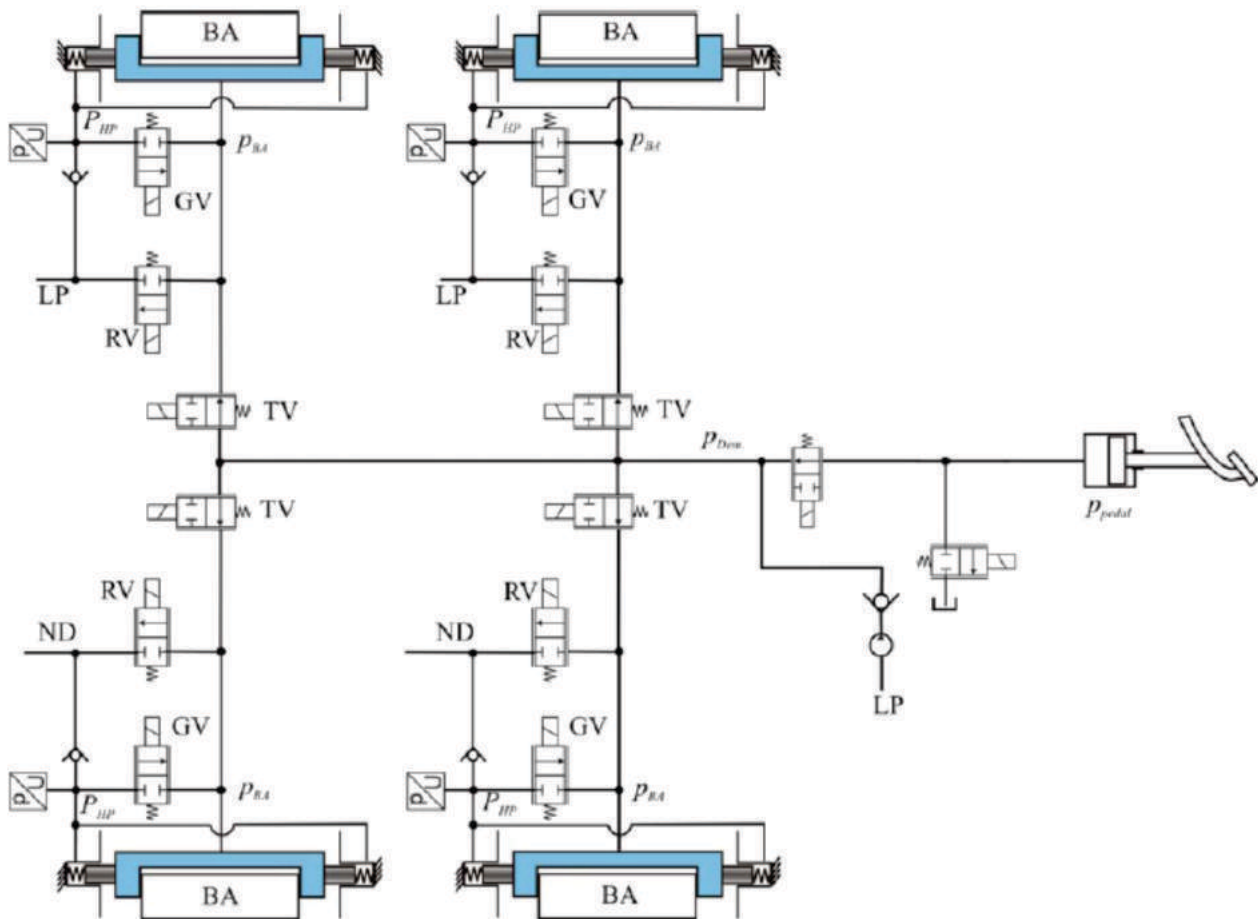


figure 2-4: SEHB for automobile applications with fail-open concept

If the driver wants to decelerate the vehicle, he initiates the brake with the pedal. Additionally, the concept provides for a pump so that the SEHB can brake independently from the driver. This is for example needed for the stability program or a driver assistance system. The pressure is led to the brake callipers which are connected to the pedal or the pump by the normally open separation valve (TV). Consequently, the brake pads are pushed towards the brake discs. As soon as a pressure slope is measured, the separation valve TV closes and the valve VV opens, enabling the self energisation. The pressure at the supporting cylinder is controlled so that the SEHB features a brake torque control in closed loop operation. The demanded deceleration is deduced from the measured pressure value at the brake pedal or set by a control device.

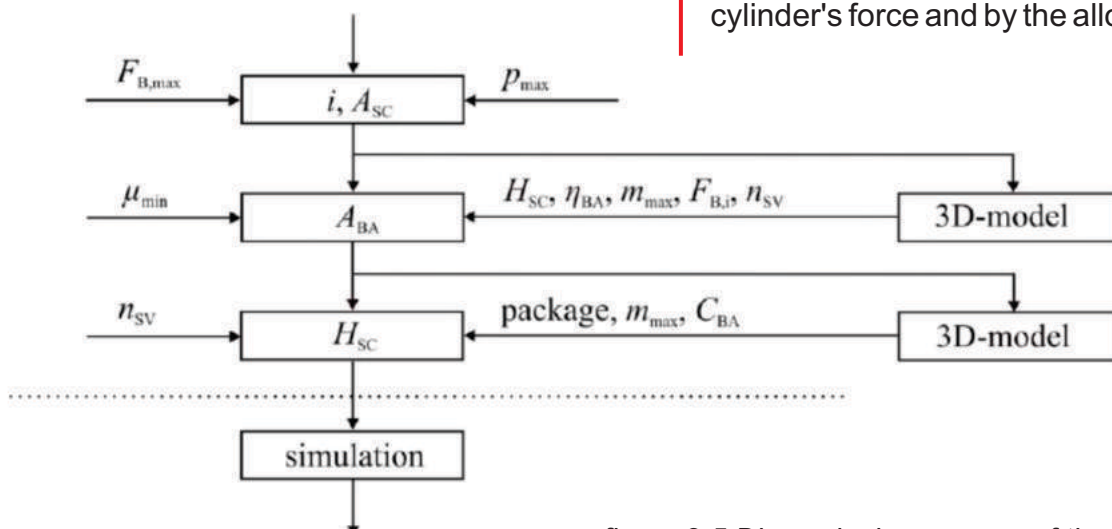
The brake pedal is connected to the reservoir and to the pump by two valves. If a brake process is initiated by the control unit and the pump, effects on the brake pedal are suppressed. In addition, because of the two valves, a pedal simulator can be easily implemented. For this purpose, compliance at the brake pedal has to be provided in the form of a small accumulator.

If there is a long ABS braking on fast changing surfaces the oil from the supporting cylinder is used up. In this case the brake control unit closes the brake calliper further by actuating the pump, as in a conventional electro-hydraulic brake.

2.3 Conflicts of aims

The requirements a brake system must satisfy can be summarized in five categories: forces and dynamics, security, package and weight, comfort and costs. In this chapter contradictions are discussed which arise from the optimisation.

The central requirement is to guarantee a specified stopping distance. For this purpose, the brake is defined. Due to the braking principle, the highest pressure in the supporting cylinder occurs at the maximum brake force. As the maximum system pressure is limited by the system components, the area of the supporting cylinder and the transmission ratio i are dimensioned first. This first step is shown in top position of **-figure25**. The transmission ratio describes the ratio between friction force and supporting force. It results from the system configuration and especially from the arrangement of the supporting cylinder. The area of the supporting cylinder is then set by the cylinder's force and by the allowed pressure.



The components, particularly the cylinders' seals, the poppet valves and the check valves have to leak as little as possible. Poppet valves show minimal leakage due to surface roughness of the valve seats and tappet /Smi08/. Plastic seals at the valve's seat minimise leakage. However, these seats are limited in the maximum pressure range. As pilot-operated valves have a long response time they can only be used in the SEHB under very limited conditions. Spool valves always leak because of the radial gap between the spool and the housing. A smaller gap reduces the leakage but increases the valve's manufacturing costs considerably. In addition, the valve becomes more vulnerable to dirt in the oil.

The second step shown in -figure25 is the dimensioning of the brake actuator's diameter A_{BA} . It can be derived from the minimal friction coefficient μ_{min} which still guarantees the functionality of the SEHB. The relation between the minimal friction coefficient and the area of the brake actuator has been derived in -eq.29. The friction coefficient during the operation of the brake depends on many influences. A water film on the brake disc is an example for a condition that implies a very low friction coefficient. To ensure the brake's functionality, the minimum brake coefficient has to be set sufficiently low. Choosing a low friction coefficient means a large braking actuator. The needed oil volume for clamping the brake increases proportionally with the area of the brake actuator. However, the volume of oil supplied by the supporting cylinder is limited. Choosing a very low minimal friction coefficient, either the supporting cylinder's stroke must be very long or the number of possible braking processes n_{sv} is small.

After this number of braking processes the supporting cylinder is exhausted and has to be reset to its original position or the pump must be activated. The supporting cylinder's stroke is mainly restricted by the available package and the allowed weight. As the brake calliper has to follow the stroke of the supporting cylinder, the needed space matches the traversed envelope. The SEHB's weight has to be particularly small if the brake calliper has to be added to the unsuspended mass, e.g. in passenger cars. In railway vehicles the brake callipers are attached to the bogie which is located behind the primary suspension. In this case a compromise has to be found, which, on the one hand guarantees the functionality at very low friction coefficients and on the other hand does not unnecessarily increase the package and the weight.

When dimensioning the supporting cylinder's stroke, the third step, further restrictions have to be considered in addition to limits of the package. First of all, to calculate the needed oil volume for clamping the brake, the stiffness of the brake calliper C_{BA} , including the brake pads and the brake disc, is decisive. During the supporting cylinder's stroke the radiuses' ratio of supporting force and brake force can change. This deviation also has to be considered when the minimal friction coefficient is set. If the directions of the supporting force and brake force vectors change, the allowed shear force at the supporting cylinder must be taken into consideration. -figure26 shows a solution to combine a small package with a long stroke of the supporting cylinder. The curved path prevents that the brake calliper exceeds the brake disc significantly. The straight parts of the path are fitted to the supporting cylinder so that the shear force is minimal.

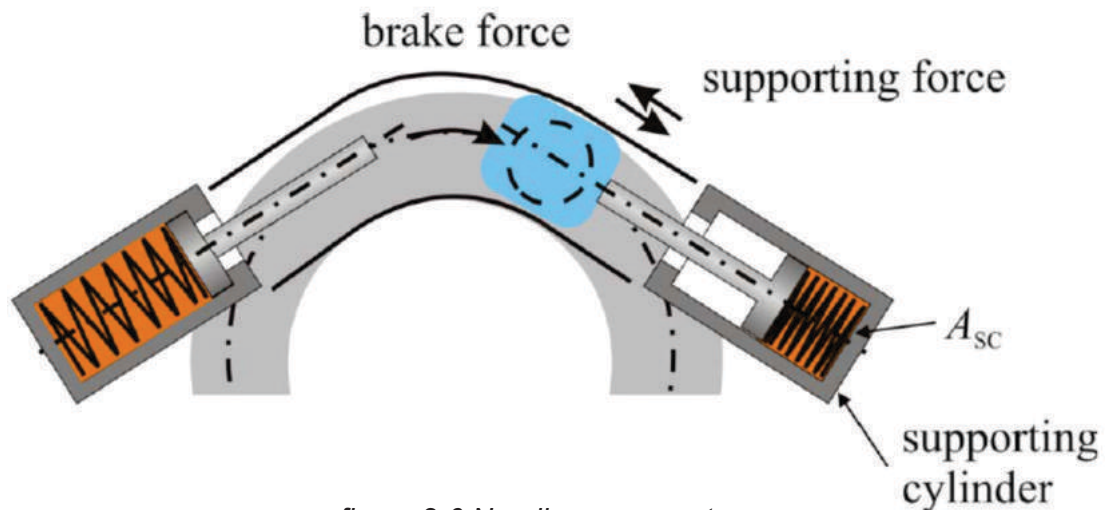


figure 2-6:Non-linear support

The minimal friction coefficient also influences the choice of the valves. When the friction coefficient is low, the valve needs a large flow area. Near the minimal friction coefficient the pressure difference at the valve is small. At the same time the brake calliper needs its maximum clamping force for deceleration. Additionally, because of the small stiffness, more compression oil is needed. In contrast, at high friction coefficients a high pressure difference at the valve occurs. A small volume flow at high pressure differences is desirable to allow a constant dynamic of the brake /Lie08/. This requirement can be fulfilled by proportionally operating valves or by using a flow control valve. Another possibility to influence the dynamic at different operating points, is to change the working areas at the cylinders.

For this purpose a brake actuator can be built up from several cylinders. The cyclic self energisation of the SEHB can be adjusted in steps if the brake is controlled adequately /Hof07/.

This idea can also be implemented in another way. figure 2-7 shows a brake actuator consisting of a differential cylinder whose cylinder housing forms the piston of a plunger cylinder which is pushed in by a spring. When the brake is released the spring presses the cylinder housing to the inner stroke limit. The differential cylinder is hold back against the spring because of a pressurised chamber B. At high friction coefficients the cylinder housing stays in this position and only the differential cylinder is active. If friction values are low, chamber A is closed by valves 1b and 2b and the supporting cylinder is connected to the plunger cylinder's chamber.

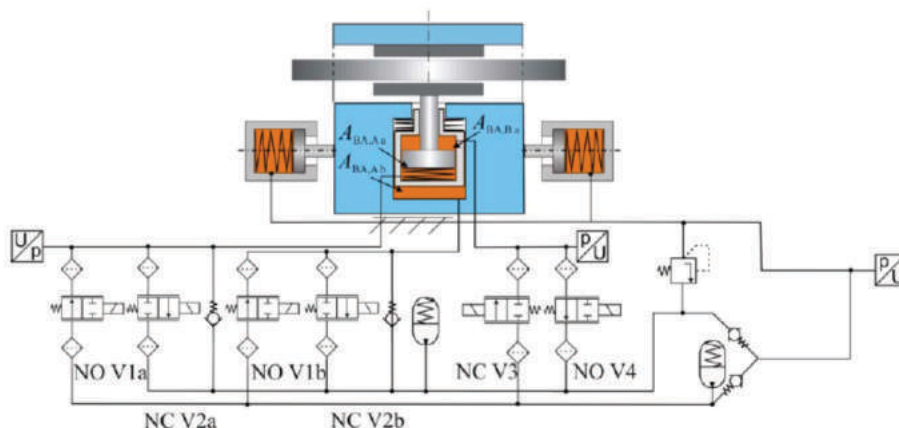


figure 2-7:Brake actuator with reinforcement cylinder

Apart from changing the area of the brake actuator, the supporting cylinder can be adjusted to the current friction value. For this purpose several supporting cylinders with the same or different areas can be used. They can be connected to high or low pressure by valves. Another possibility is designing them like the brake actuator in - **figure27**. If friction coefficients are low, only a small area of the supporting cylinder is activated. Thus, a high closed-loop gain is implemented. In case of high friction coefficients, the active area of the supporting cylinder is enlarged, improving the controllability.

It is also possible to design the supporting cylinder in a way that at first a small area is active. After a short stroke, the first cylinder step moves against a stroke limiter and the friction force is supported by the whole cylinder area.

1 SEHB prototype

figure31 shows the prototype built up at the IFAS. The brake calliper is a floating calliper with a differential cylinder as brake actuator. It rides on guide bolts. A purchased block cylinder is used as the clamping cylinder. On its backside, depicted on the left side of **figure31**, the valve block is directly flanged. On the front side of the cylinder a tensioned spring is installed in axial direction to provide for the fail-closed behaviour.

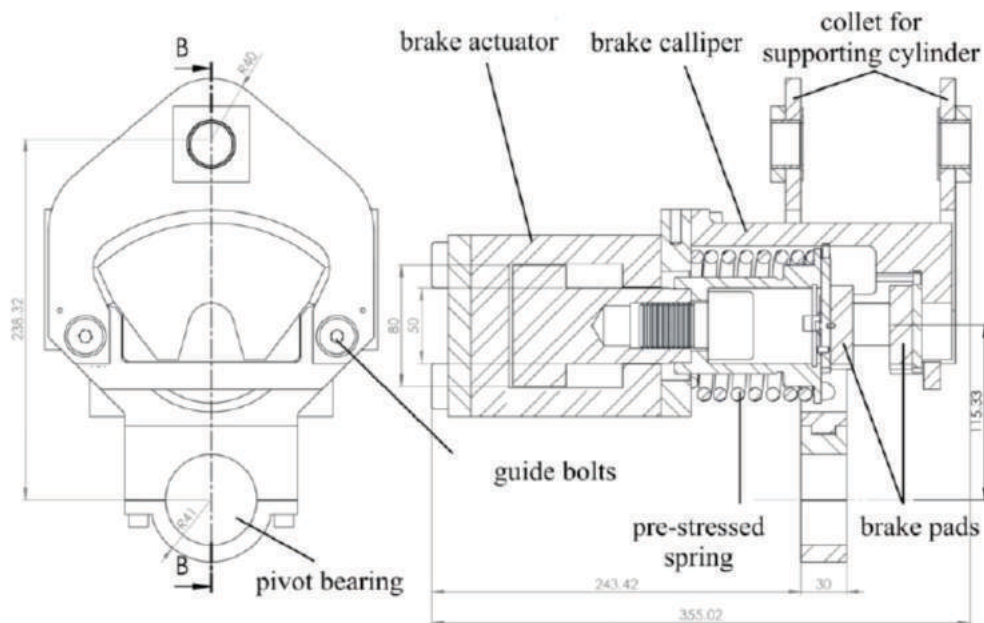


figure 3-1: Brake actuator of the SEHB prototype

A pivot bearing connects the floating calliper to the machine bed. The rotating axis is coaxial to the rotating axis of the brake disk. Due to this fact, the brake pad is directed on the brake disc with a constant friction radius. Contrarily to the brake principle shown in - **figure11**, the supporting cylinder is designed as a double rod cylinder. Thus, a standard hydraulic cylinder is used. The spring reset is not integrated into the cylinder, it is mounted to one side of the cylinder.

The resulting demand for more construction space is accepted for the prototype. Both chambers of the cylinder are connected to the valve block by hoses.

The high and the low pressure accumulators are connected to the valve block by hoses, too. They are mounted onto the machine bed next to the brake. A piston accumulator with a volume of about 7 ml is used as the high pressure accumulator. The volume of the low pressure accumulator is much larger due to the necessary compensation of wear resulting in the brake actuator's stroke.

The prototype is mounted in the institute's test field as shown in figure 3-2. It is driven by a flywheel powered by a hydraulic motor, shown on the right side of figure 3-2. The friction force is controlled by a real-time rapid prototype control processor.

The test stand software includes maps that compensate the valves' pressure-dependant behaviour allowing for a delicate brake force control. The calculated control signal for the valves is the current in the valves' solenoids

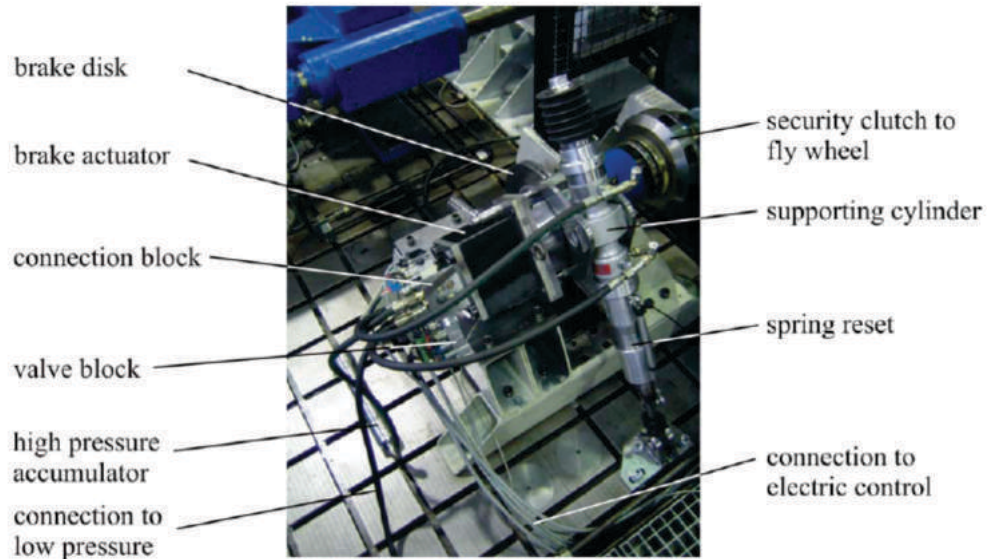


figure 3-2: Prototype on machine bed

3.1 Valve unit

The valve unit consists of a connection block which is directly screwed on the brake actuator and of the valve block itself. The connection block is manufactured from steel. It includes the check valves as well as the connections of the hydraulic lines to the accumulators and to the supporting cylinder. In addition, the pressure sensors are installed onto the connection block.

The solenoid valves depicted in figure 11 are fit into the valve block. To control the flow at the valve unit in a broad range, the valves are doubled. 2/2-way valves from an automotive brake application are used. These valves feature a low price, low leakage, high dynamics and a small need of package. The valves are fitted into the valve block as shown in figure 33. When pressed into the block, the valves' housing seals by a knife edge.

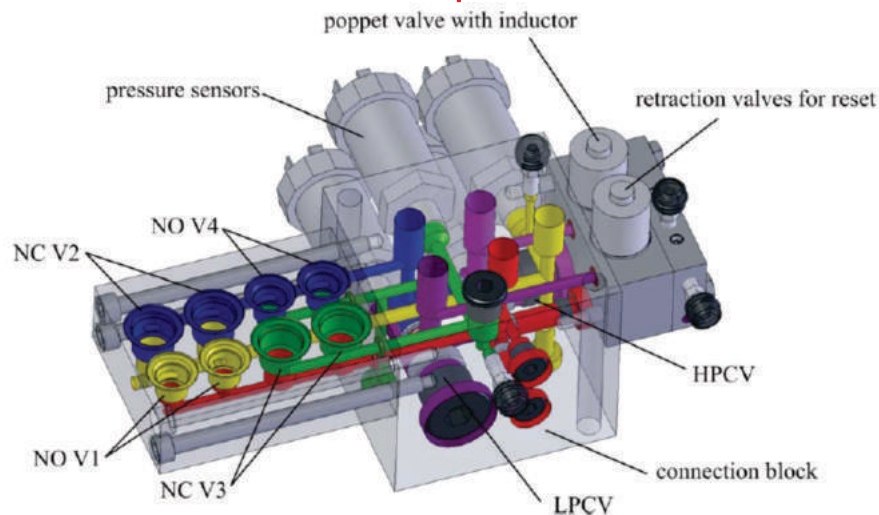


figure 3-3: valve block

Since a double rod cylinder is used, an additional valve is necessary. It connects the two chambers of the supporting cylinder to reset it to its original position. This valve function is included in a small valve block which is mounted on the connection block, too. As reset valves, two more normally closed valves are installed back to back. This arrangement is necessary because the normally closed valves open in one direction like check valves. -figure33 shows both valves with attached solenoid.

4 Measurement results

In the last chapter a measurement is exemplarily presented and analysed. **figure41** shows a measurement during which the brake force is varied between two levels in the form of a ramp /Ewa08/. The upper measurement plot shows the reference brake force and the actual brake force calculated from the pressure sensor at the supporting cylinder.

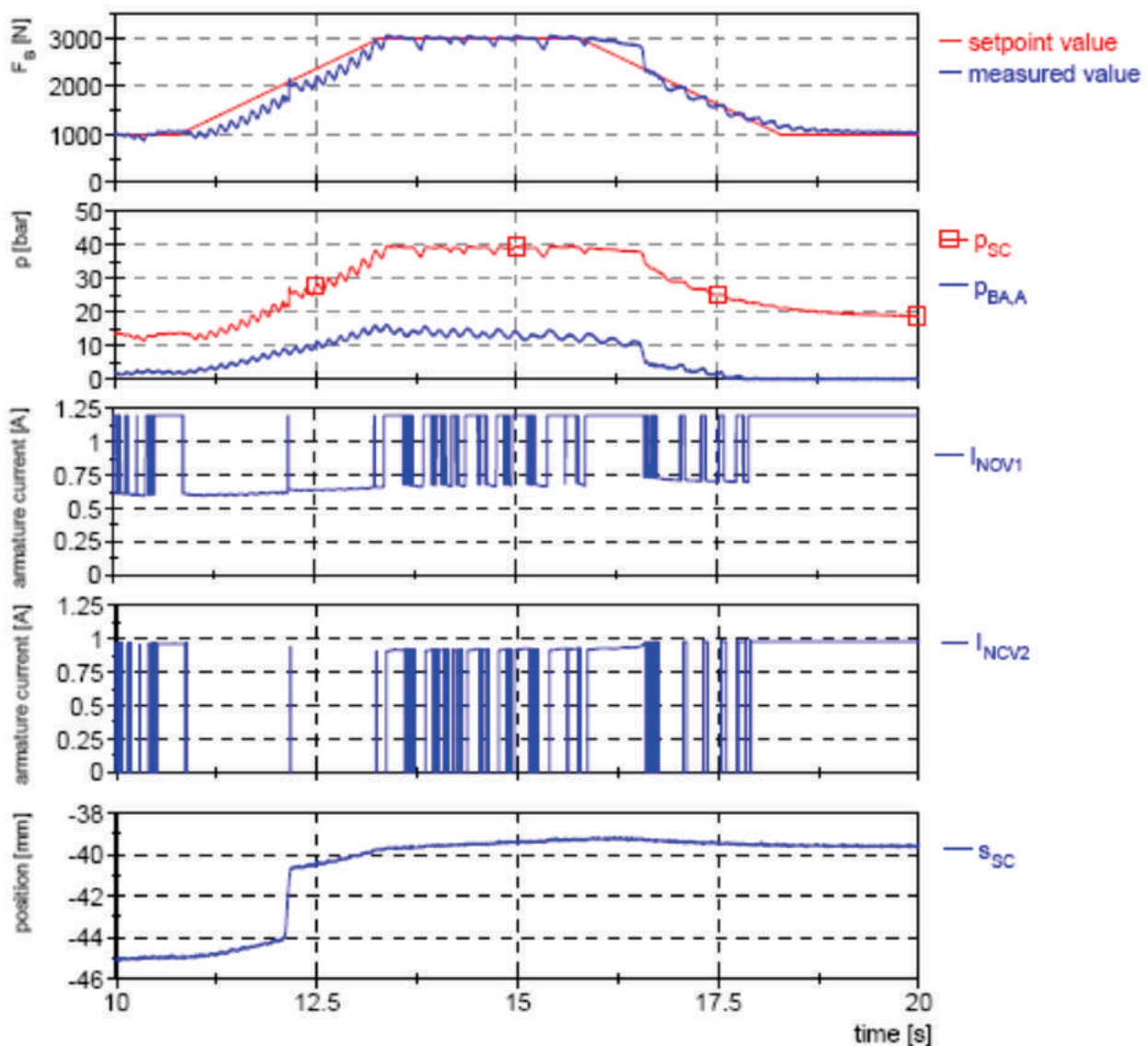


figure 4-1: measurement results /Ewa08/

In the second plot the pressure values in the brake actuator and in the supporting cylinder are shown. The pressure in the supporting cylinder is directly proportional to the braking force. Therefore it is constant when the braking force does not change. The slight pressure decline in the brake actuator at a brake force of 3000 N is explained by an increasing friction value due to the heating up of the brake disc and the brake pads.

The two measurement plots in the middle show the electric actuation in the valve solenoids. These currents are given by the control unit and generated by an amplifier card. The value of the current grows when the reference brake force increases since the poppet valves are influenced by the pressure difference at the valve's tappet. The steps in the current profile are due to changes of the valve's operating mode. There is a hysteresis between the value of the current, at which the valve is safely closed and the value at which it starts opening. Starting in the middle of these values, the control unit adjusts the current to set the desired opening of the valve.

The measurement plot at the bottom shows the position of the supporting cylinder. The high slope at about 12 s is a consequence of filling the high pressure accumulator. The stroke of the supporting cylinder during this measurement is 5.5 mm. Thereby 3 mm are needed to fill the accumulator. Since the stored oil is needed to release the brake completely, this part of the supporting cylinder's stroke only occurs once during a braking process.

1 Summary and Perspective

The presented dimensioning of the SEHB provides a good insight to the mechatronical system of the SEHB. The dimensioning requires that all parameters are considered carefully which influence the self energisation. The examination of the SEHB at low friction coefficients is indispensable to guarantee the functionality of the SEHB in all situations.

The presented prototype demonstrates the functionality of the SEHB. In further development steps the characteristics of the reinforcement can be examined with the prototype. A simulation model can be calibrated to measurements at different operating points. The verified simulation model allows realistic conclusions about dynamic characteristics and controllability. In a static dimensioning this is only possible in terms of quality.

The SEHB can be built in different system configurations. Therefore it is appropriate for applications in different environments with different requirements and security concepts. In this article a fail-closed security concept is presented, which meets the security concept of railway vehicles. The SEHB for automobile applications pursues a fail-open security concept. It also includes a fall back level with a direct hydraulic connection between the brake pedal and the wheel brakes.

6. Bibliography

- /AN07/---„Aachener bremsen besser“, Aachener Nachrichten, 08.05.2007
- /Bre04/ Breuer, Bert; Bill, Karlheinz H.- „Bremsenhandbuch – Grundlagen, Komponenten, Systeme, Fahrdynamik“; 2. edition 2004, Vieweg Verlag
- /Ewa08/ Ewald, Julian; Liermann, Matthias; Stammen, Christian; Murrenhoff, Hubertus - „Application of proportional seat valves to a self-energising electro-hydraulic brake“, in: *Fluid power and motion control*: (FPMC 2008), Bath, GB, Centre for Power Transmission and Motion Control
- /Gom06/ Gombert, Bernd; Gutenberg, Philipp - „Die elektronische Keilbremse – Meilensteine auf dem Weg zum elektronischen Radantrieb“, in *ATZ*, 108(11), 2006
- /Her08/ Hermanns, Marcel; Hennen, Martin; Liermann, Matthias; Stütze, Thorsten - „Intelligentes, integriertes Einzelrad-Antriebs-Brems-Modul (EABM)“, in: *Eisenbahntechnische Rundschau*. Hamburg : DVV Media Group, Eurailpress. - 57 (2008)
- /Hof07/ Hofmann, Dirk; Baumann, Dietmar Disk brake, patent DE102007016250A1, 04.04.2007
- /Lie06/ Liermann, Matthias; Stammen, Christian - „Selbstverstärkende hydraulische Bremse für Schienenfahrzeuge: Intelligentes, Integriertes Einzelrad-Antriebs-Brems-Modul“, in: *O + P* Nr. 50 (2006)
- /Lie08/ Liermann, Matthias - „Self-energizing Electro-Hydraulic Brake“, dissertation, 2008, Shaker Verlag
- /Mur08/ Murrenhoff, Hubertus - „Servohydraulik – Geregelte hydraulische Antriebe“, Shaker Verlag 2008
- /Smi08/ Schmidt, Matthias; Murrenhoff, Hubertus; Lohrberg, Henrik; Körber, Franz-Josef - „Influencing parameters on tightness of hydraulic seat valves“, in: *Fluid power and motion control*: (FPMC 2008), Bath, GB, Centre for Power Transmission and Motion Control
- /Tou64/ Tournier, Yves; Henri, Beauchamp - Disk brake, patent FR19630941849, 18. Juli 1963

INFLUENCE OF AIR CONTENT ENTRAINED IN FLUID OF OPERATING PARAMETERS OF VANE PUMP WITH DOUBLE EFFECT

Radovan S. Petrovic ¹⁾, Wang Zheng Rong ²⁾, Andrzej Banaszek ³⁾

¹⁾ Center for automatic control and fluid technics Faculty of Mechanical Engineering Kraljevo University of Kragujevac, Serbia

²⁾ Dept. of Fluid power and control, LAN Zhou University of technology, LAN Zhou, China

³⁾ Technical University of Szczecin, Faculty of Maritime Technology Poland

Abstract

In developing the vane pumps the fundamental basis is experimental research and mathematical modeling of nonstationary hydraulic processes inside the pump, in thrust space and suction and thrust pipeline. By means of experimental research and results of mathematical modeling and software package KRILP, it is possible to determine the parameters of operating processes of vane pumps precisely enough.

This research examines the idealized and actual flow ripple of a high-pressure vane within vane type pump. For the idealized case, a 'perfect' pump is examined in which the leakage is considered to be zero and the fluid is considered to be incompressible. Based upon these assumptions, expressions describe the characteristics of the idealized flow-ripple are derived. Next, the actual flow-ripple of the pump is examined by considering the fluid compressibility and for computing these results a numerical program is used. From the idealized analysis it is shown that the idealized flow-ripple is determined by geometrical flow property

Keywords: vane pump, mathematical modeling, software, hydrodynamic processes, incompressible, flow-ripple, axial clearance, radial clearance, rotor, stator, experiment.

1. Introduction

Modern methods of designing and constructing the hydraulic pumps can not be done without using the appropriate mathematical models of effects and processes happening in real pump structures. The mathematical model of a process is analytical interpretation of the process with certain assumptions. In order to reach the mathematical model it is necessary to make detailed theoretical research based on the laws of fundamental sciences and explanation of processes, what is the basis for adopting the assumptions and defining the model equations.

2. Mathematical model of pressure change in the operating chamber

The level of noise made by vane pump with double effect is crucially influenced by pressure rise and fall in the pump chambers in the areas of change of operating cycles. Constant conversion of thrust pressure into operating pressure in the installation and vice versa is an important assumption for lowering the noise level. There are a great number of researches done in order to define the optimal geometry of working volume when one operating cycle converts into another one [9]. The processes occurring at the area of pressure change and their relation can be researched by experiments and by mathematical modeling by means of adequate software packages. For these researches the software KRILP has been developed and it has been written in program language Digital Visual Fortran 5.0.

The increase of rotation number provides better tightness of working chamber at the area of pressure change which can be explained by the increase of centrifugal force acting on the vanes and pressing them against the inner surface of the stator. When the vanes are separated from the operating stator profile, pressure pulsation and amplitude changes are registered. These changes often occur with low number of revolutions and they lead to oil coming back from thrust area towards suction area. When chambers are not sealed tight, i.e. when clearances are large, the pressure does not rise enough in the area of pressure change, what leads to unexpected relation between the chamber and thrust port and also leads to pressure balance. Thus the leakage between the suction and thrust zone is being increased as well as the amplitude of pressure pulsation.

Due to the influence of the clearance on the tightness in the chamber, the pressure change in the chamber should be presented by mathematical model depending on volumetric losses and it is necessary to make certain simulations on the computer. On the basis of data obtained by experiments and simulations we should determine geometries of suction and thrust ports as well as partitions between them at valve plate. The following phases can be distinguished in simulating the pressure change in the chamber while passing over the partition separating suction and thrust zones :

- the chamber is closed, i.e. there is no connection between the chamber and neither suction zone and nor thrust zone
- the chamber is connected to thrust port through the slot
- the chamber is fully connected to thrust port.

Vane pump with double effect is shown in Fig.1.

Technical data:

Speed: $500-3500 \text{ min}^{-1}$

Pressure: $210 \cdot 10^5 \text{ Pa}$

Specific Flow: $16.5 \text{ cm}^3 / \text{o}$

Number of vanes: 10



Fig.1. Vane pump with double effect

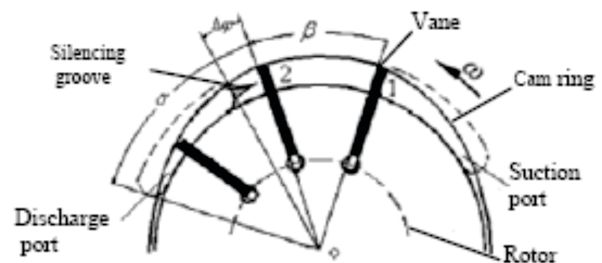


Fig.2. In order to gain the instantaneous fluid pressure within chamber in transition region

1.1. Volumetric losses affecting the speed of pressure change in the operating chamber at the zone of pressure change

In order to operate properly the pump must have appropriate clearances between vane rotor and valve plates. There is a certain flow through these clearances. Volumetric losses in the chamber can be classified as follows [8]:

- losses at vane side made by axial clearances $Q_{an} (n = 1, 2)$

- losses over vane top made by radial clearances Q_{rn} ($n=1,2$)
- losses made by flow withdrawal Q_{pr}
- losses through the slot at valve plate Q_{pz}
- losses through the gap made by the vane in rotor groove Q_{pc}

1.1.1. Losses made by axial clearances

If we assume that the flow is streamline the losses through the axial clearances are:

a) volumetric losses for the chamber in front of the vane can be presented by following equation:

$$Q_{a1} = \frac{(r_i - r) \cdot z_{a1}^3}{12\eta s} |p_r - p_k| \text{sign}(p_r - p_k), \quad (1)$$

b) volumetric losses for the chamber behind the vane can be presented by following equation:

$$Q_{a2} = \frac{(r_i - r) \cdot z_{a2}^3}{12\eta s} (p_k - p_u), \quad (2)$$

where:

r_i - variable radius of the stator;

r - smaller radius of the stator

z_{a1}, z_{a2} -values of axial clearance;

s - vane thickness

η -dynamic viscosity of working fluid;

p_u - suction pressure

p_k - pressure in the chamber

p_r - operating pressure

1.1.2. Losses made by radial clearances

Between the inside surface of the stator and vane top working flow leaks what can be presented as follows:

a) volumetric losses for the chamber in front of the vane can be presented by following equation:

$$Q_{r1} = \frac{b \cdot z_{r1}^3}{12\eta s} |p_r - p_k| \text{sign}(p_r - p_k), \quad (3)$$

b) volumetric losses for the chamber behind the vane can be presented by following equation:

$$Q_{r2} = \frac{b \cdot z_{r2}^3}{12\eta s} (p_k - p_u), \quad (4)$$

z_{r1}, z_{r2} - values of radial clearances

b – the width of the vane

1.1.3. Losses made by flow withdrawal

The mean value of losses made by flow withdrawal at the vane is presented by the expression:

$$Q_{pr} = \frac{z_{a1/2} \omega (R+r)(R-r)}{4} \quad (5)$$

where are:

ω - angular speed of rotor;

φ - angle of rotor rotation

R, r - bigger and smaller radius of stator

1.1.4. Losses through the slot at valve plates

Losses through the slot in thrust port at valve plate are determined in the following manner:

$$Q_{pz} = \mu A \sqrt{\frac{2}{\rho} (p_r - p_k) \text{sign}(p_r - p_k)} \quad (6)$$

where are:

μ - outflow coefficient;

A - cross-sectional area

ρ - density of working fluid

1.1.5. Losses made by the vane in rotor groove

If the pressure in the chamber is higher than working pressure of the pump there is a gap in rotor groove made by front vane tilting because of tangential load and there is oil leakage which can be presented by:

$$Q_{pc} = \frac{bz_{pc}^3}{12\eta l_r} (p_k - p_r) \quad (7)$$

where are:

z_{pc} - clearance in the gap;

$l_r = l - (r_i - r_r)$ - length of the front vane when rotor is in transmission area.

r_r - radius of rotor

1.2. Speed of pressure change in the chamber when suction and thrust zones are being separated

If initial volume V is lowered for $dV = V_1 - V = -(V - V_1)$,

due to pressure rise $dp = p_1 - p$ the relative volume - dV/V , calculated per pressure unit:

$$S = -\frac{1}{dp} \cdot \frac{dV}{V}, \quad (8)$$

is compressibility coefficient.

The reciprocating value of compressibility coefficient is called the compressibility modulus (ϵ_s),

$$\epsilon_s = \frac{1}{S} = -\frac{dp}{dV/V} \quad (9)$$

which has the same dimension as the pressure.

In previous expressions the minus sign shows that pressure rise corresponds to volume decrease and vice versa. The previous expression can be also presented in the following form, in case of final changes of pressure and volume

$$-\frac{\Delta V}{V} = \frac{\Delta p}{\epsilon_s} \quad (10)$$

which represents so called Hooke's law. The marks in previous expression are:

$\Delta p = p_1 - p$ - pressure increment

$\Delta V = V_1 - V$ - change of volume

V_1 - fluid volume at the pressure p_1

In this study, the compression of oil in the transition regions is considered as adiabatic change. For the transition time is about 1ms at the speed of rotation $n = 1800 \text{ min}^{-1}$ and the angle of the transition regions is $\Delta\varphi = 10^\circ \sim 12^\circ$.

Mathematically the fluid bulk modulus varying with the content of air is expressed

$$S' = S'' \frac{1 + (V_{a0}/V_{f0})(p_0/p)^{2/k}}{1 + (V_{a0}/V_{f0})(p_0/p)^{1/k}(S''/kp)} \quad (11)$$

Where S' is the bulk modulus of oil containing air, $S'' = 1660 \text{ MPa}$ is the bulk modulus of pure oil, p is the absolute pressure of oil, p_0 is absolute atmosphere, $k = 1.4$ is adiabatic exponent, V_{a0} is volume of air at absolute atmosphere, V_{f0} is volume of oil at absolute atmosphere. The volumetric content of air in oil at absolute atmosphere is given by

$$x_0 = \frac{V_{a0}}{V_{a0} + V_{f0}} \quad (12)$$

So:

$$\frac{V_{a0}}{V_{f0}} = \frac{x_0}{1 - x_0} = x_1 \quad (13)$$

Substituting (12) into (13) yield the fluid bulk modulus S' in following form

$$S' = S'' \frac{1 + x_1 p_o^{2/k} p^{-2/k}}{1 + x_1 p_o^{1/k} p^{-1/k} S''/k} \quad (14)$$

The pressure increment in the working chamber of vane pump with double effect can be reached from the following expression:

$$\Delta p_k = \frac{\epsilon_s}{V_{k(R)}} (\Delta V)_{k(R)}, \quad (15)$$

where are:

Δp_k - pressure increment in the chamber between the vanes $p_u < p_k < p_p$

ϵ_s - compressibility modulus of working fluid

p_u - suction pressure of working fluid

p_p - thrust pressure of working fluid

$V_{k(R)}$ - volume of the chamber (when the chamber is in the zone of pressure change constrained by angle φ and bigger stator radius R)

Volume $V_{k(R)}$ is calculated like this:

$$V_{k(R)} = \frac{b}{2} (R^2 - r_r^2) (\beta - \sigma), \quad (16)$$

where are:

$(\beta - \sigma)$ [rad] - angle between two adjacent vanes

b - vane width

The speed of pressure change in the chamber is obtained by differentiating the expression (15) with respect to time t :

$$\frac{\Delta p_k}{\Delta t} = \frac{\varepsilon_s}{V_{k(R)}} \frac{\Delta V_{k(R)}}{\Delta t}, \quad (17)$$

in case when $\Delta t \rightarrow 0$; $\Delta V_{k(R)} \rightarrow dV_{k(R)} \rightarrow 0$ and $\Delta p_k \rightarrow dp_k \rightarrow 0$, previous equation has differential form:

$$\frac{dp_k}{dt} = \frac{\varepsilon_s}{V_{k(R)}} \frac{d}{dt} (\Delta V)_{k(R)} \quad (18)$$

If we put the expressions for volumetric losses (1) to (7) into the expression (18) for speed of pressure change in the chamber we obtain the following expression:

$$\frac{dp_k}{dt} = \frac{\varepsilon_s}{V_{k(R)}} \left(\frac{dV_{k(R)}}{dt} + 2Q_{a1} - 2Q_{a2} + Q_{r1} - Q_{r2} - Q_{pr} + Q_{pz} + Q_{pc} \right) \quad (19)$$

After replacing the values for volumetric losses we get required expression for speed of pressure change in relation to the clearance in the chamber of vane pump with double effect:

$$\begin{aligned} \frac{dp_k}{dt} = \frac{\varepsilon_s}{V_{k(R)}} & \left[\frac{dV_{k(R)}}{dt} + 2 \frac{(\rho - r) \cdot z_{a1}^3}{12\eta s} |p_r - p_k| \text{sign}(p_r - p_k) - \right. \\ & - 2 \frac{(\rho - r) \cdot z_{a2}^3}{12\eta s} (p_k - p_u) + \frac{b \cdot z_{r1}^3}{12\eta s} |p_r - p_k| \text{sign}(p_r - p_k) - \\ & - \frac{b \cdot z_{r2}^3}{12\eta s} (p_k - p_u) - \frac{z_{a1} \cdot 2\omega(R+r)(R-r)}{4} + \\ & \left. + \mu A \sqrt{\frac{2}{\rho} (p_r - p_k) \text{sign}(p_r - p_k)} + \frac{b z_{r1}^3}{12\eta l_r} (p_k - p_r) \right] \end{aligned} \quad (20)$$

The expression of p is given by

$$p \approx \frac{[(V_{a0}/V_{f0})] p_0}{1 + (V_{a0}/V_{f0}) (p_0/p)^{1/k} (S''/kp)} \quad (21)$$

Where p_0 is the density of pure oil.

Substituting (13) into (21) yield p in following form

$$p \approx \frac{(1+x_1) p_0}{1 + x_1 (p_0/p)^{1/k} (S''/kp)} \quad (22)$$

For simulation purposes, the above equation can be rearranged as

$$\begin{aligned} \frac{dp}{d\phi} = & - \frac{1}{1 - \frac{\Delta p}{S'} \frac{dS'}{dp}} \frac{S'}{V} \frac{dV}{dt} \left(\frac{-B\omega}{2} (R^2 - r_1^2) + \right. \\ & \left. + bs \frac{dr_1}{dt} + c_q A_0 (2 \Delta p/p)^{1/2} \right) \frac{1}{\omega} \end{aligned} \quad (23)$$

Eq.(23) can be solved numerically for the instantaneous pressure of the chamber in transition regions. Example for one type high-pressure vane within vane pump, Fig.3 shows p/p_s vary with the configuration of silencing groove under condition of $p_s = 17.5 \text{ MPa}$, $n = 1800 \text{ min}^{-1}$ and $x_0 = 1\%, 3\%, 5\%, 7\%$.

Substituting the numerical results of p into Eq.(23) can yield the pressure gradient $dp/d\phi$ vary with the content of air in fluid, as shown in Fig.4.

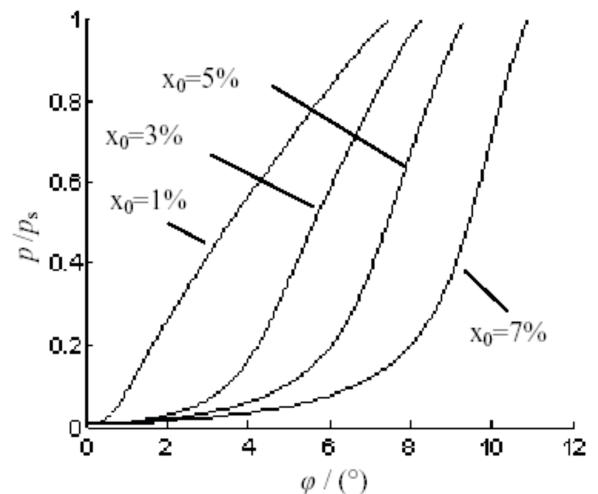


Fig.3. Instantaneous pressure varying with the air content

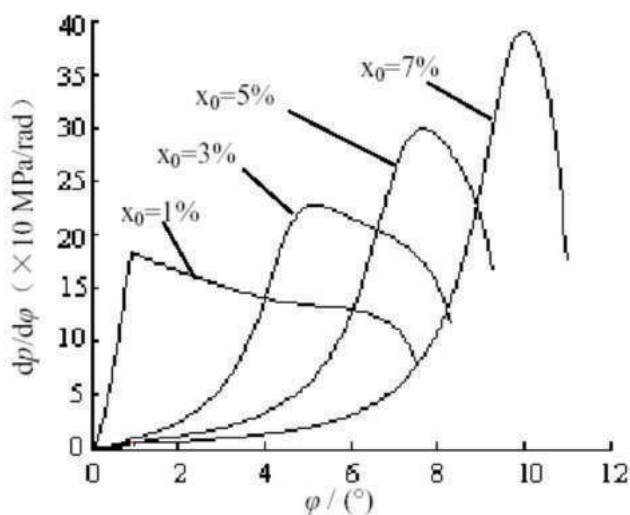


Fig.4. Pressure gradient varying with the air content

Next section shows diagrams of speed of pressure change depending on the clearance in the operating chamber of vane pump with double effect. They are obtained by simulation of expression (20) by means of software package KRILP.

2 Results of simulating the pressure change in the chamber of vane pump with double effect

Results of simulating the expression for speed of pressure change in the chamber for various values of slot cross section are shown in Fig.5.

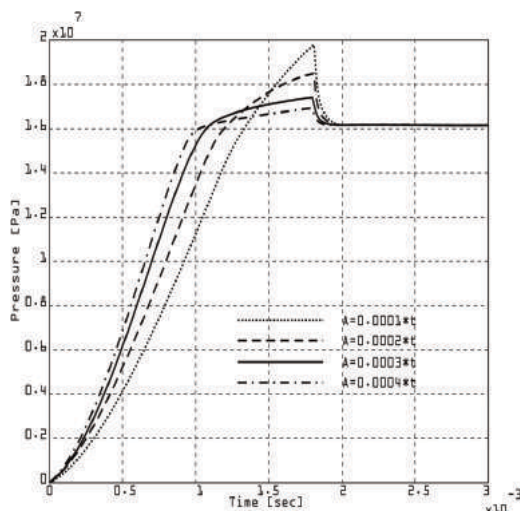


Fig.5. Speed of pressure change in the chamber for various values of slot cross section

Results of simulating the expression for speed of pressure change in the chamber for various values of axial clearance at the first vane are shown in Fig.6.

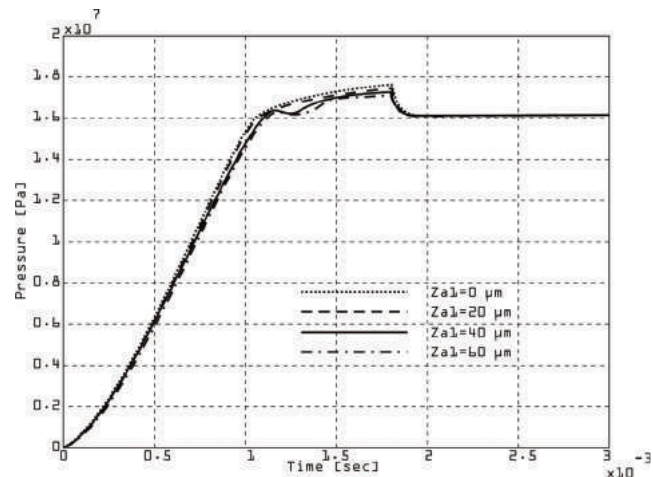


Fig.6. Speed of pressure change in the chamber for various values of axial clearance at the first vane

Results of simulating the expression for speed of pressure change in the chamber for various values of axial clearance at the second vane are shown in Fig.7.

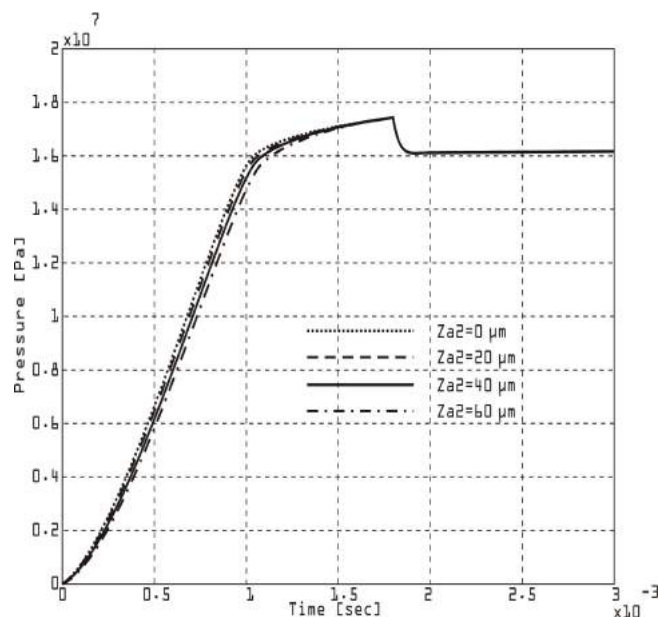


Fig.7. Speed of pressure change in the chamber for various values of axial clearance at the second vane

Results of simulating the expression for speed of pressure change in the chamber for various values of radial clearance at the first vane are shown in Fig.8.

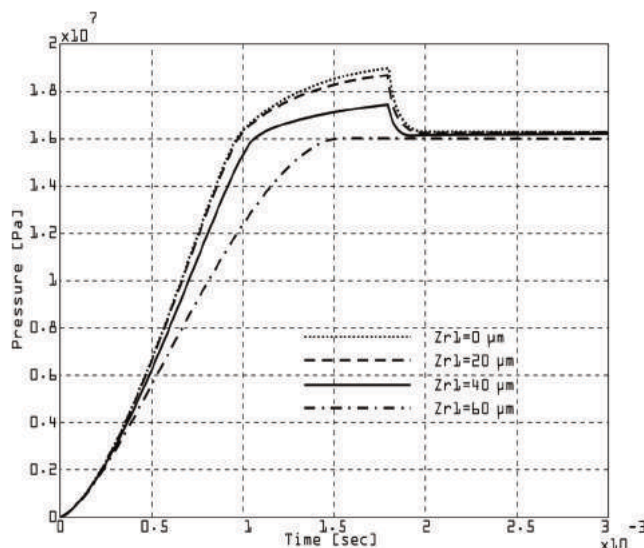


Fig.8. Speed of pressure change in the chamber for various values of radial clearance at the first vane

Results of simulating the expression for speed of pressure change in the chamber for various values of radial clearance at the second vane are shown in Fig.9.

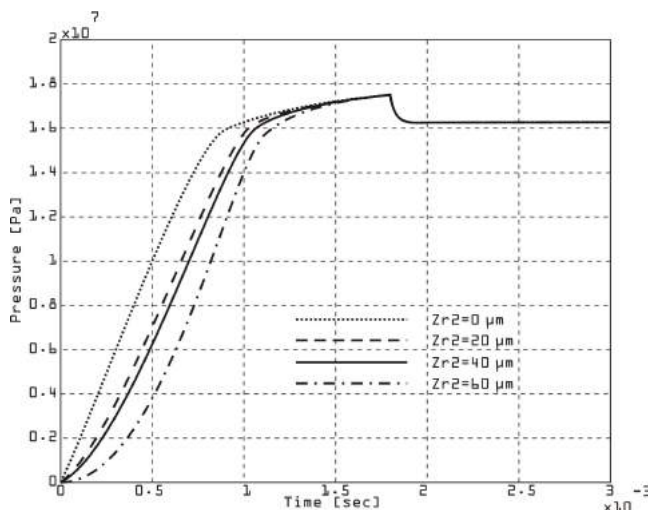


Fig.9. Speed of pressure change in the chamber for various values of radial clearance at the second vane

Results of simulating the expression for speed of pressure change in the chamber for various values of the gap in rotor groove are shown in Fig.10.

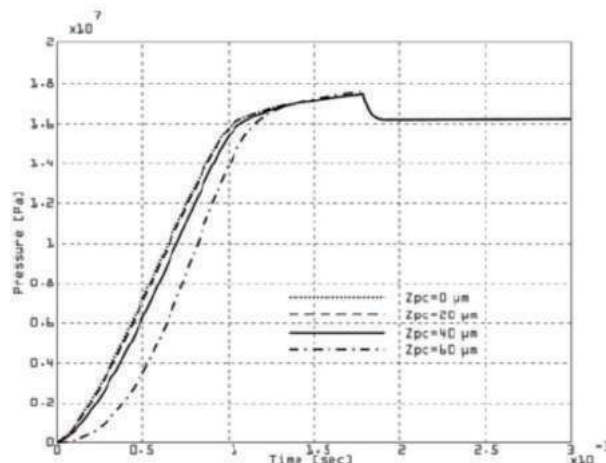


Fig.10. Speed of pressure change in the chamber for various values of the gap in rotor groove

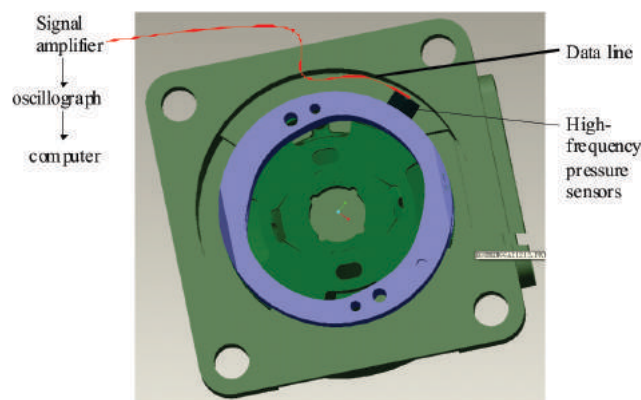


Fig.11. The overall structure of experiment

4 CONCLUSION

It is not possible to determine precisely enough the parameters of hydrodynamic process of the vane pump with double effect neither by experiments nor by mathematical modeling only. Accurate working parameters can be reached by combined application of experimental measuring, mathematical modeling of hydrodynamic process and nonlinear optimization but at the same time the system errors of measuring and unknown parameters can be determined.

The program KRILP developed for mathematical modeling, identification and optimization of vane pumps provides developing of a whole family of vane pumps in further research of hydrodynamic processes along with the analysis of advantages and disadvantages of vane pumps with double effect.

5 REFERENCES

- [1] Petrovic, R. Mathematical modeling and identification of multicylindrical axial piston pump parameters. *PhD Thesis, Faculty of Mechanical Engineering*, Belgrade, 1999.
- [2] Petrović, R. Mathematical Modeling and Experimental Research of Characteristic Parameters Hydrodynamic Processes of a Piston Axial Pump, *Strojniški vestnik - Journal of Mechanical Engineering* 55(2009)4, UDK 621.785.4
- [3] Petrović, R. Mathematical Modeling and Experimental Verification of Operating Parameters of Vane Pump With Double Effect *Strojniški vestnik - Journal of Mechanical Engineering* 55(2009)1 UDC 621.9.04
- [4] Radovan S. Petrovic, Jožef Pezdirnik, Petar R. Ivanovic,
Development of methodologies and software for engineering, simulation and optimization of oil-hydraulic cylinders of large measurements and strengths, *Proceedings of the Seventh International Conference on Fluid Power Transmission and Control (ICFP 2009)*, China
- [5] C.L.Na, The distribution theory of axial piston pump in considering the compression of fluid, Beijing, Weapons Industry Press, (2003) 17. (in Chinese)
- [6] Y.Q.Na, *Journal of Lanzhou University of Technology*, Vol.30, No.3 (2004)58. (in Chinese)

[7] Z.R.Wang, *Proc. 6th Int. Symp. on Fluid Power Transmission and Control*, Hangzhou, International Academic Publishers (2005)527.

[8] Banaszek A.: The influence of liquid cargo viscosity on discharge rate of hydraulic submerged cargo pumps used in transport at sea, *Archives of Transport No 4/2006*, p.25-32, Polish Academy of Sciences, Warsaw 2006,

MECATRONICĂ ȘI TEHNICA MĂSURĂRII INTELIGENTE



**EOSINT M 270
Titan Version**

**Laboratorul
Micro-Nanotehnologii
"Rapid Prototyping"**



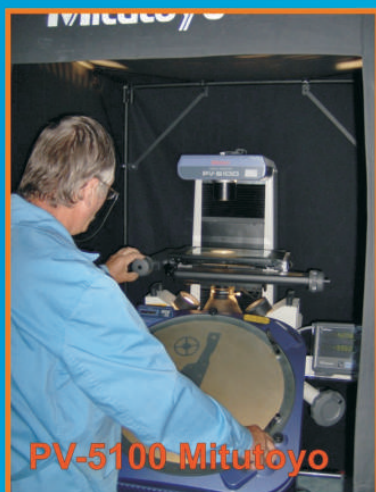
Leitz Reference 600

**Micro - Laboratorul
Măsurări dimensionale
ultraprecise în 3D**



Microscop de Forță Atomică

**Laboratorul nanometrie
"Microscop de Forță Atomică"**



PV-5100 Mitutoyo



OPTIMAR 100 Mahr

**Echipamente mecatronice
HIGHTECH**



**SISTEM VISION
Starrett Galileo**

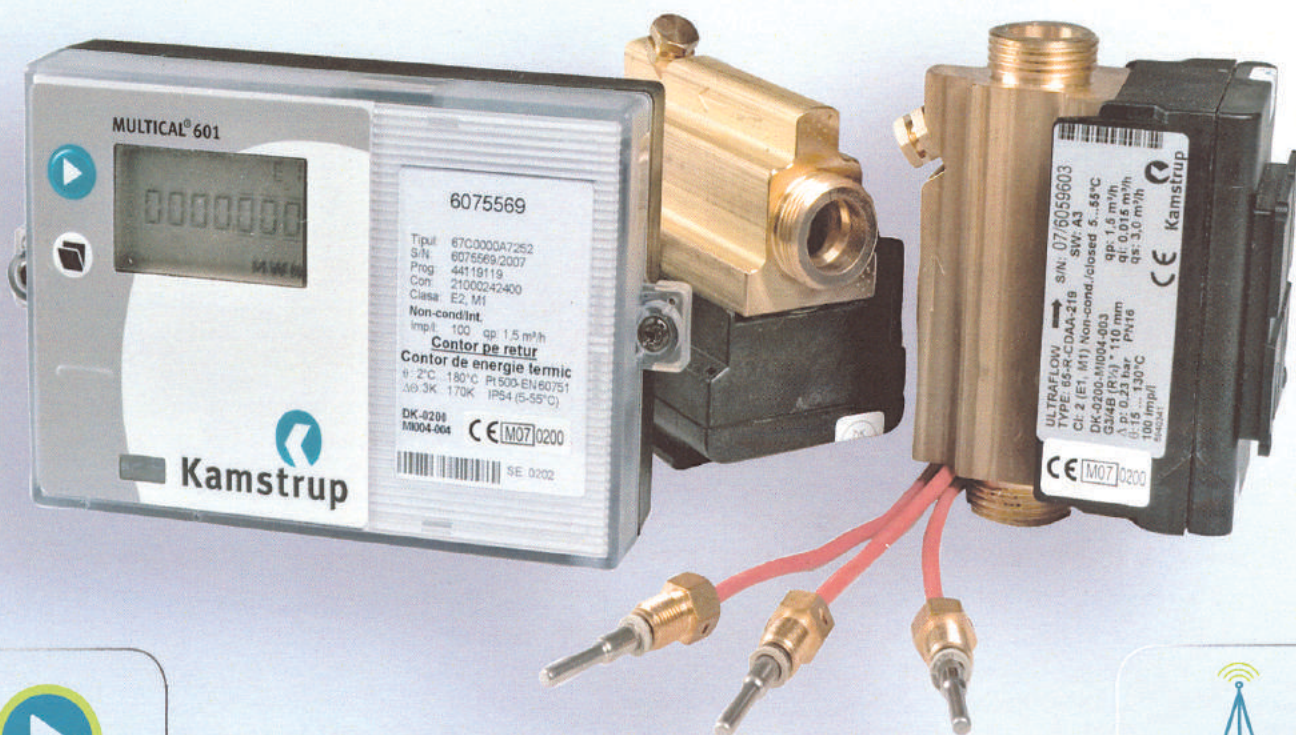
- ◆ **SISTEME ȘI ECHIPAMENTE
MECATRONICE DE MĂSURARE**
- ◆ **APARATURĂ INTELIGENTĂ
MEDICALĂ**
- ◆ **TEHNOLOGII INOVATIVE**
- ◆ **MERKETING, STRATEGII,
TRANSFER TEHNOLOGIC**

- ◆ **CERCETARE DEZVOLTARE
ȘI INOVARE**
- ◆ **STUDII, STRATEGII ȘI
CONSULTANȚĂ**
- ◆ **ANALIZE, TESTĂRI ȘI
CERTIFICARE**



**INSTITUTUL NAȚIONAL DE CERCETARE DEZVOLTARE PENTRU
MECATRONICĂ ȘI TEHNICA MĂSURĂRII**

Șos. Pantelimon nr. 6 + 8, sector 2, 021631, București, ROMÂNIA
Tel: +4021. 252.30.68/69; Fax: +4021. 252.34.37;
E-mail: cefin@cefin.ro; incdmtm@incdmtm.ro



Mod de operare

Display intuitiv si
simplu de utilizat

MULTICAL® 601

CONTORIZAREA CONSUMURILOR DE CALDURA PENTRU INCALZIRE
SI APA CALDA, PE BAZA PRINCIPIULUI ULTRASONIC DE MASURA



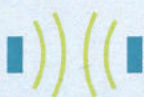
Citire la distanta

M-Bus, Radio,
LONWorks, etc.



Memorie

Standard, cu jurnale
de date protejate



Ultrasonic

Sistem de masura
precis, cu durata
lunga de viata



Standarde

Conform MID si
EN 1434:2004



Flexibil

Noi functiuni si
interfete pot fi
oricand incorporate



Kamstrup

- metering solutions

DETERMINATION OF THE ACTUATION FORCE OF SPOOL VALVES WITH ZERO COVERAGE

(1st Report, Theoretical Analysis)

Ph.D.eng. Dragos Ion Guta ¹, Ph.D.eng. Teodor Costinel Popescu ¹,
Ph.D.stud.eng. Catalin Dumitrescu ¹

¹INOE 2000-IHP Bucharest, ROMANIA

Abstract:

The adjustment elements of hydraulic parameters flow and pressure are complex closed loop systems, which involve phenomena associated with fluid flow, electromechanical phenomena, as well as phenomena specific to automatic adjustment. Due to complexity of such phenomena, determination of optimal solutions to their design and implementation is iterative. A key problem to be solved in order to design / develop / optimize a hydraulic directional control valve is to determine the force necessary for displacement of slide valve. Hydrodynamic forces that arise due to the flow of the working fluid through the section delimited by the shoulders of the spool valve and the edges of the sleeve tend to stop distribution. Meeting the performance requirements involves the use of modeling processes and numerical simulation based on realistic models, obtained by calibration of equations systems based on experimental data.

Keywords: proportional directional valve, axial flow forces, solenoid actuator

1. Introduction

Directional control valves are hydraulic components used to make different connections and adjust the flow along the circuits created between joints. The most widespread directional control valves consist of a cylindrical slide with translational motion and a fixed body provided with toroidal inner channels. Between the shoulders of the slide valve and the toroidal chambers several variable throttles are placed simultaneously which regulate the flow. The less complicated directional control valve has two positions and two joints, actually being a throttle used to control flow or for interruption of hydraulic circuits. The most widespread directional control valves have four joints and three positions. In terms of the scheme of connections, directional control valves can have closed, open or partially open centre.

Since the change of a mechanical parameter causes variation of a hydraulic parameter, directional control valves can be considered mechano- hydraulic converters. Using an electromechanical conversion stage (proportional magnet) with a mechano-hydraulic converter (directional control valve) allows creation of a complex subsystem (electrohydraulic amplifier) which performs conversion of signal from electrical signal into a hydraulic one [1]. These are referred to as amplifiers because the ratio of hydraulic controlled power and electrical control power is greater than 1 (usually 103... 106). Direct command of slide valves can be performed by means of proportional force or position electromagnets.

Proportional force electromagnets (Fig. 1) ensure proportionality between the coil current and the force axially developed inside plunger. Force provided by the electromagnet is proportional to intensity of control current and is affected by hysteresis.

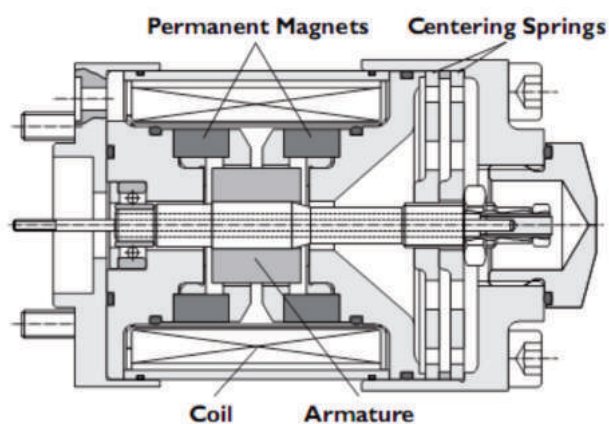


Fig.1. Moog linear force motor [4]

For small strokes force inside the rod of plunger is independent of its position (Fig. 2). Bearings of plunger are usually made of sintered and rayon bronze and are immersed in oil.

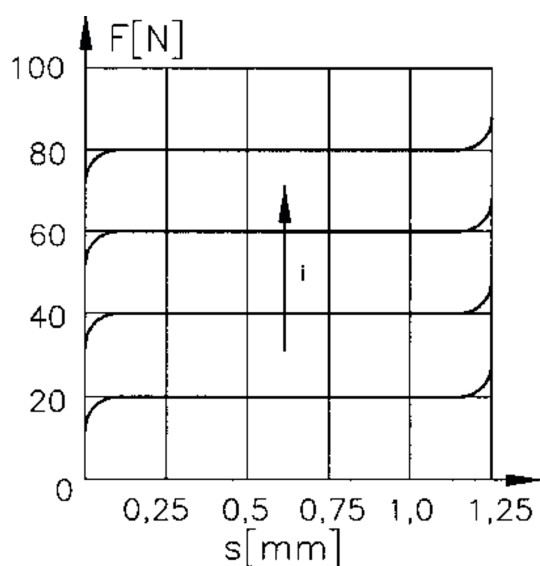


Fig.2. Stationary characteristic of a proportional force electromagnet

Proportional stroke electromagnets (Fig. 3) are made of a block comprising a proportional force electromagnet, an inductive position transducer and a servo controller.

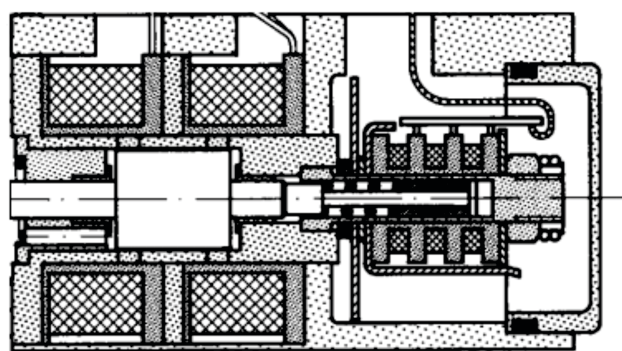


Fig.3. Bosch Rexroth control solenoid with position transducer [5]

Electromechanical converters [2] of such type contain a closed feedback loop in servo controller supported by position information received from the inductive transducer. Axial force inside plunger (Fig.4) depends on its position.

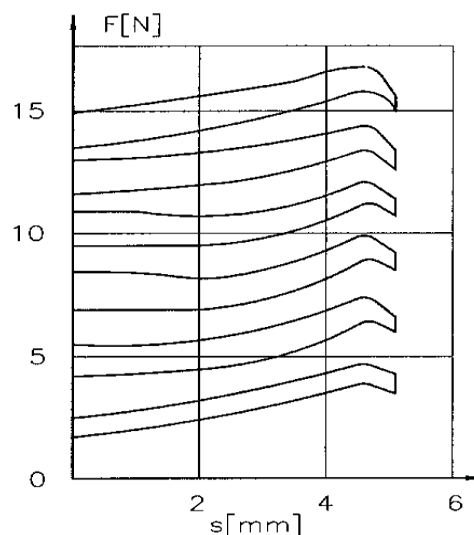


Fig.4. Stationary characteristic of a proportional stroke electromagnet

Design of proportional electromagnets used to control the slide valves of hydraulic directional control valves raises the issue: reducing electromagnetic gauge when increasing oil flows decanted through the directional control valve. Decrease of gauge, electric power consumption and consequently of production and use costs of proportional electromagnets requires their optimization depending on the axial forces that need to be developed for displacement of slide valves.

2. Mathematical modeling of axial forces needed for displacement of the slide valve

Axial forces needed for displacement of slide valves of hydraulic directional control valves consist of inertial forces, frictional forces, elastic forces of centering springs and hydrodynamic forces [3] due to the flow of working fluid through holes of variable area.

Q – volumetric flow
 A0 – area of flow section
 Cc – coefficient of contraction
 Cd – coefficient of flow
 ρ – density of working fluid
 θ – jet angle
 F – force
 P – pressure
 w – area gradient

2.1. Determination of hydrodynamic forces due to flow

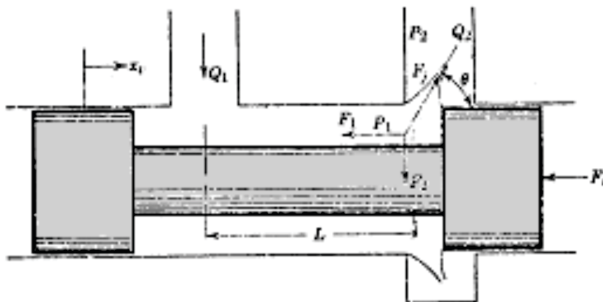


Fig.5. Flow forces due to flow

The most important component of the actuation force is of hydrodynamic type. Force developed due to flow through the section formed between the slide valve edges and sleeve:

$$F_j = \rho \cdot V \frac{Q_2^2}{A_2 \cdot V} = \frac{\rho \cdot Q_2^2}{A_2} = \frac{\rho \cdot Q_2^2}{C_c \cdot A_0} \quad (1)$$

Components (axial and lateral) of the equal and opposite force caused by Fj:

$$F_1 = -F_j \cdot \cos \theta \quad (2)$$

$$F_2 = -F_j \cdot \sin \theta \quad (3)$$

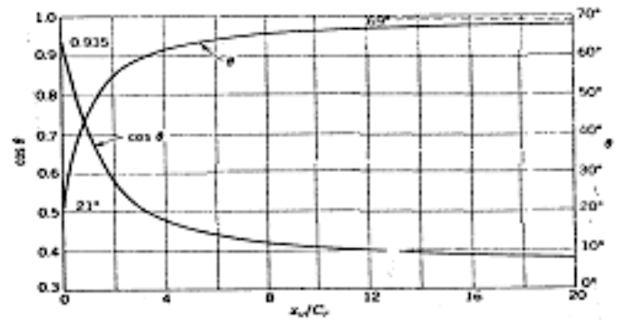


Fig.6. Effect of radial clearance on the jet angle

Neglecting the fluid compressibility inside the directional control valve and considering flow conservation:

$$Q_1 = Q_2 = C_d \cdot A_0 \sqrt{\frac{2}{\rho} (P_1 - P_2)} = C_c \cdot C_v \cdot A_0 \sqrt{\frac{2}{\rho} (P_1 - P_2)} \quad (4)$$

It results:

$$F_1 = 2 \cdot C_d \cdot C_v \cdot A_0 \cdot (P_1 - P_2) \cos \theta \quad (5)$$

$$F_1 = 2 \cdot C_d \cdot C_v \cdot w \cdot (\Delta P) \sqrt{x_v^2 + C_r^2} \cos \theta \quad (6)$$

In the transitory regime:

$$F_3 = M \cdot a = \rho \cdot L \cdot A_v \frac{d\left(\frac{Q_1}{A_v}\right)}{dt} = \rho \cdot L \frac{dQ_1}{dt} \quad (7)$$

$$F_3 = L \cdot C_d \cdot w \sqrt{2 \cdot \rho \cdot (P_1 - P_2)} \frac{dx_v}{dt} + \frac{L \cdot C_d \cdot w \cdot x_v}{\sqrt{\left(\frac{2}{\rho}\right) (P_1 - P_2)}} \frac{d(P_1 - P_2)}{dt} \quad (8)$$

In the dynamic regime force due to flow depends on the displacement speed of the slide valve and variation of pressure drop. Usually the influence of pressure drop is neglected, considering that it has no significant impact on system dynamics [3]. Component determined by the displacement speed of the slide valve is considered more important as it represents a factor of attenuation.

2.2. Determination of axial forces needed for displacement of the slide valve

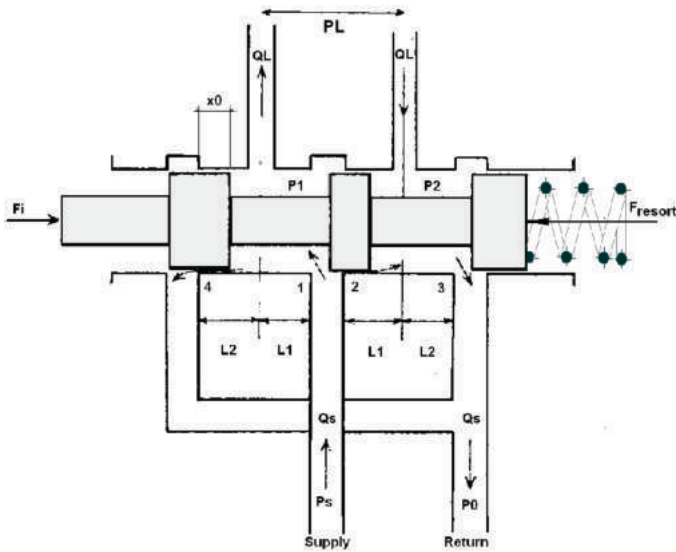


Fig.7. Three-joint four-way spool valve

Axial force needed for displacement of the slide

$$F_R = 2 \cdot C_d \cdot C_v \cdot (\cos \theta) \cdot w \cdot x_v \cdot (P_s - P_1) - L_1 \cdot \rho \frac{dQ_1}{dt} + 2 \cdot C_d \cdot C_v \cdot (\cos \theta) \cdot w \cdot x_v \cdot P_2 + L_2 \cdot \rho \frac{dQ_3}{dt} + F_{resort} \quad (9)$$

$$P_1 = \frac{P_s + P_L}{2} \quad (10)$$

$$P_2 = \frac{P_s - P_L}{2} \quad (11)$$

$$Q_1 = C_d \cdot A_1 \cdot \sqrt{\frac{2}{\rho} (P_s - P_1)} \quad (12)$$

$$Q_3 = C_d \cdot A_3 \cdot \sqrt{\frac{2}{\rho} P_2} \quad (13)$$

$$F_R = 2 \cdot C_d \cdot C_v \cdot w \cdot (\cos \theta) \cdot (P_s - P_1) \cdot x_v + (L_2 - L_1) \cdot C_d \cdot w \cdot \sqrt{\rho \cdot (P_s - P_L)} \cdot \frac{dx_v}{dt} + F_{resort} \quad (14)$$

3. Test system

Device for determining the actuation force of directional control valves with zero coverage (Fig. 10) was designed and developed in the Laboratory of General Hydraulics of INOE 2000 – IHP. In order to measure the actuation force for moving the slide valve, this device was equipped with a precise manual drive device, namely a micrometric screw.

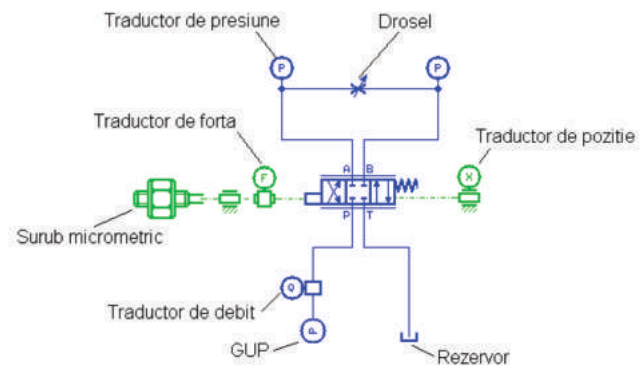


Fig.8. Basic schematic diagram of the device for measurement of axial forces

The device (Fig. 8) drives the control rod by means of a force transducer. Rod position is measured with an inductive position transducer. Return of the slide valve to initial position is made with a spring (Fig. 9) located on the side of the slide valve which is opposite to the one operated by the micrometric screw.

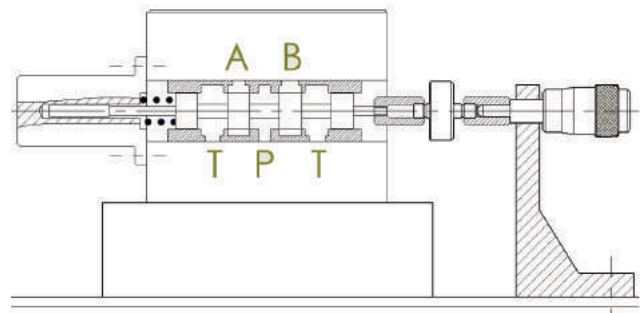


Fig.9. Actuation device used for positioning of the slide valve

Hydraulic parameters are measured by manometers placed on the joints A and B of the directional control valve. Hydraulic load can be achieved by changing the flow section of the throttle valve located between the joints A

and B of the directional control valve. The device is supplied with pressurized oil from a generator block. Oil flow is measured using the flow meter located on the joint P. All transducers are connected via an acquisition board to a PXI NI system.

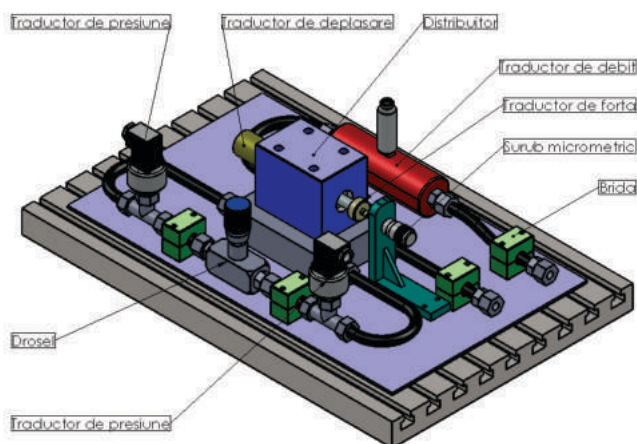


Fig.10. Device for measurement of axial forces

4. Conclusions

Complexity of natural phenomena usually doesn't allow systemic development of "perfect" mathematical models. Verification and tuning of mathematical models based on experimental data acquired from the processes of interest is mandatory in any study.

In the second part of the paper, "Determination of the actuation force of directional control valves with zero coverage (2nd Report, Experimental Results)", will be presented in full procedures for determining the axial forces, the experimental results and the procedure for adjusting parameters of mathematical model based on experimental data acquired.

References

- [1] Eng. Mircea RADULESCU, Eng. Niculae IONITA , Eng. Danut ROTARU, Ph.D.Eng. Adrian MIREA "Mechatronics systems achievement for driving, adjusting and control of pressure-flow parameters to some hydraulic and pneumatic equipment" HIDRAULICA 2/iulie 2009
- [2] Eng. Mircea RADULESCU, Eng. Ionita Niculae, Eng. Rotaru Danut, Eng. Anghel CONSTANTIN "Mechatronic system of hydraulic pressure adjustment with high flow proportional valve" HIDRAULICA 1/martie 2009
- [3] Merrit, H.E. – "Hydraulic Control Systems". John Wiley and Sons Inc., New York, London, Sydney, 196
- [4] Moog - www.moog.com
- [5] BoshRexroth www.bosch.com.ro



CHAMBER OF COMMERCE
AND INDUSTRY VALCEA



HYDRAULICS AND PNEUMATICS
RESEARCH INSTITUTE
BUCHAREST



On November 10 – 12, 2010 in CALIMANESTI – CACIULATA, VALCEA - ROMANIA
will take place

the 18th Edition of International Salon of Hydraulics, Pneumatics,
Sealing Elements, Fine Mechanics, Tools,
Specific Electronic Equipment & Mechatronics

- HERVEX 2010,

the most significant international scientific reunion
in the field of Fluid Power
in Romania, held under the patronage
of CETOP and with supported of ANCS.

This international salon is organized by:

- Hydraulics and Pneumatics Research Institute, Bucharest, Romania - IHP
- and
- Chamber of Commerce and Industry Valcea, Romania – CCIVL

in partnership with:

- POLITEHNICA University of Bucharest, Romania
- "Gheorghe Asachi" Technical University of Iasi, Romania
- PIA Institute in Aachen, Germany
- Wroclaw University of Technology, Poland.

hervex@fluidas.ro

www.hervex.ro

CONTRIBUTIONS CONCERNING RHEOLOGICAL METHODS FOR EVALUATING THE DURABILITY OF INDUSTRIAL LUBRICANTS

Irina RADULESCU*, Alexandru RADULESCU**

*S.C. I.C.T.C.M. S.A. Bucharest, ROMANIA, ** University POLITEHNICA Bucharest, RO.

ABSTRACT

The paper propose a method for diagnosing the wear degrees of lubricants based on determination of the rheological properties, more precisely the reducing of the viscosity values during the time. An exponential relation is proposed for the variation of the viscosity versus the equivalent distance covered by the motor vehicle. The two parameters characteristics are the initial viscosity for the fresh oil and the wear intensity coefficient. These values are determined using the regression analysis method.

1. INTRODUCTION

At this moment of time, an important problem of the world economy is the continuous grow of waste and residue as result of the human's activities and with a devastator ecological impact to the environment. From this point of view, it is important to develop a new method of fast diagnosis of industrial lubricants, starting from the idea that the deadline for changing the oil is imposed to be made when it is complete used and not based on the theoretical recommendations of the products.

In some case, at motor vehicles, the oil is changed more frequently that is necessary, in order to be sure that its properties were not all vanished. This type of procedure is not dangerous, from theoretical point of view, but it is expensive. The degradation of lubricant oil, collected directly from „working” conditions depends on many factors, the most important being the oxidation and impurity. The level of impurity and the period of used oil depend on the exploitation conditions, the quality of oil, the construction and the technical state of engine, [1], [2].

This paper propose a method for diagnosing the wear degrees of lubricants based on determination of the rheological properties, more precisely the reducing of the viscosity values during the time. The rheological model proposed for the industrial lubricant is the Newtonian behaviour, expressed as:

$$\tau = \eta \frac{du}{dy} \quad (1)$$

This relation shows the direct proportionality between the shear stress and the velocity gradient, and the proportional coefficient is the viscosity. The experimental stand used for measuring the rheological parameters of the lubricants is a cone and plate viscometer, which offers absolute viscosity determination with precise shear rate and shear stress information.

In order to estimate the wear degree of the used oils, a theoretical relation is proposed [3], which established the variation of the viscosity versus the equivalent distance covered by the motor vehicle:

$$\eta = \eta_0 e^{-Kd} \quad (2)$$

The two parameter characteristics for Eq. 2 are the initial viscosity η_0 for the fresh oil and the wear intensity coefficient K . These values are determined using the regression analysis method, [4].

2. EXPERIMENTAL PROCEDURES

Experimental investigations were undertaken with the aim to check the assumed theoretical method. They were carried out at the ambient temperature of 20 °C using a cone and plate Brookfield viscometer, presented in Figure 1.

In the same figure, the spindle geometry of the viscometer and its characteristic parameters are presented. They offer absolute viscosity determinations with precise shear rate

and shear stress information readily available. The sample volumes required are extremely small and temperature control is easily accomplished.



CAP SPINDLES

SPINDLE	SHEAR RATE	SAMPLE VOLUME	CONE ANGLE	CONE RADIUS
CAP-01	15.3H sec ⁻¹	67 µL	0.45	1.511cm
CAP-02	15.3H sec ⁻¹	58 µL	0.45	1.200cm
CAP-03	15.3H sec ⁻¹	24 µL	0.45	0.955cm
CAP-04	3.3H sec ⁻¹	154 µL	1.8	1.200cm
CAP-05	3.3H sec ⁻¹	67 µL	1.8	0.955cm
CAP-06	3.3H sec ⁻¹	50 µL	1.8	0.702cm
CAP-07	2.0H sec ⁻¹	1700 µL	5.0	2.599cm
CAP-08	2.0H sec ⁻¹	400 µL	5.0	1.511cm
CAP-09	2.0H sec ⁻¹	100 µL	5.0	0.955cm
CAP-10	5.0H sec ⁻¹	170 µL	1.2	1.511cm

Figure 1: Brookfield cone and plate viscometer, [5]

In order to obtain practical informations concerning the durability of the lubricants, three types of oils have been tested, coming from motor vehicles with different wear degrees:

- ELF EXCELLIUM LDX 5W-40 from a Diesel motor vehicle with 130000 km way;
- ELF PERFORMANCE EXPERTY 10W-40 from an essence motor vehicle with 38000 km way;
- ELF COMPETITION ST 10W-40

from an essence motor vehicle with 80000 km way.

For each type of oil, the mean life time recommended by the producers is 10000 km. During this period, a few samples of lubricants have been collected, corresponding at different wear degrees: for fresh oil (at 0 km) and for used oil (approx. at 3000 km, 7000 km and 10000 km).

The physical and chemical properties of the fresh tested lubricants are presented in Table 1.

Characteristical parameter	ELF EXCELLIUM LDX 5W-40	ELF PERFORMANCE EXPERTY 10W-40	ELF COMPETITION ST 10W-40
Density at 15°C	849 kg/m ³	871 kg/m ³	883 kg/m ³
Viscosity at 40°C	86.5 cSt	96 cSt	98.5 cSt
Viscosity at 100°C	14.2 cSt	14.4 cSt	14.6 cSt
Viscosity Index	170	139	170
Viscosity CCS at 30°C	6500 cP	6700 cP	6900 cP
Pour point	-41° C	-33° C	-35° C
Flash point COC	226° C	230° C	235° C
TBN	10.4 mg KOH/g	12 mg KOH/g	10.4 mg KOH/g
Volatile factions	11 %	10.5 %	12 %
Viscosity HTHS (150°C)	3.8 cP	3.9 cP	3.7 cP
Colour (ASTM)	L 3.5	L 3.0	L 3.5

Table 1: Physical and chemical properties of lubricants, [6]

3. RESULTS

The characteristic rheograms obtained with the Brookfield cone and plate viscometer, for all the tested oils, are presented in Figures 2, 3 and 4. In each figure, four curves are

presented, corresponding for different wear degrees for the tested oils. It can be observed that the viscosity decreases once with equivalent distance of the motor vehicle, and clearly depends of the oil type.

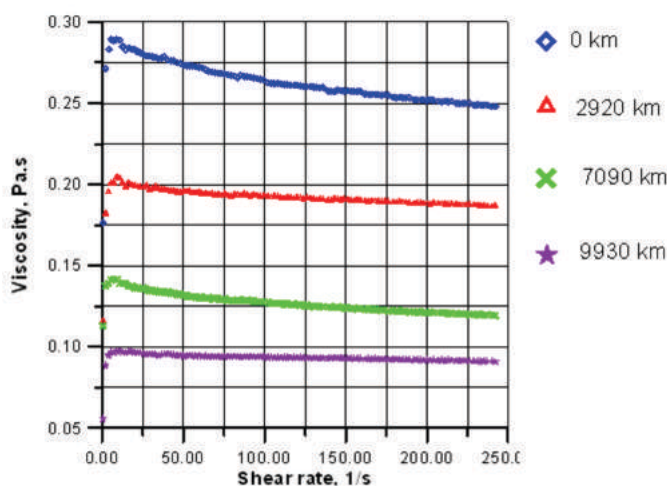


Figure 2: Experimental rheogram for ELF EXCELLIUM LDX 5W-40 oil

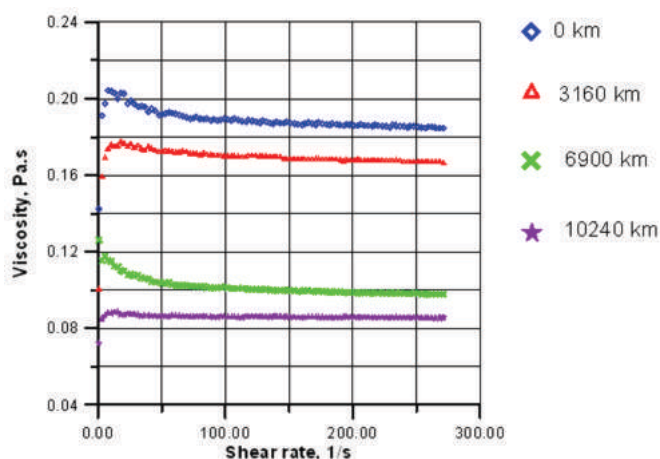


Figure 3: Experimental rheogram for ELF PERFORMANCE EXPERTY 10W-40 oil

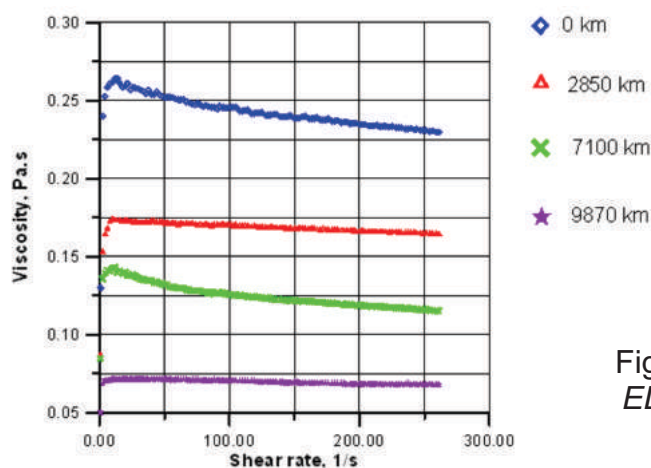


Figure 4: Experimental rheogram for ELF COMPETITION ST 10W-40 oil

The experimental data have been numerically analyzed with the regression analysis method, in order to obtain the mean values of the viscosity, for fresh and used oils (see Table 2).

The same table presents the values of the correlation coefficient, which is an indicator of the correlation level between the theoretical Newtonian model and the experimental data.

Type of oil	Wear degree	Equivalent distance, km	Viscosity, Pa.s	Correlation coefficient
ELF EXCELLIUM LDX 5W-40	Fresh oil	0	0.186	0.963
	Used oil	2920	0.167	0.982
		7090	0.086	0.991
		9930	0.099	0.994
ELF PERFORMANCE EXPERTY 10W-40	Fresh oil	0	0.253	0.957
	Used oil	3160	0.189	0.978
		6900	0.122	0.989
		10240	0.092	0.995
ELF COMPETITION ST 10W-40	Fresh oil	0	0.229	0.968
	Used oil	2850	0.164	0.975
		7100	0.118	0.988
		9870	0.068	0.990

Table 2: Regression parameters for tested oils

In order to obtain the main values of the initial viscosity η_0 for the fresh oil and the wear intensity coefficient K (see Eq. 2), the data from Table 2 are numerically treated and the results are presented in Table 3.

The wear characteristics of the tested oils, which include the experimental data and the theoretical fitted curves, are plotted in Figure 5.

Type of oil	Initial viscosity, Pa.s	Wear intensity coefficient, km^{-1}	Correlation coefficient
ELF EXCELLIUM LDX 5W-40	0.188	$7.793 \cdot 10^{-5}$	0.811
ELF PERFORMANCE EXPERTY 10W-40	0.254	$10.092 \cdot 10^{-5}$	0.996
ELF COMPETITION ST 10W-40	0.234	$11.582 \cdot 10^{-5}$	0.964

Table 3: Main values of the initial viscosity and wear intensity coefficient

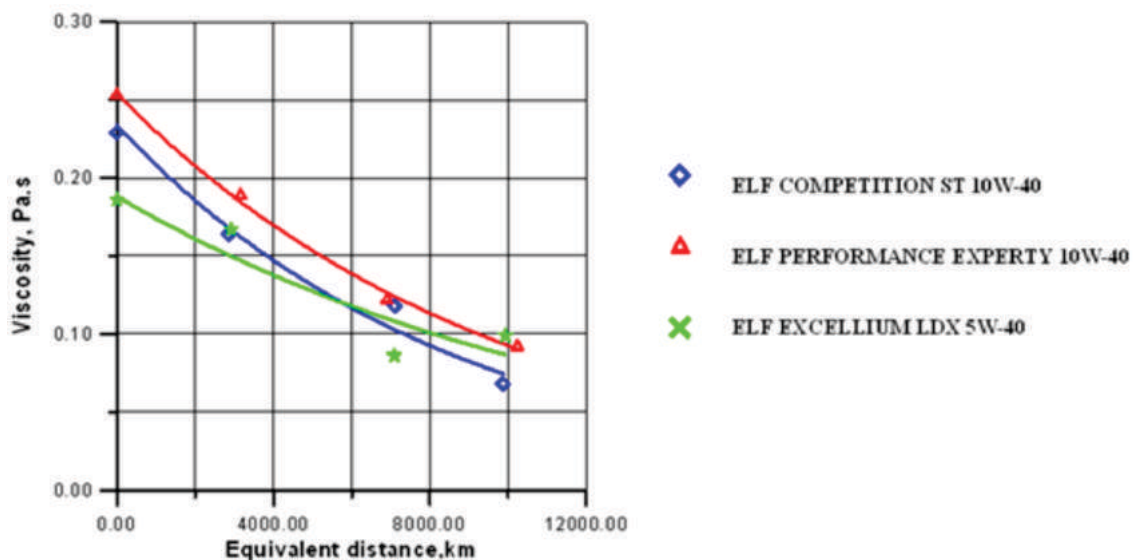


Figure 5: Wear curves for the tested lubricants

4. CONCLUSIONS

As a scientific theoretic research in technical science domain, these ideas are very important, by the thematic approach and by the novelty degree brought. Also, the possibility of changing the oil when it is really used, and not after the theoretical recommendation of the producer, gives a good economical and ecological impact, considering the practical character of the method.

On the international plan, two main directions and orientations are guided in the preventive mentenability domain and they can be applied in any closed system of lubrication:

- the management of wear products (residue) to determine the quantitative volume of wear particles;
- the management of the stage of lubricants based on physical, chemical and rheological test.

Analyzing the experimental results obtained with this rheological method, it can be observed an important tendency of viscosity decreasing during the working time. Using the determination of the two characteristic parameters, the initial viscosity η_0 for the fresh oil and the wear intensity coefficient K , a new criteria for the wear degree of the oils is obtained.

Finally, the principal result of this research is a new methodology, efficient, performed and ecological for the evaluation and quantification of the wear degree and lubricants durability. In addition, it is important that a new complex device can be performed for the diagnosis of "life reserve" for industrial lubricants.

REFERENCES

- [1] Alliston-Greiner A.F. Test methods in tribology, Proc.1 st World Tribology Congress, London, 1997, pp. 146-150
- [2] *** The real costs of lubrication, [www.maryngroup.com /Archives/ Technical/2002/CIM%20Real%20Cost%20 Paper.pdf](http://www.maryngroup.com/Archives/Technical/2002/CIM%20Real%20Cost%20Paper.pdf)
- [3] Czarny, R. "A study of thixotropy phenomen in lubricating greases", EUROTRIB' 89, Vol. IV, Helsinki, sept.1989, pp. 198-203
- [4] Crocker, D.C. "How to use regression analysis in quality control", American Society for Quality Control, Vol. IX, 1983
- [5] *** CAP 2000+ viscometer, www.brookfieldengineering.com/products/viscometers/laboratory-cap-2000.asp
- [6] *** ELF Lubricants, www.lubricants.elf.com/lub/lubroot.nsf/

S.C. ROMFLUID S.A.

Cuțitul de Argint nr. 14, sector 4,
cod 040557, BUCUREȘTI
Tel: 021 336 18 78 / 021 336 37 65
Fax: 021 336 37 05
E-mail: romfluid@romfluid.ro
www.romfluid.ro



**EXECUȚIE ȘI
MONTAJ
sisteme de
tâmplărie
cu geam
termopan**



HYDAC Romania

Ploiesti, Str. Vanatori, nr. 5 B, cod 100576
Tel: 0244575778, Fax: 0244575779
www.hydac.ro



HYDAC



ORIGINAL CONSTRUCTION AND MATHEMATICAL MODEL OF A PNEUMO-HYDRAULIC POSITIONING UNIT

Prof.PhD Eng. Mihai AVRAM*, Lect.PhD Eng. Despina DUMINICĂ*,
Prof.PhD Eng. Constantin Bucșan*, Eng. Victor CONSTANTIN*
*„POLITEHNICA” University of Bucharest

Abstract

The paper presents an original solution of pneumo-hydraulic positioning unit, as well as its mathematical model. The principle of the solution consists of the control of the position by using a hydraulic circuit governed by a proportional throttle. The unit contains a pneumatic cylinder with incorporated position sensor and a hydraulic cylinder whose rods are mounted in continuation. The load speed is thus rigorously controlled. Full stop is achieved by blocking the hydraulic circuit. The system is interfaced with a personal computer via specialized input-output electronic modules.

The dynamic behavior of the unit was simulated using SIMULINK. LabVIEW was used for developing control software. Experimental researches proved that the pneumo-hydraulic unit assured the positioning of the actuated load in any point of the working stroke with an accuracy of ± 0.1 mm.

Keywords: mechatronics, positioning system, pneumatics, control software

INTRODUCTION

Pneumatic positioning systems only in the past two decades have been associated with the accuracy concept. Until then, the main reasons of choosing such a positioning system were its simplicity, robustness, high reliability and the attractive price. In order to achieve a good positioning accuracy, the main disadvantages of the working fluid must be diminished through research: low viscosity and high compressibility. Those are the main barriers that stand against building advanced precise pneumatic systems.

Today more and more applications demand precise positioning, some only in specific points, and others in any point of the working range. There are different approaches for those situations. For the first category there are several existing solutions; all depends in how many stops are needed. The stop points can be the ends of the working range or intermediary points, marked by mechanical stop mechanisms. Once the stop points number rises, the positioning becomes more and more difficult. There are several special motors that can deal with this problem, but they had a low penetration into the market.

The problem that has not been solved yet properly is accurate positioning in any point of the working range. A way of overtaking this deadlock is the use of a hydraulic control circuit. In this situation, the unit becomes a pneumo-hydraulic unit.

In this context, the authors developed at the National Research and Development Center for Mechatronics, in the frame of “POLITEHNICA” University of Bucharest, an original solution of accurate pneumo-hydraulic unit, as part of a research project [1].

DESIGN AND CONSTRUCTION OF THE PNEUMO-HYDRAULIC UNIT

The principle of the solution consists of the control of the position by using a hydraulic circuit governed by a proportional throttle; in this way the liquid flow is accurately controlled. The unit speed is controlled rigorously and full stop is achieved by blocking the hydraulic circuit.

A series of general design considerations were observed during the design of the solution, among them being the following ones:

- § modular structure of the units;
- § use of actuators with integrated positioning sensors;

- § distribution equipment placed on the motor stator;
- § integrated control electronic circuitry;
- § PC-based electronic control system;
- § appropriate placement of various sensors in order to compensate the eventual perturbation factors.

The connection diagram of the proposed solution is presented in figure 1.

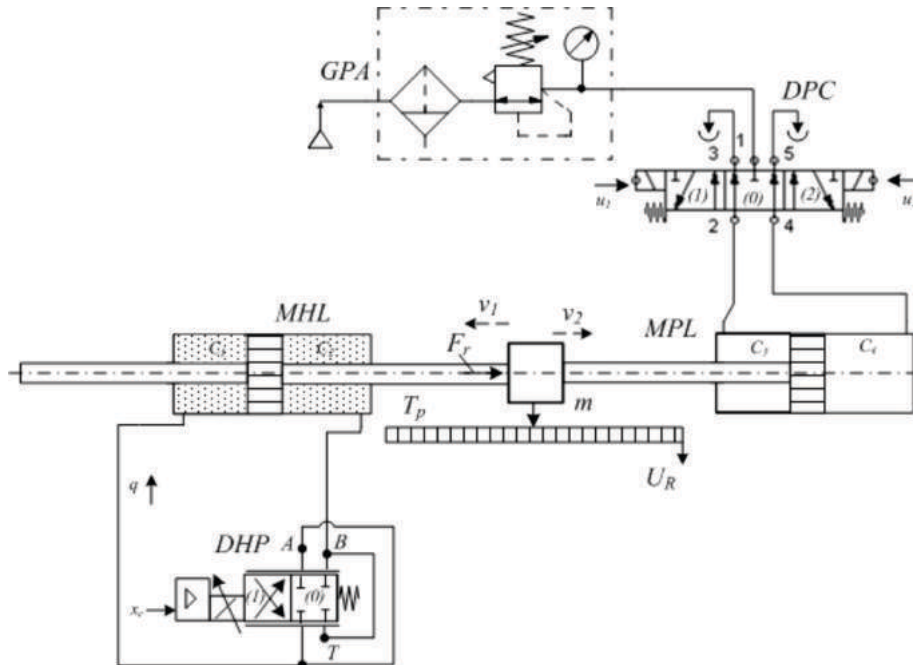


Fig. 1 The connection diagram

The following notations are used: MPL - Linear pneumatic motor; MHL - Linear hydraulic motor; DPC – Classical pneumatic direction control valve; DHP –Hydraulic proportional throttle; Tp - Position sensor; GPA- Modular air filter/regulator.

The construction of the pneumo-hydraulic unit is presented in more detail in [2].

Figure 2 presents the obtained physical model.

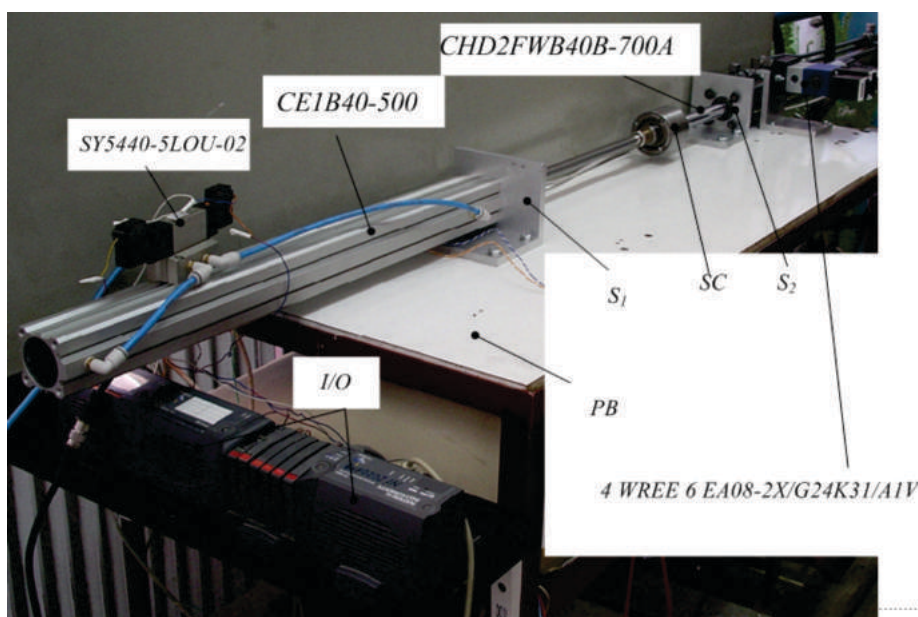


Fig.2 Physical model of the pneumo-hydraulic unit

The rods of the pneumatic cylinder with incorporated position sensor *CE1B40-500* and of the hydraulic cylinder *CHD2FWB40B-700A* are mounted in continuation and coupled via a special system *SC* that includes a spherical joint for the compensation of contingent deviations caused by non-coaxiality. The classical pneumatic direction control valve *SY5440-5LOU-02* is mounted directly on the sleeve of the pneumatic motor. The hydraulic control subassembly consists of the hydraulic motor with bilateral rod and the hydraulic proportional throttle *4 WREE 6 EA08-2X/G24K31/A1V*, mounted on the connection way between the two motor chambers. Other notations used in fig.2 are: S_1, S_2 – supports; *PB* – base plate; *I/O* - specialized input-output modules manufactured by National Instruments that allow the interfacing with the personal computer.

MATHEMATICAL MODEL

In order to study the dynamic behavior of the pneumo-hydraulic unit, the authors developed its mathematical model starting from the scheme presented in figure 1. Table 1 presents the used notations.

The movement of the mobile assembly will start if a flow section is established through the proportional throttle

The model consists of the following equations:

§ the equation that describes the movement of the load:

$$M \cdot \frac{d^2x}{dt^2} + B \cdot \frac{dx}{dt} + F_r = (P_3 - P_4) \cdot S_1 - (P_2 - P_1) \cdot S_2 \quad (1)$$

the variations of the pressures in the chambers of the hydraulic motor

$$\frac{dP_1}{dt} = \frac{E}{V_1(x)} \cdot \left(q - S_2 \cdot \frac{dx}{dt} \right) \quad (2)$$

$$\frac{dP_2}{dt} = \frac{E}{V_2(x)} \cdot \left(-q + S_2 \cdot \frac{dx}{dt} \right) \quad (3)$$

§ the variations of the pressures in the chambers of the pneumatic motor:

$$\frac{dP_3}{dt} = \frac{\chi}{V_3(x)} \cdot \left(\dot{m}_3 \cdot R \cdot T_a - S_1 \cdot P_3 \cdot \frac{dx}{dt} \right) \quad (4)$$

$$\frac{dP_4}{dt} = \frac{\chi}{V_4(x)} \cdot \left(-\dot{m}_4 \cdot R \cdot T_a - S_1 \cdot P_4 \cdot \frac{dx}{dt} \right) \quad (5)$$

Used notation	Significance
B	Damping factor
c	Maximum travel of the rods
d_n	Nominal diameter
D_s	Diameter of the throttle slide valve
E	Oil elasticity module
F_r	External force
K	Constant factor
\dot{m}_3, \dot{m}_4	Mass flow rates in the chambers of the pneumatic cylinder
M	Mass of the mobile assembly piston – rod - load
P_a	Supply pressure
P_i	Pressures in the chambers of the motor; $i=1 \dots 4$
P_0	Atmospheric pressure
q	Oil flow rate through the throttle
R	Universal gas constant
S_i	Active sections of the motor, $i=1 \dots 4$
S_c	Flow section through the throttle
T_a	Absolute temperature
V_i	Volumes of the motor chambers, $i=1 \dots 4$
x	Displacement of the two cylinder rods mounted in continuation
y	Displacement of the throttle slide valve
y_n	Nominal opening of the throttle
α_1	Shape factor
χ	Adiabatic factor
ρ	Oil density

Table 1 Notations used in the model of the pneumo-hydraulic unit

The variable volumes that appear in equations (2)...(5) have the following expressions:

$$V_1(x) = V_{10} + x \cdot S_2 \quad (6)$$

$$V_2(x) = c \cdot S_2 + V_{20} - x \cdot S_2 \quad (7)$$

$$V_3(x) = V_{30} + x \cdot S_1 \quad (8)$$

$$V_4(x) = c \cdot S_1 + V_{40} - x \cdot S_1 \quad (9)$$

The oil flow rate between the two chambers of the hydraulic cylinder can be computed as:

$$q = \begin{cases} S_C \cdot \sqrt{\frac{2}{\rho} \cdot (P_2 - P_1)} & \text{if } P_2 > P_1 \\ 0 & \text{if } P_2 = P_1 \\ -S_C \cdot \sqrt{\frac{2}{\rho} \cdot (P_1 - P_2)} & \text{if } P_2 < P_1 \end{cases} \quad (10)$$

The flow section through the throttle is equal to:

$$S_C = 2 \cdot \alpha_1 \cdot \pi \cdot D_S \cdot y \quad (12)$$

The variation of the position of the throttle slide valve can be deduced from the characteristic diagram offered by the manufacturer [4], presented in figure 3:

$$y = \begin{cases} \frac{0.5}{0.04} \cdot y_n \cdot t & \text{if } 0 \leq t \leq 0.04 \\ 0.5 \cdot y_n & \text{if } t > 0.04 \end{cases} \quad (13)$$

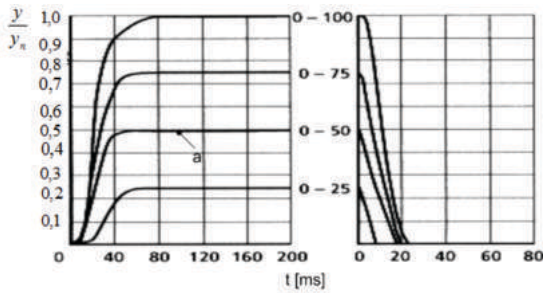


Fig. 3 Characteristic diagram of the throttle (available on the manufacturer's site)

The nominal opening y_n that appears in (13) can be deduced from the continuity of the flow section:

$$\frac{\pi \cdot d_n^2}{4} = \pi \cdot D_S \cdot y_n \quad (14)$$

The model can be simplified if it is supposed that there is a delay between the actuation of the direction control valve DPC and of the proportional hydraulic throttle DHP (fig. 1). Therefore the initial conditions of the model become, as shown in figure 4:

$$\begin{cases} P_3 = P_a \\ P_4 = P_1 = P_0 \\ P_2 = P_1 + \frac{(P_3 - P_4) \cdot S_1 - F_f}{S_2} \end{cases}$$

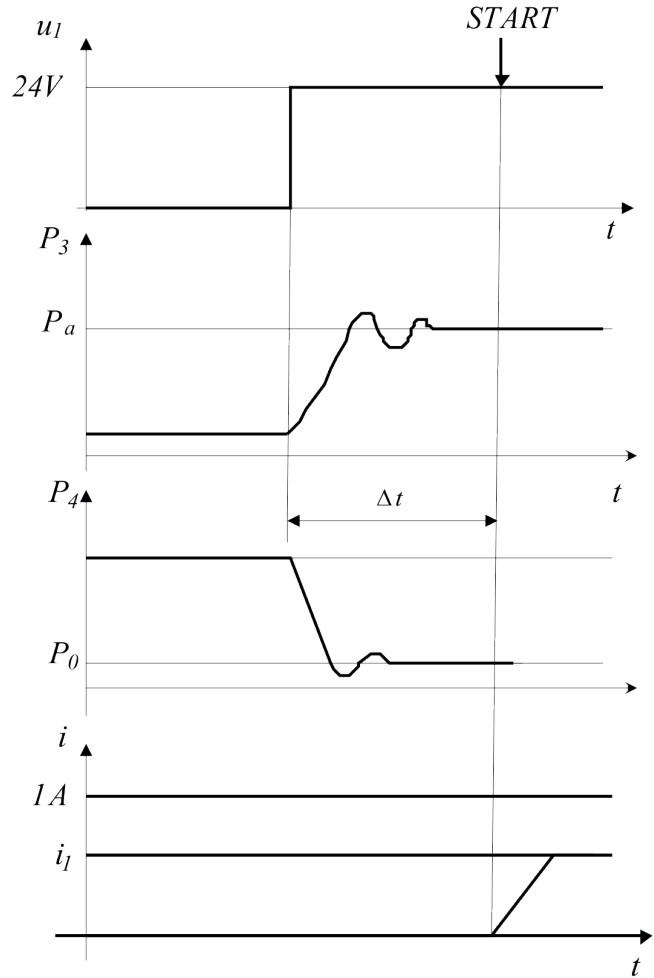


Fig. 4 Initial conditions

Consequently, the flow sections through the pneumatic direction control valve DPC can be computed as:

$$A_1 = A_2 = A_n = \alpha_2 \cdot \frac{\pi \cdot D_n^2}{4} \quad (15)$$

The flow rates controlled by the DPC are equal to:

$$\dot{m}_3 = \begin{cases} \frac{K \cdot P_a}{\sqrt{T_a}} \cdot A_n \cdot N\left(\frac{P_3}{P_a}\right) & \text{if } 0 < \frac{P_3}{P_a} < 1 \\ 0 & \text{if } \frac{P_3}{P_a} = 1 \\ -\frac{K \cdot P_3}{\sqrt{T_a}} \cdot A_n \cdot N\left(\frac{P_a}{P_3}\right) & \text{if } 1 < \frac{P_3}{P_a} \end{cases} \quad (16)$$

$$\dot{m}_4 = \begin{cases} \frac{K \cdot P_4}{\sqrt{T_a}} \cdot A_n \cdot N\left(\frac{P_0}{P_4}\right) & \text{if } 0 < \frac{P_0}{P_4} < 1 \\ 0 & \text{if } \frac{P_0}{P_4} = 1 \\ -\frac{K \cdot P_0}{\sqrt{T_a}} \cdot A_n \cdot N\left(\frac{P_4}{P_0}\right) & \text{if } 1 < \frac{P_0}{P_4} \end{cases} \quad (17)$$

where:

$$N(x) = \begin{cases} 1 & \text{if } 0 \leq x \leq 0.528 \\ 3.8 \cdot \left[\frac{2}{x^{\frac{\chi+1}{\chi}}} - x^{\frac{\chi+1}{\chi}} \right] & \text{if } 0.528 < x < 1 \end{cases} \quad (18)$$

CONTROL SOFTWARE

In order to perform experimental researches of the pneumo-hydraulic unit, the authors developed a series of four original subroutines using LabVIEW 7.1, each useful either in determining certain parameters of the unit or actually positioning it. The algorithms used as starting point for the routines are presented in [3].

Starting from this mathematical model, the dynamic behavior of the unit was simulated using SIMULINK. Figure 5 presents the software simulation scheme. Some relevant diagrams obtained from the simulation are presented in figures 6 and 7.

It can be noticed from figure 6 that, after a transitory period, the acceleration decreases to zero, leading to a constant-speed translation of the two cylinder rods mounted in continuation.

Figure 7 presents the variation of the pressures installed in the two chambers of the hydraulic cylinder.

Figure 8 shows the front panel of the application. For ease of use, the panel is divided into several areas. The left area consists of a Menu Ring list that allows the user to select which subroutine is to be used. The subroutines are as follows

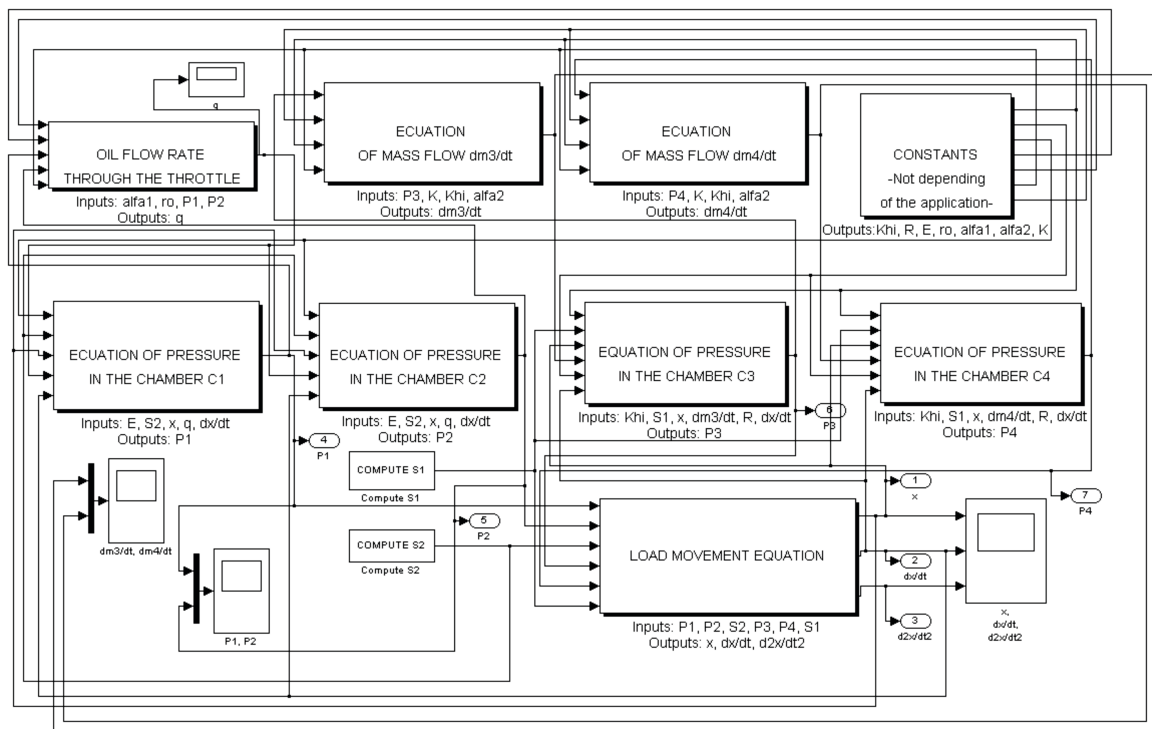


Fig. 5 Simulation scheme

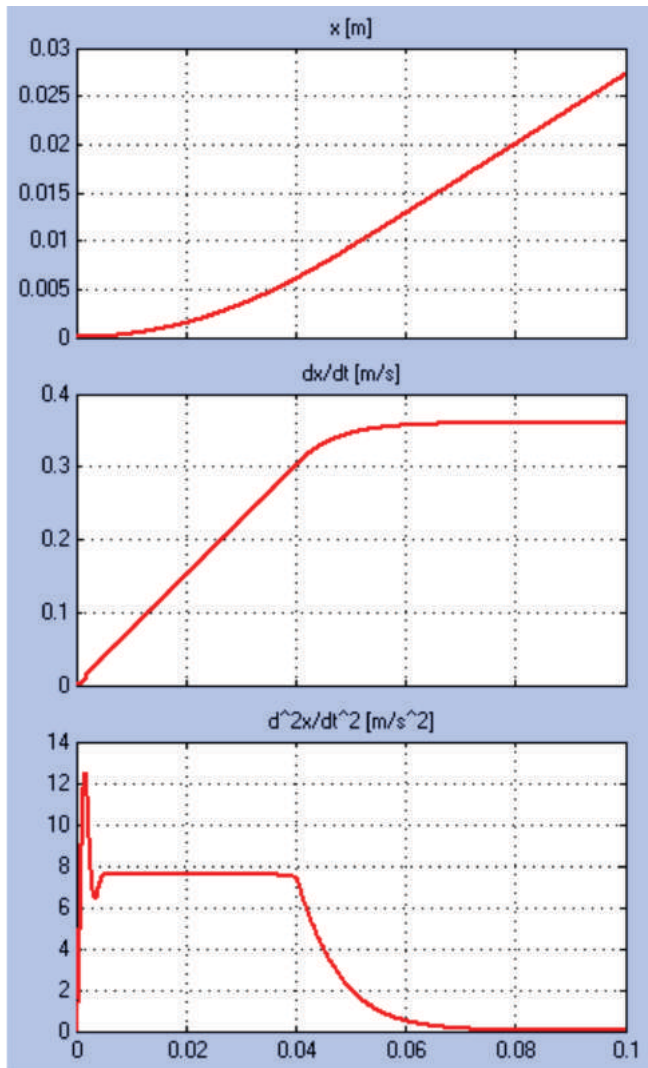


Fig. 6 Displacement, speed and acceleration of the two cylinder rods mounted in continuation

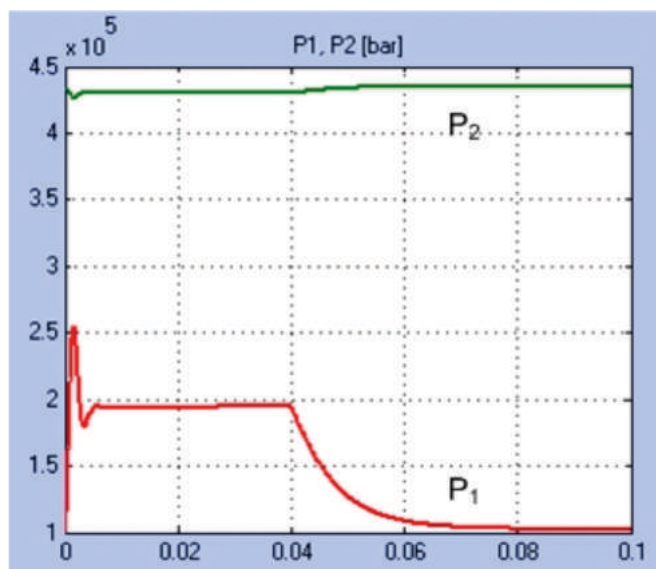


Fig. 7 Variation of the pressures in the two chambers of the hydraulic cylinder.

§ "Manual"; in this case, the central area will feature a three position toggle switch: advance – right position, backwards – left selector and stop – center position

§ "Return to 0"; the center area will display a LED indicator that turns on when the proximity sensor is activated.

§ "Optimum speed test"; for this option, the central area will reveal the controls relevant to the braking algorithm; the front panel will feature several numeric controls allowing the operator to set the input parameters for this subroutine: target position, the decrement for the command voltage per unsuccessful attempt, the reference point for a new attempt (input is a percentage of the total distance)

§ "Auto"; upon launching this routine the program will perform the actual positioning algorithm; the central area of the front panel will feature several numeric controls (input parameters for the algorithm), a numeric indicator for the current position of the unit and a LED indicator activated when an appropriate control voltage has been found inside the results.txt file. Also, the area features a indicator that reveals the current state of the search progress of the results.txt file, file that contains the results of the "Optimum speed test" subroutine.

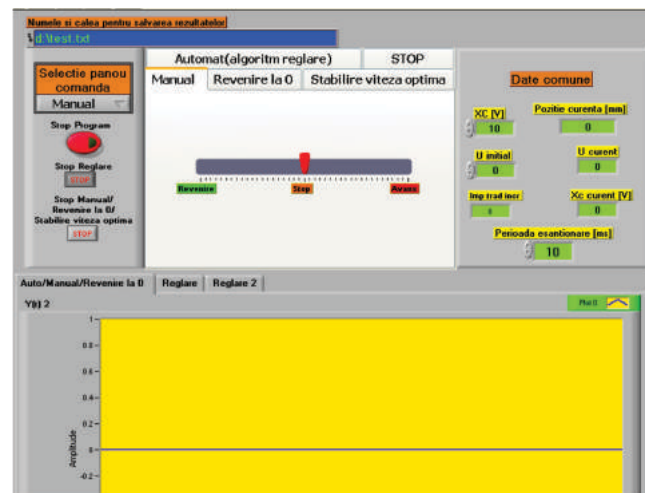


Fig. 8 Front panel of the application.

The left area also contains three on/off toggle switches:

§ "Stop program" that halts the program and all equipments involved in the process;

§ "Stop Auto"; this button is used only for stopping the "Auto" algorithm;

§ "Stop Manual/Return to 0/Optimum speed test"; the button is used for stopping any of the three algorithms, provided they are currently in use.

The right area contains three numeric controls used for setting the initial values of the maximum voltage for the hydraulic proportional control valve, the initial state of the two electromagnets that are part of the pneumatic way valve and the number of samples/second for the FieldPoint modules. Also, the area features four numeric indicators that show the current value of the control voltage for the proportional electromagnet, the current state of the electromagnets that control the pneumatic way valve, current position in mm.

Figure 9 shows a chart depicting the position of the unit during the "Optimum speed test" subroutine. Figure 10 features the movement of the load over time.

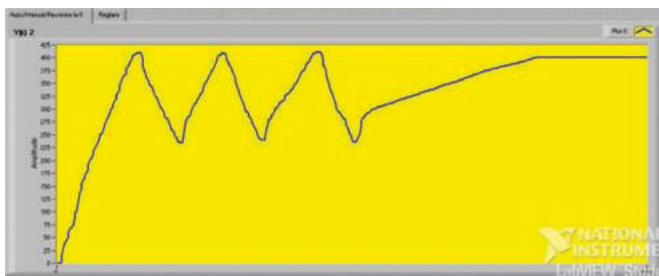


Fig. 9 Optimum speed test position chart.

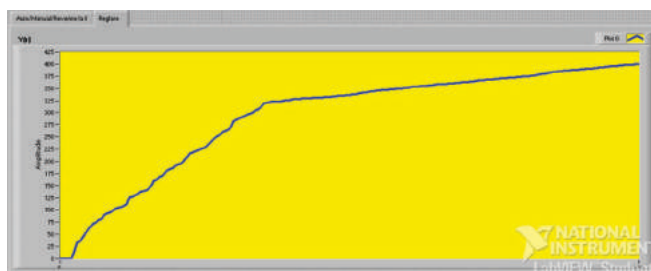


Fig. 10 Position chart for Auto subroutine.

For this test, the desired position was 400 mm and the initial position was 0 mm. The desired tolerance was $\text{mm}5.0 \pm$ and the positioning was done within $\text{mm}2.0 \pm$ of the target.

CONCLUSIONS

The experimental researches proved that the pneumo-hydraulic unit assured the positioning of the actuated load in any point of the working stroke with an accuracy of $\pm 0.1 \text{ mm}$. Further increase of the positioning accuracy can be obtained by developing appropriate control algorithms and software.

ACKNOWLEDGMENTS

This work was supported by the National Authority for Scientific Research in the frame of the National Research Program PNCDI II - PARTENERIATE.

REFERENCES

- [1] Research Project no.71-090/2007 "Modular rotary and linear pneumatic units", 2007-2009.
- [2] Avram, M., Bucşan, C., Bogatu, L., Duminićă, D., "Pneumo-hydraulic Positioning Unit - Part I: Construction and Operation", Romanian Review of Precision Mechanics, Optics and Mechatronics 2009, No.35, pag.39...41.
- [3] Avram, M., Bucşan, C., Constantin, V., "Pneumo-hydraulic Positioning Unit - Part II: Control Algorithms", Romanian Review of Precision Mechanics, Optics and Mechatronics 2009, No.36.
- [4] http://www.boschrexroth.com/country_units/america/united_states/sub_websites/brus_brh_i/en/GoTo/6_proportional_valves/4WREE/index.jsp

HYDRAULICS & PNEUMATICS RESEARCH INSTITUTE



HYDRAULICS & PNEUMATICS RESEARCH INSTITUTE is a unit specialized in research-design-production, being a subsidiary of Inoe 2000 National RESEARCH-DEVELOPMENT Institute.

The institute is structured on several research, design & execution divisions and laboratories, well equipped and employing highly qualified manpower, with more than 50 year-experience in its specific activity field.

RESEARCH LABORATORIES

Laboratory for Tribology and Lubrication Equipment
Laboratory for Electro Hydraulics Adjustment Equipment
Laboratory for Basic Hydraulics
Laboratory for Pneumatics Equipment
Laboratory for Mechatronics and Robotics Equipment
Laboratory for Sealing Systems
Laboratory for Environmental Protection
Laboratory for Fluid Mechanics
Laboratory for Electronics Equipment
Laboratory for Hydrostatic Transmissions

TESTING LABORATORIES

Testing Laboratory of hydraulic equipment for high pressure adjustment
Testing Laboratory of hydraulic equipment for medium and high pressure
Testing Laboratory of lubrication system and equipment



HYDRAULICS & PNEUMATICS RESEARCH INSTITUTE
is a founder member of the FLUIDAS Association
www.fluidas.ro



HYDRAULICS & PNEUMATICS RESEARCH INSTITUTE
is a co-organizer of the National Salon of Hydraulics and Pneumatics HERVEX
www.hervex.ro

No 14, Cutitul de Argint Street, Bucharest - ROMANIA
Phone: +4021 336 39 91; Fax: +4021 337 30 40;
e-mail: ihp@fluidas.ro ; <http://www.ihp.ro>



ASSISTED RESEARCH OF THE ELEMENTS AND THE SYSTEMS BY USING THE ELEMENTAR TRANSFER FUNCTIONS AND VIRTUAL INSTRUMENTATION

Prof.univ.Ph.D.Eng.Adrian Olaru¹ and Ph.D.Eng.Serban Olaru²

¹University Politehnica of Bucharest Romania

²RomSYS Mechatronics Company

Abstract:

In the optimisation stage of the systems one of the more important step is the optimisation of the dynamic behavior of all elements with priority the elements what have the slow frequency, like motors. The paper try to show how will be possible to optimise very easily the dynamic behavior of elements and systems, using LabVIEW propre instrumentation and the application of the transfer functions theory. By appling the virtual LabVIEW instrumentation is possible to choose on-line the optimal values for each constructive and functional parameters of the elements and the systems to obtain one good dynamic answer: maximal acceleration without vibration, minimum answer time and maximal precision. The paper presents some of the more important used transfer functions in the assisted analyse of the elements and systems and some practical results of the assisted optimisation.

1. Introduction

The transfer functions theory applied to the elements and the systems using the LabVIEW non linear components assure one very easily mode of the modeling, simulation and validation of the elements and systems, finally to obtain by sinthesys one integrated and intelligent system. Now, in the world, this theory and virtual LabVIEW instrumentation isn't applied to optimise the systems, perhaps of the difficulties to find the corespondent validated transfer functions for each component of the system, or some complex transfer functions what assures one minimum errors of validation. In the paper will be presented one virtual LabVIEW propre library for the assisted research of the electrical and hydraulic elements and systems with many results what will be possible to use in the curently research.

2. Transfer functions theory

The created virtual LabVIEW instrument library contents one specify elementar transfer function for each components of the electrical, mechanical, hydraulic or complex systems. With these elementar transfer functions will be possible to exted the library with many others more complex, like for exemple PT_6 –proportional- inertial system with six inertial order by serial link of three elementar transfer functions PT_2 , or PD_2T_2 - proportional- derivative

and inertial of the second order by serial link of two PDT_1 , and s.o. In the table 1 you can see more of these complex transfer functions using the elementar functions and in the table 2 some of the more important transfer functions used in many modeling and simulations of the elements and systems [1], [2], [3], [4], [5]. With the elementar transfer functions theory and by using the non linear functions from LabVIEW library is possible to simulate any complex servo driving systems. The propposed method contents in two ways of optimization: the first is to choose all constructive and functional parameters of the components by on-line work of the propre virtual complex LabVIEW system to obtain the desired dynamic results- perhaps one minimum acceleration time without oscilations, or one output characteristics without vibrations indifferent of the acceleration time, or one Fourier spectrum to the higher field, etc[6], [7], [8], [9]. All these situation is possible to show by on-line work of the VI; the second will be to introduce in to the initial schema of many corrections, choose the regulator and controllers parameters, or to introduce complex control laws. These will be possible very easy by using the transfer functions, because it is know the action to the dynamic behavior of each of them.

For example to attenuate the inertial action of the second order it is indicated to introduce in to the initial schema of one control law of the type PD₂- proportional derivative of the second order, what control the inertial term, the damper term

and the stiffness term of the system. By using this control law was possible to minimise the acceleration time and to obtain one answer without any vibrations, like you can see forward in the paper.

Table 1. Some expressions and virtual LabVIEW instruments of transfer functions


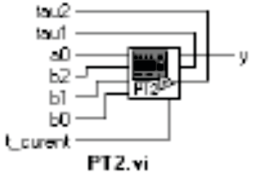
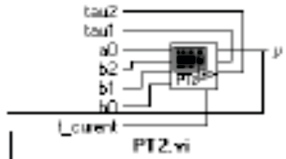
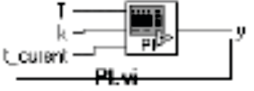
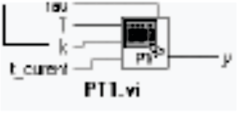

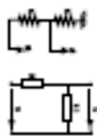
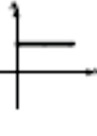


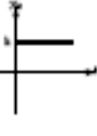

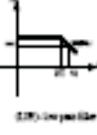


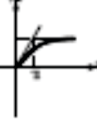


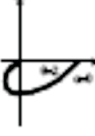

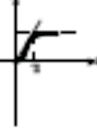

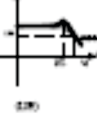
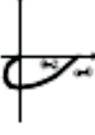

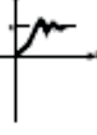

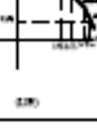
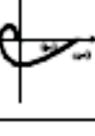

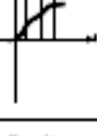
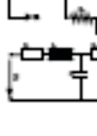

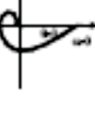

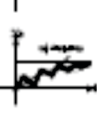
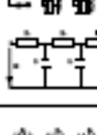
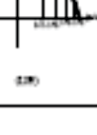
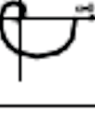
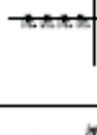
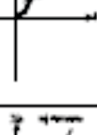
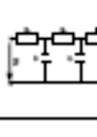


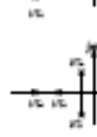

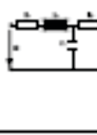
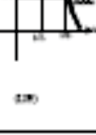







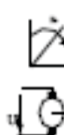
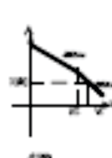

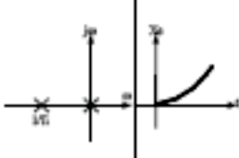

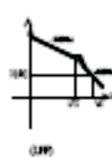

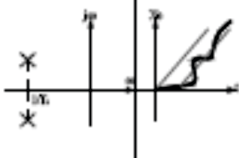

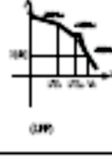

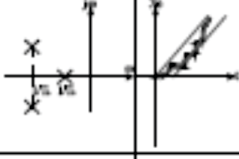
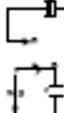
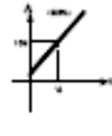


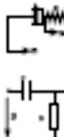
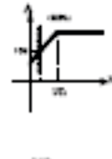

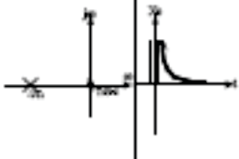
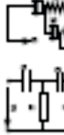
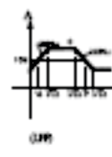

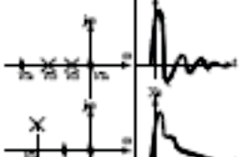



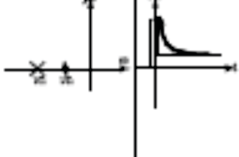
Type	Expresion of transfer function	Virtual LabVIEW instrument
PT ₁	$H(s) = \frac{k}{T_s s + 1}$	
PT ₂	$H(s) = \frac{k}{(s+a)(s+b)}$ $\xi > 1$	
	$H(s) = \frac{k}{s^2 + a^2}$ $\xi = 0$	
	$H(s) = \frac{k}{(s+a)^2}$ $\xi = 1$	
	$H(s) = \frac{k\omega_n^2}{s^2 + 2\xi\omega_n s + \omega_n^2}$ $0 < \xi < 1$	
PT ₃	$H(s) = \frac{k}{(s+a)(s+b)(s+c)}$	
PT ₄	$H(s) = \frac{k}{(s+a)(s+b)(s+c)(s+d)}$	
I	$H(s) = \frac{k}{s}$	
IT ₁	$H(s) = \frac{k}{s} \cdot \frac{1}{T_s s + 1}$	
PDT ₁	$H(s) = \frac{k(T_d s + 1)}{T_s s + 1}$	
DT ₁	$H(s) = \frac{T_d s}{T_s s + 1}$	
PID	$H(s) = k(1 + T_d s + \frac{1}{T_s s})$	
PID T ₁	$H(s) = k(1 + T_d s + \frac{1}{T_s s}) \cdot \frac{1}{T_s s + 1}$	

Table 2

Some models of transfer functions and his characteristics, mathematical and physical models

P	$H(s) = K$					
PT1	$H(s) = \frac{K}{T_1 s + 1}$					
PT2	$H(s) = \frac{K}{(T_1 s + 1)(T_2 s + 1)}$					
	$H(s) = \frac{K}{(T_1 s + 1)(T_2 s + 1)}$					
PT3	$H(s) = \frac{K}{(T_1 s + 1)(T_2 s + 1)(T_3 s + 1)}$					
	$H(s) = \frac{K}{(T_1 s + 1)(T_2 s^2 + T_3 s + 1)}$					
PT4	$H(s) = \frac{K}{(T_1 s + 1)(T_2 s + 1)(T_3 s + 1)(T_4 s + 1)}$					
	$H(s) = \frac{K}{(T_1 s + 1)(T_2 s + 1)(T_3 s^2 + T_4 s + 1)}$					
	$H(s) = \frac{K}{(T_1 s^2 + T_2 s + 1)(T_3 s^2 + T_4 s + 1)}$					

I	$H(s) = \frac{K}{s}$				
IT1	$H(s) = \frac{K}{s} \frac{1}{T_i s + 1}$				
IT2	$H(s) = \frac{K}{s} \frac{1}{T_{i2} s^2 + T_{i1} s + 1}$				
IT3	$H(s) = \frac{K}{s} \frac{1}{(T_i s + 1)(T_{i2} s^2 + T_{i1} s + 1)}$				
D	$H(s) = T_D s$				
DT1	$H(s) = \frac{T_D s}{T_i s + 1}$				
D2T2	$H(s) = \frac{T_{D2} s^2 + T_{D1} s}{T_{i2} s^2 + T_{i1} s + 1}$				
PDT	$H(s) = \frac{K(T_D s + 1)}{T_i s + 1}$ $T_D > T_i$				

PDT1	$H(s) = \frac{K(T_D s + 1)}{T_I s + 1}$ $T_D < T_I$						
PD2T2	$H(s) = \frac{s^2 + (a_1 + b_2)s + a_1 b_2}{s^2 + (a_2 + b_1)s + a_2 b_1}$ $a_1 b_2 = a_2 b_1; (a_1 + b_2) > (a_2 + b_1)$						
PD2T2	$H(s) = \frac{s^2 + (a_1 + b_2)s + a_1 b_2}{s^2 + (a_2 + b_1)s + a_2 b_1}$ $a_1 b_2 = a_2 b_1; (a_1 + b_2) < (a_2 + b_1)$						
PD2T2	$H(s) = \frac{s^2 + (a_1 + b_2)s + a_1 b_2}{s^2 + (a_2 + b_1)s + a_2 b_1}$ $a_1 b_2 = a_2 b_1; (a_1 + b_2) > (a_2 + b_1)$ $a > b$						
PD2T2	$H(s) = \frac{s^2 + (a_1 + b_2)s + a_1 b_2}{s^2 + (a_2 + b_1)s + a_2 b_1}$ $a_1 b_2 = a_2 b_1; (a_1 + b_2) > (a_2 + b_1)$ $a < b$						
PID	$H(s) = \left(1 + T_D s + \frac{1}{T_I s} \right) K$ $4T_d > T$						
PIDT1	$H(s) = K \left(1 + T_d s + \frac{1}{T_I s} \right) \frac{1}{T_i s + 1}$						
PIDT1	$H(s) = K \left(1 + T_d s + \frac{1}{T_I s} \right) \frac{1}{T_i s + 1}$						

PIDT2	$H(s) = K \left(1 + T_d s + \frac{1}{T_i s} \right) \frac{1}{T_k s^2 + T_k s + 1}$					

In the modeling of the elements and systems one more important thing is to approximate better the real function of the systems. For that will be necessary the following steps: write the mathematical model and to apply the Laplace transformation; determine the transfer elementary function of each component; simulation of the elements and compare the results with the real characteristics of the researched elements, in this case LHM (linear hydraulic motor); the validation of the model or changing them to obtain one minimum errors between the model and the real one. After these assisted research will be possible to optimise the results only by numerical simulation because the mathematical model was validated and completed with some new coefficients what results from the validation step.

3. The LHM mathematical model and the experimental validation [10], [11], [12], [13], [14]

The applied mathematical model, in this case for the LHM, was developed in one complex matrix form to take in to the research all input and output data.

The general matrix form of one mathematical model with two output and two input data is:

$$[H(s)] = \frac{\begin{bmatrix} x_{e1}(s) \\ x_{e2}(s) \end{bmatrix}}{\begin{bmatrix} x_{i1}(s) \\ x_{i2}(s) \end{bmatrix}} = \begin{bmatrix} H_{11} & H_{12} \\ H_{21} & H_{22} \end{bmatrix} \quad (1)$$

The LHM is one inertial of the second order type of the transfer function like this:

$$T_1 T_2 \frac{dx_e^2}{dt^2} + h(T_1 + T_2) \frac{dx_e}{dt} + x_e = kU \quad (2)$$

Finally, the matrix form in the state space will be:

$$\begin{pmatrix} \dot{x}_1 \\ \dot{x}_2 \end{pmatrix} = \begin{bmatrix} 0 & 1 \\ -\frac{1}{T_1 T_2} & -\frac{h(T_1 + T_2)}{T_1 T_2} \end{bmatrix} \begin{pmatrix} x_1 \\ x_2 \end{pmatrix} + \begin{pmatrix} 0 \\ \frac{k}{T_1 T_2} \end{pmatrix} U(t) \quad (3)$$

$$Y = \begin{pmatrix} 1 & 0 \end{pmatrix} \begin{pmatrix} x_1 \\ x_2 \end{pmatrix} \quad (4)$$

General for of the state space relation will be:

$$\begin{aligned} \dot{x}'(t) &= [A]x(t) + [B]u(t) \\ y(t) &= [C]x(t) + [D]u(t) \end{aligned} \quad (5)$$

After application of the Laplace transformation, the output will be:

$$Y(s) = C^T [sI - A]^{-1} x_0 + \bar{C}^T [sI - A]^{-1} B U(s) + D U(s) \quad (6)$$

where:

$$\begin{aligned} T_1 T_2 &= \frac{m \frac{A_1 c}{2E}}{A_1^2 (1 - c_{fu}) + a_m b_m}; h(T_1 + T_2) = \frac{m a_m + \frac{A_1 c}{2E} b_m}{A_1^2 (1 - c_{fu}) + a_m b_m}; \\ kU &= \frac{A_1 (1 - c_{fu}) Q}{A_1^2 (1 - c_{fu}) + a_m b_m}. \end{aligned} \quad (7)$$

and where: Q is the flow 20-100 [cm³/s]; A – active motor area 50-80 [cm²]; c - active movement 30-40 [cm] ; a_m - proportional gradient of loss flow with pressure 0.2-0.7[cm⁵/daNs]; p - loss pressure 4-6 [daN/cm²]; V – hydraulic volume of the motor 500- 1000 [cm³]; m - reduced mass on the motor axis 0.1-0.6 [daNs²/cm]; b_m - gradient of loss forces proportional with velocity 0.8-1.8 [daNs/cm]; F – resisting forces 10-30[daN].

Relation (6) is the real output and will be change in to the following form, if the all input data will be step type:

$$Y(s) = c^T [sI - A]^{-1} \frac{x_0}{s} + c^T [sI - A]^{-1} B \frac{U}{s} + D \frac{U}{s} \quad (8)$$

Finally, after changes of the product in the sum and after applied the inverse Laplace transformation the relation for the velocity of LHM will be:

$$y_1 = k(1/\psi_2) * q * (1 - (1/e^{(\omega * \psi_2 * dt)}) * (1/\psi_2) * \sin(\omega * \psi_2 * dt + \text{atan}(\psi_2/\psi_1))) - (F + a_0) * (a_m/b_0) * (1 - 1/e^{(b_0 * dt / (a_m * m))})$$

$$a_{00} = k * q * (1/\psi_2) - ((F + a_0) * (a_m/b_0))$$

$$a_0 = p * A_1$$

$$b_0 = ((A_1^2) * 0.86) + a_m * b_m$$

$$b_1 = M * a_m + (A_1 * c * b_m / (30000))$$

$$b_2 = M * A_1 * c / (30000)$$

$$b_{00} = A_1 * 0.86$$

$$k = b_{00}/b_0$$

$$\psi_1 = b_1 / (2 * \sqrt{b_2 * b_{00}})$$

$$\omega = \sqrt{b_0/b_2}$$

$$\psi_2 = \sqrt{1 - \psi_1^2}$$

The results after the simulation step and the experimental research of the LHM were obtained the characteristics from the fig.1.

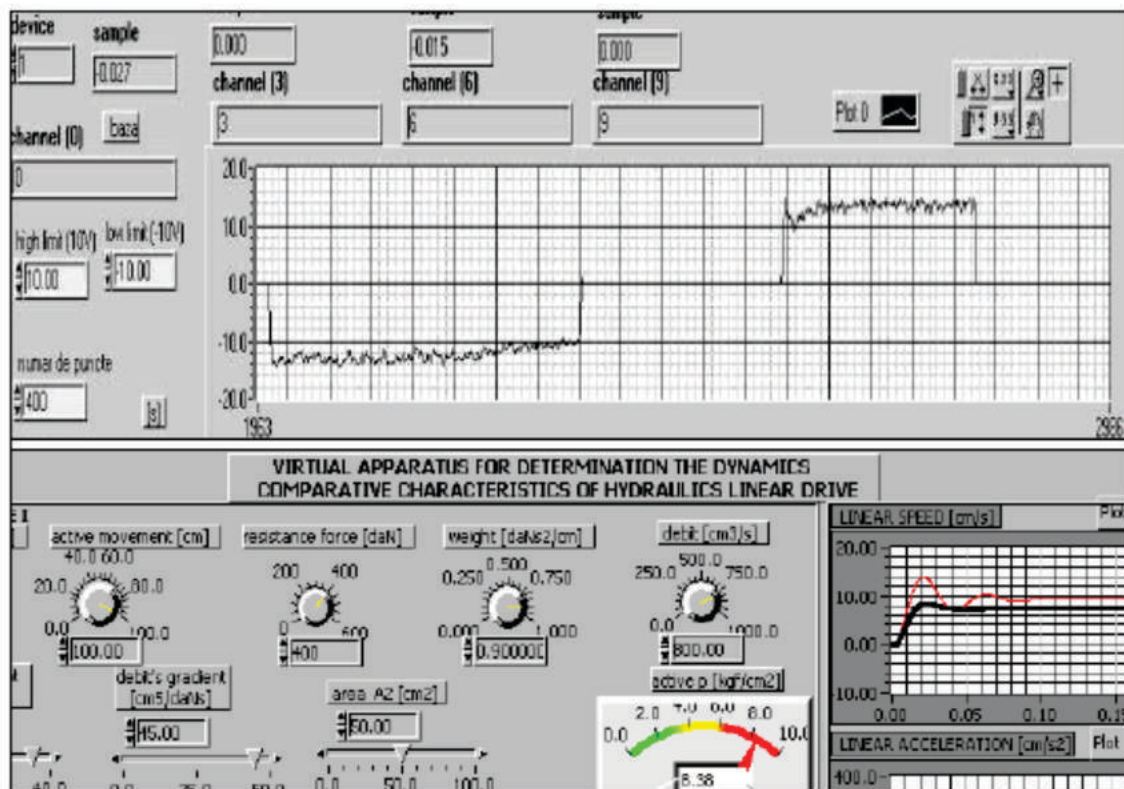


Fig.1. Validation of the LHM mathematical model- comparative analyze of the experimental and simulation results

4. Assisted optimisation of the LHM using the propre LabVIEW instrumentation

The assisted optimisation used the validated mathematical model of the LHM and by changing some constructive or functional parameters. In the figs.2-4 were changed the flow loss and the force gradients, a_m , b_m , the active area A_1 , the movement of the motor stem, c .

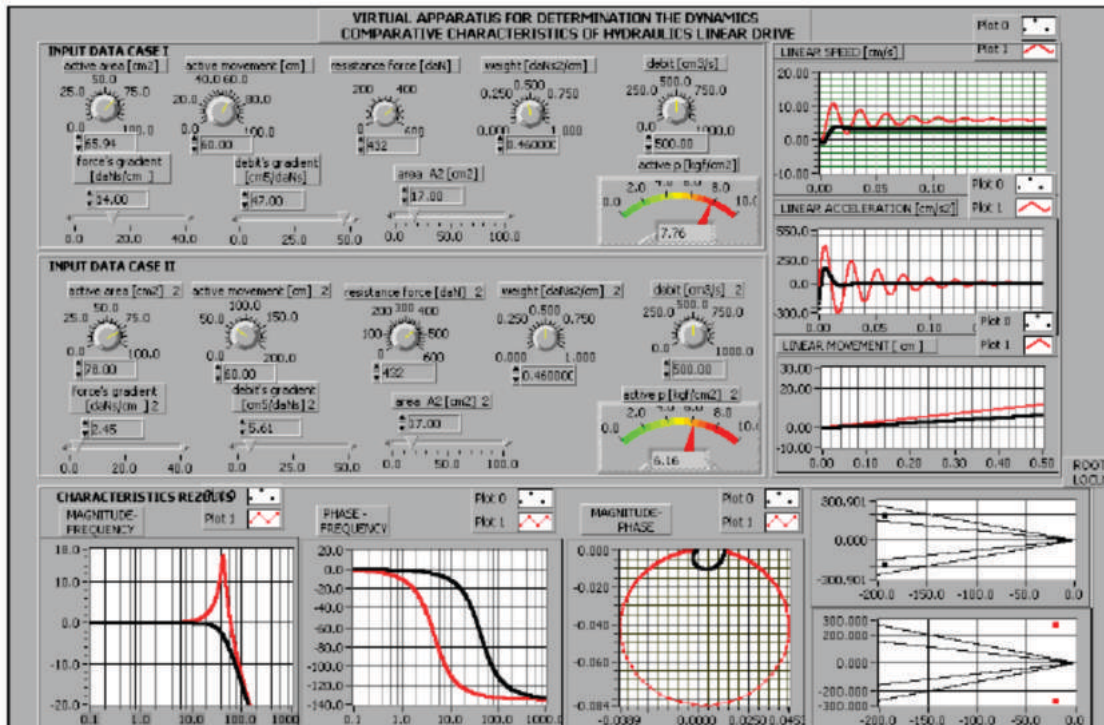


Fig.2. Front panel of the virtual LabVIEW LHM instrument for the comparative analyze, when was changed the flow and resistance force gradients, a_m , b_m

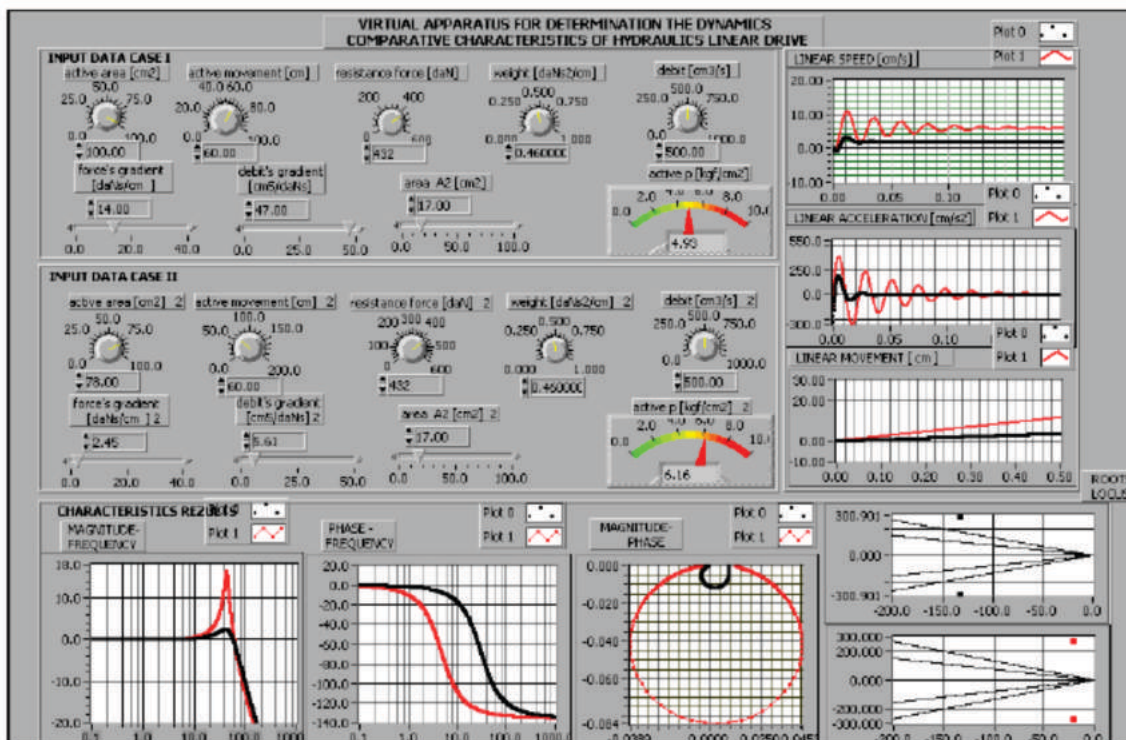


Fig.3. Front panel of the virtual LabVIEW LHM instrument for the comparative analyze, when was changed the active area, A_1

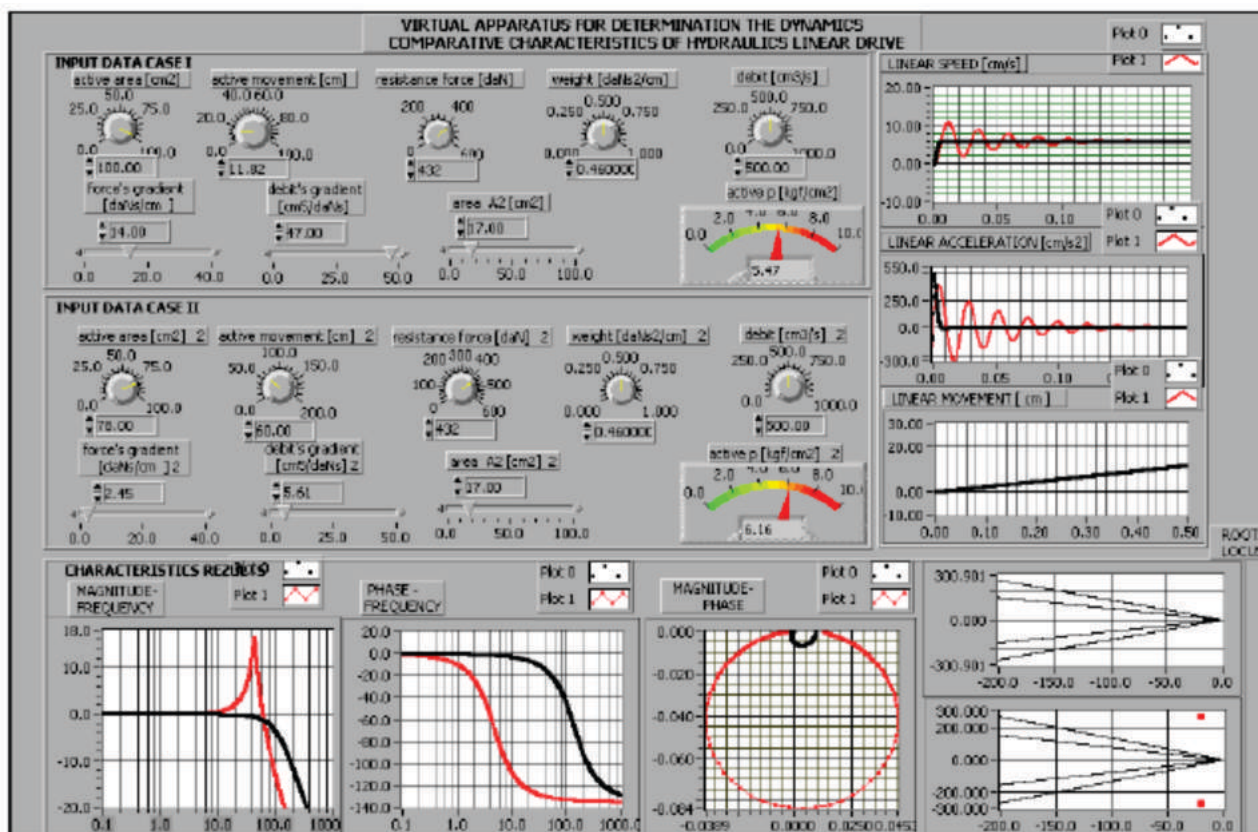


Fig.4. Front panel of the virtual LabVIEW LHM instrument for the comparative analyze, when was changed the active area and the movements of motor steam, A_v , c

Analyzing the optimization applied LHM LabVIEW proper VI results the following remarks: by increase the flow and force gradients were obtained some transfer of the poles in the plane poles- zeros to the stability field, velocity were obtained without any vibrations, fig.2; by increase the active area was obtained the displacement of the poles outside of the precision – stability field but one magnification of the answer with decrease of the acceleration time with the effect in to the increase of the movement precision, fig.3; by decrease of the active movement of the LHM steam was obtained one magnification of the velocity output with the same acceleration time with the second example, but without any vibrations of the velocity output, fig.4. By this method is possible to choose the constructive or functional values of the LHM to obtain one good dynamic behavior answer to obtain one good precision, or stability, or better solving the compromise precision- stability problem. Without on-line work of the proper LabVIEW VI-s is not possible to obtain these results.

5. Assisted optimisation of the hydraulic systems with many closed loops and different control laws

The assisted optimization of the complex hydraulic systems contents the construct of the complex virtual schema with many elementary transfer functions and some closed loops and different control laws. For that were used some proper LabVIEW subVI-s linked one to other in the magnifying factor. In the paper were simulated the system CFP- LHM (constant flow pump- linear hydraulic motor) [15], [16], [17], [18], VFP- RHM with regulator (variable flow pump- rotate hydraulic motor), CFP- PD- LHM (constant flow pump- proportional distribution-linear hydraulic motor), LHM-OHM (linear and oscillate hydraulic motor). For the control of the command signals were used some proper subVI-s by manually, automat or using the intelligent systems with some neural networks, to control the electrical command signals. All the examples of the numerical simulations of these complex hydraulic servo driving systems were presented in the figs.5-11 and the control of the electrical command signal in the figs.12-13.

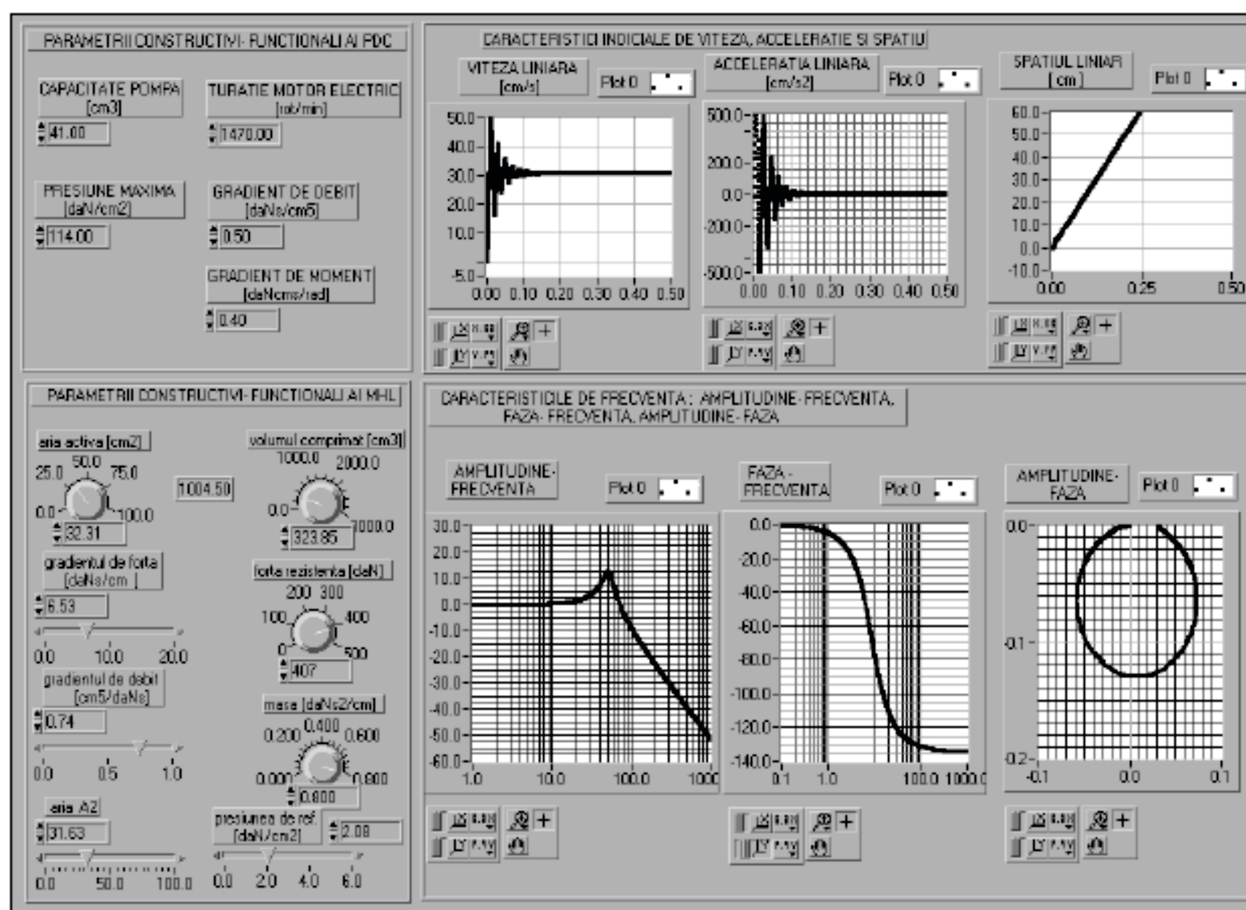


Fig.5. Indicial and frequency characteristics for the servo driving CFP-LHM after changing the inertial mass m

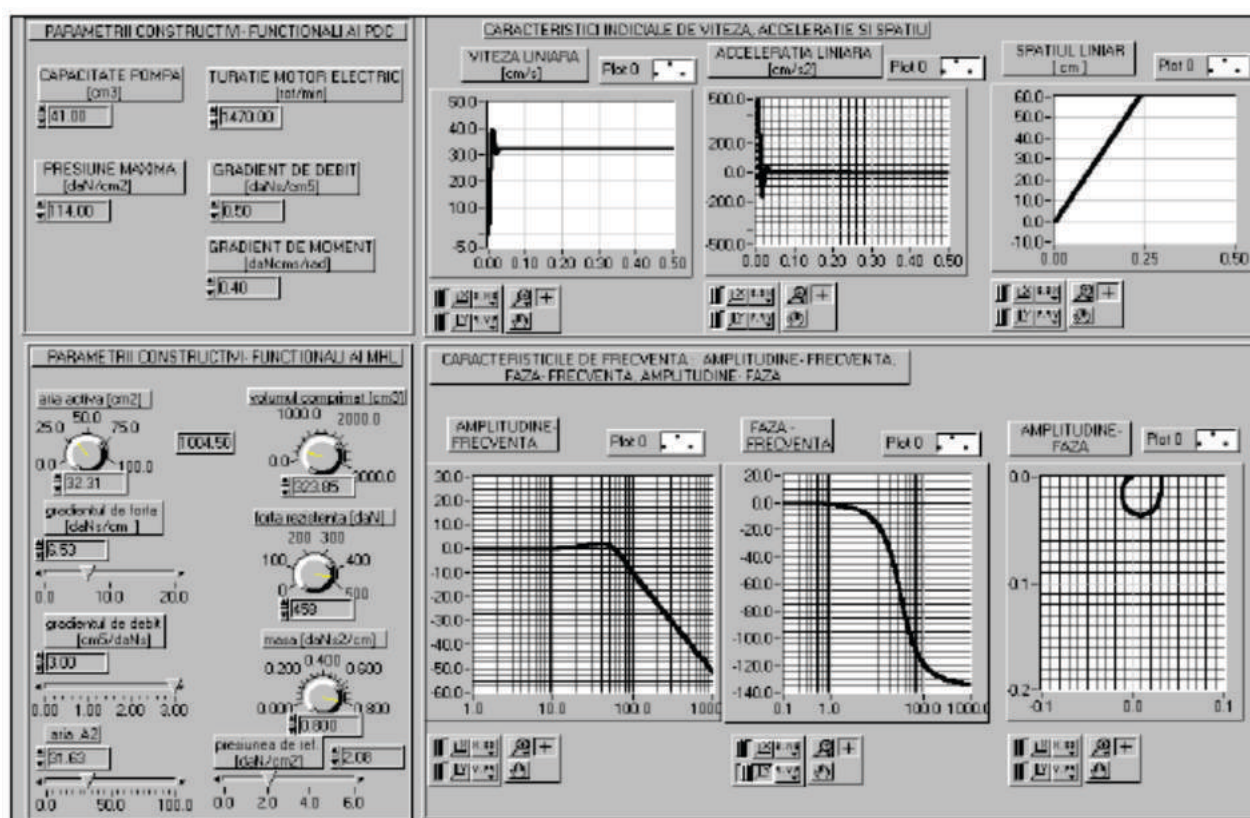


Fig.6. Indicial and frequency characteristics for the servo driving CFP-LHM after changing the flow loss gradient a_m

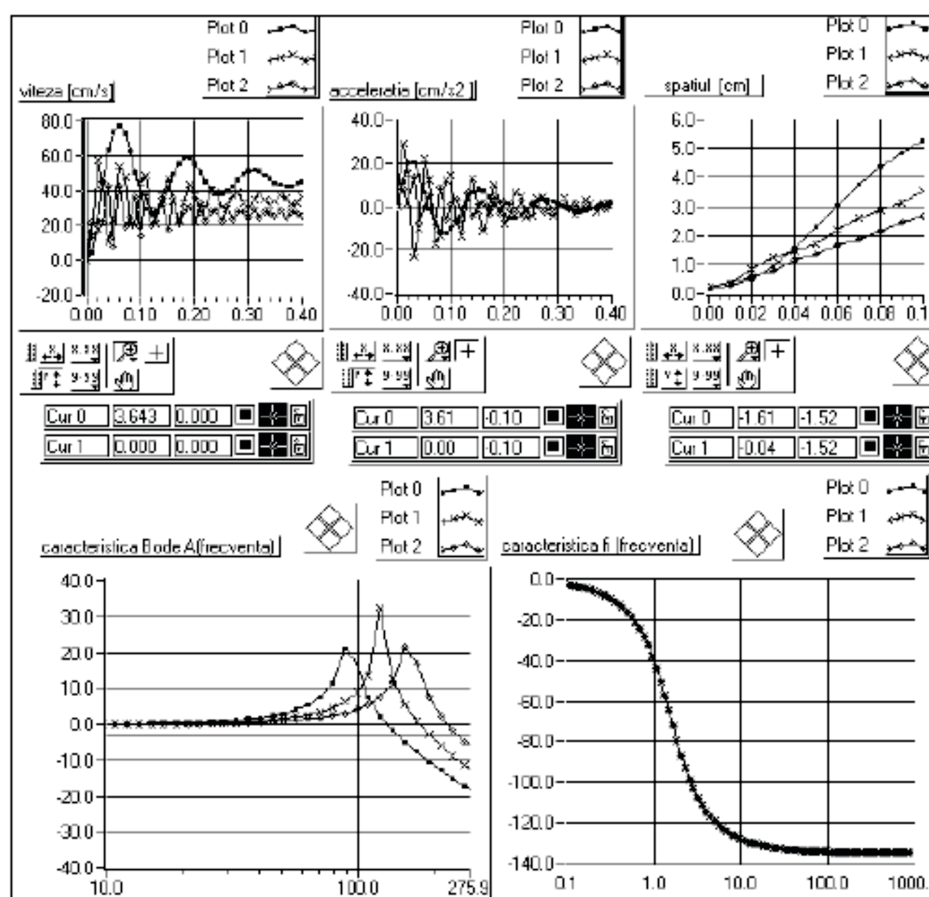


Fig.7. Indicial and frequency characteristics obtained by changing the diameters of the discrete distribution D_m

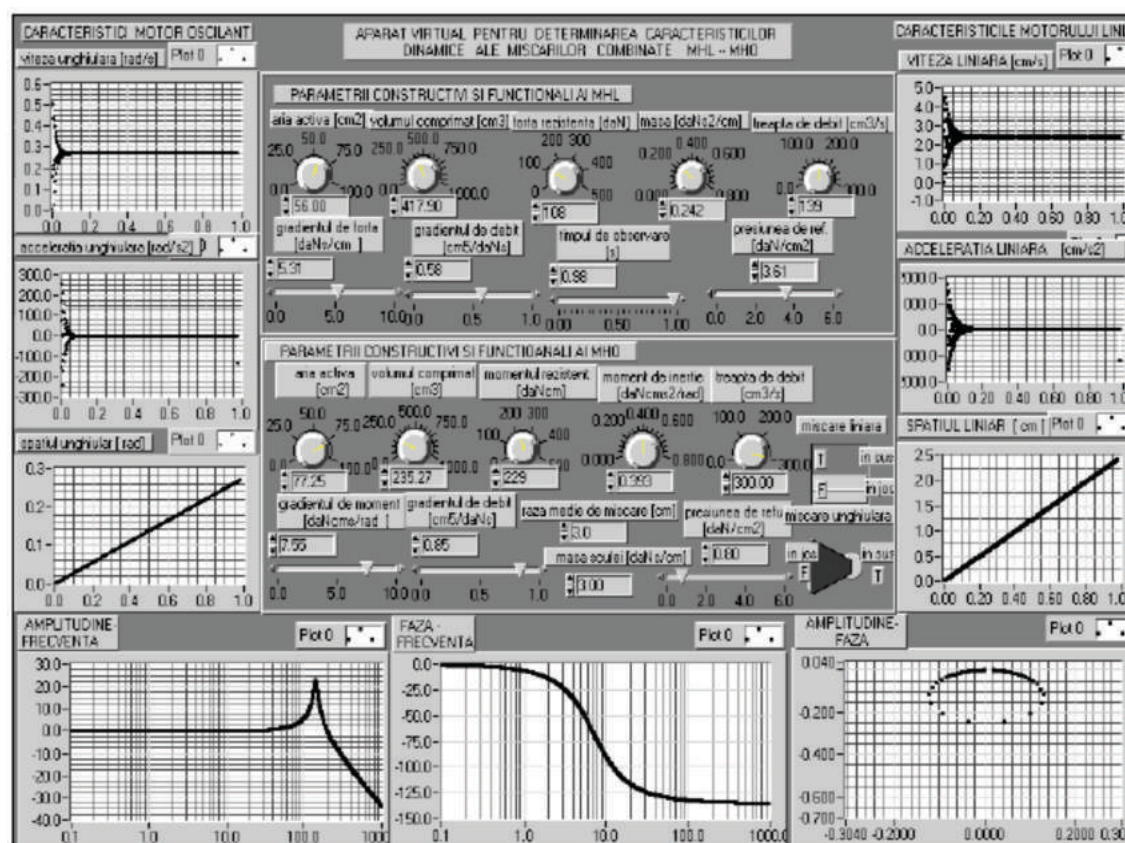


Fig.8. Indicial and frequency characteristics for the servo driving of one mechanical arm for the tools changing magasin

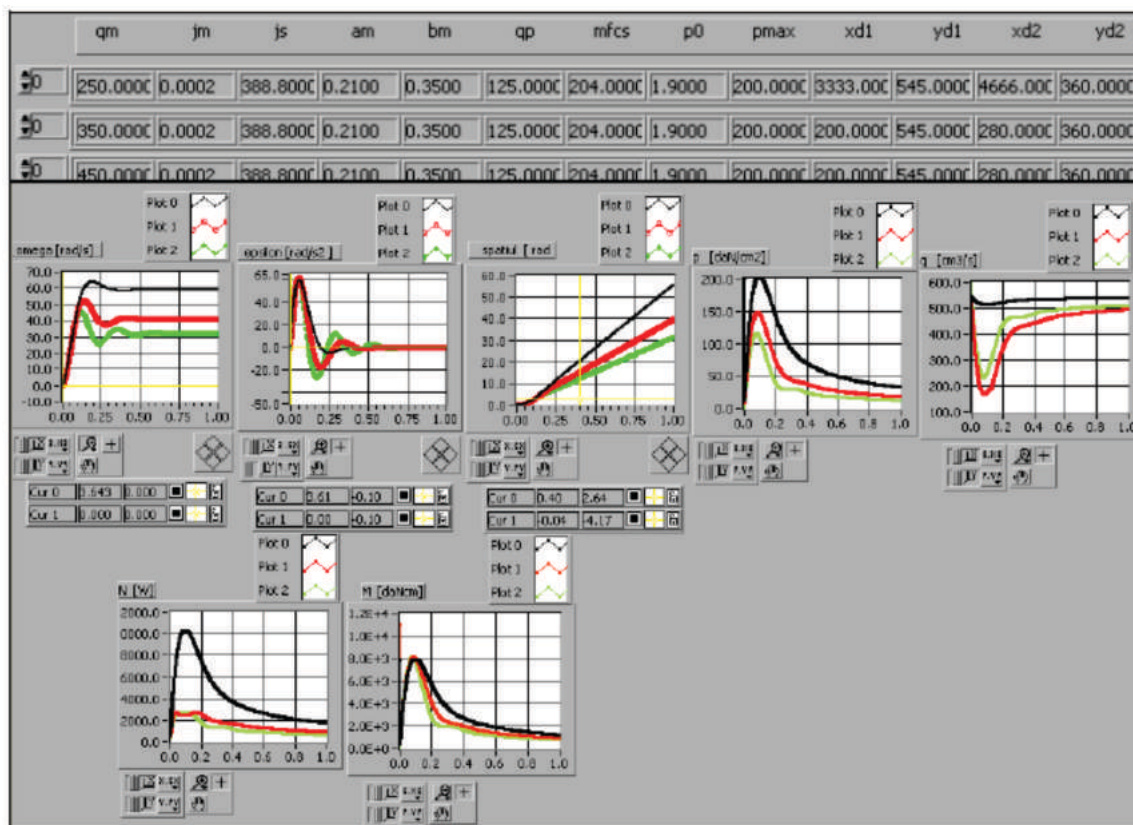


Fig.9. The input data and the characteristics of velocity, acceleration, pressure, flow, moment and power when was changed the flow

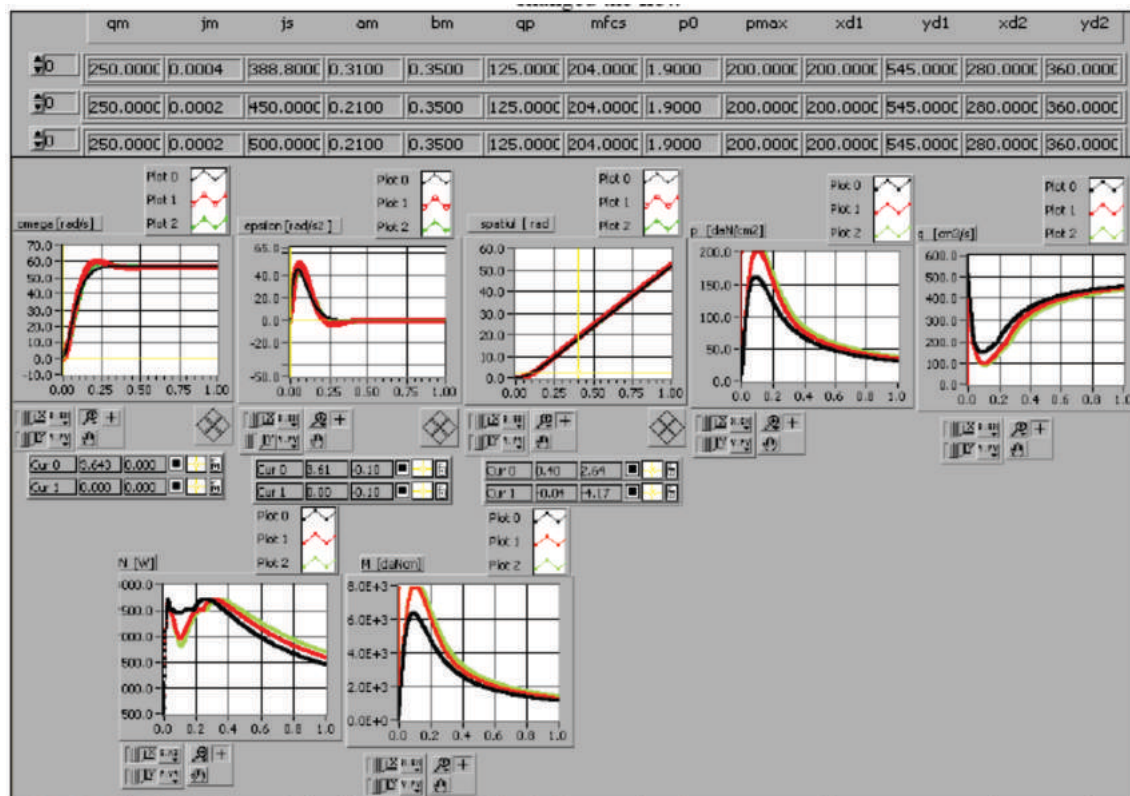


Fig.10. The input data and the characteristics of velocity, acceleration, pressure, flow, moment and power when was changed the inertial term

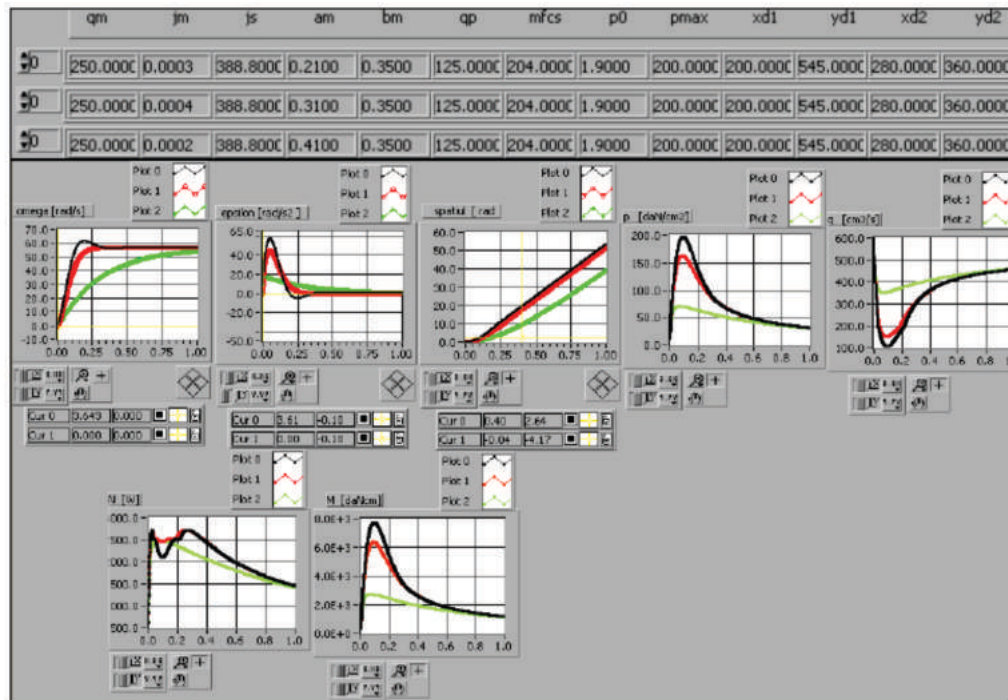


Fig.11. The input data and the characteristics of velocity, acceleration, pressure, flow, moment and power when was changed the loss flow between the motor rooms

After analyzing the results from the figs. 5-11 we can do the following remarks: by changing the inertial mass m we can control the vibrations and the output velocity, fig.5; by changing the flow loss gradient a_m we can determine the attenuation of the vibration with increase of the acceleration time and the damper force, fig.6; by changing of the discrete distribution diameter, D_m we can obtain one

increase of the frequency field, of magnitude to the resonance, and one approach to the stability limits, fig.8. By changing the flow in the servo system VFP-RHM were obtained the decrease of the power magnitude oscillations, fig.9, by increase of the inertial term, increase the power oscillations, fig.10, by increase the flow loss between the motor rooms, determine the decrease of the moment oscillations, and power, fig.11.

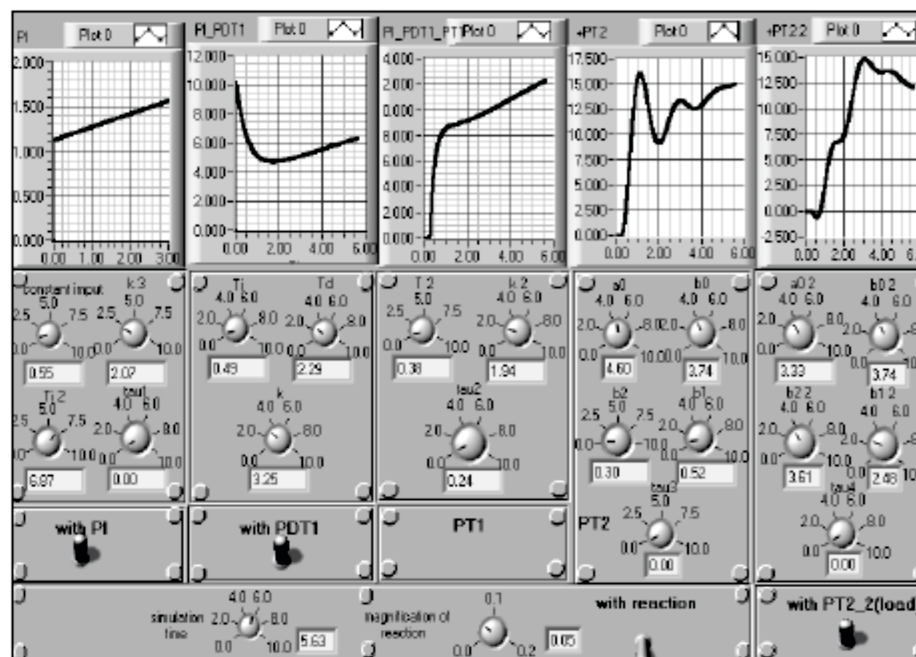


Fig.12. The indicial characteristics for the applied control law to the electrical command signals

To adjust some answer results we can use one complex control schema, fig.12, what assure on-line control of the electrical command signal of elements and systems. This signal we can optimise by on-line work of this VI and by choosing all his parameters. The signal control VI used some transfer functions: PI, PDT₁, PT₁, PT₂, PT₂ in some different variants with or

without reaction. The control of the electrical comand signal is possible to adjust using some complex intelligent systems with neural network with Linear or Perceptron neurons and complex neural network schema with three differents layers with differents number of neurons[19] [20].

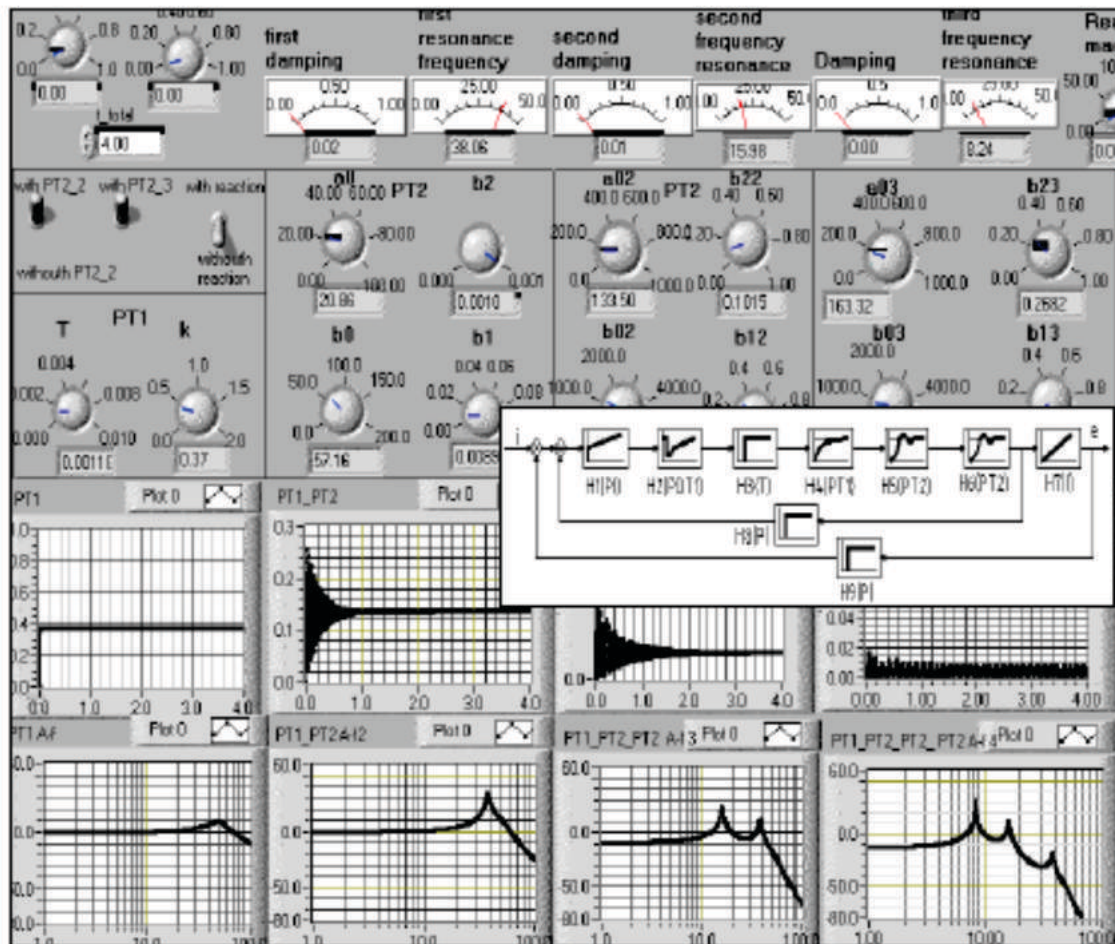


Fig.13. Front panel with the real and frequency characteristics for one complex schema with two closed loops and proportional control low

6. Conclusions

The assisted theoretical and experimental results assure for many researchers in this filed some important conclusions what will be possible to apply in the future research activity. The designed propre virtual LabVIEW instrumentation we can use in many other application and the research of many electrical, hydraulic or combined systems. The transfer function method and the used mathematical model for the LHM or for some other showed systems we can apply in many future research.

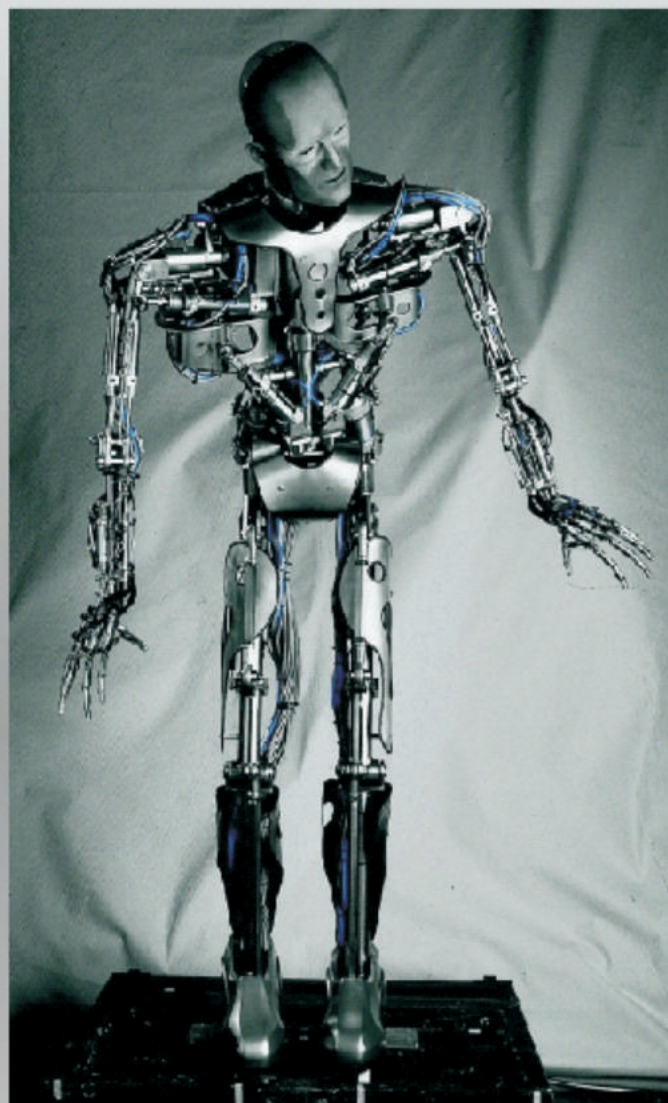
The virtual LabVIEW library what contents many hydraulic, electric elements and many servo systems we can use in the theoretical and experimental research to optimise the dynamic behavior answer, to decrease the research time activities and to obtain some good results in to the developing and implementing in the future the intelligent systems.

7. References

- [1] **Olaru, A.** *Dynamic of industrial Robots- Modeling dynamic behavior of the elements and the systems utilized in construction of the industrial robots*, Bren Edition 2001, ISBN 973-8143-65-9.
- [2] **Oprean, A., Olaru A., Ioanid, P.** *Computer aided research for dynamic behavior of forging manipulators orientation modulus*, IMEC, Manufacturing Engineering 2000 and Beyond, Freud, SUA, 1996, pag 345-352, 1996.
- [3] **Oprean, A., Olaru, A.** *Theoretical and experimental analyze of position and velocity at articulated arm industrial robot* SISOM 2001 Bucharest.
- [4] **Olaru, A.** *Theoretical and experimental cinematic research of industrial robots*, The 12th International DAAM Symposium " Intelligent Manufacturing & Automation: Focus on Precision Engineering " 24-27th October 2001, Jena, Germany
- [5] **Olaru, A., Staicu, St.** *Theoretical and experimental research dynamic behavior of industrial robots* University "Politehnica" Bucharest Publishing House 2001.
- [6] **Olaru Serban , Oprean Aurel, Olaru Adrian,** *Assisted research of the rheological dampers with LabVIEW instrumentation*, The 1st European DAAAM International Young Researchers' and Scientists' Conference, 24-27th October 2007, University of Zadar, Zadar, Croatia, 2007.
- [7] **Olaru, A., Olaru, S.** *Research Of The Industrial Robot Dynamic Behavior With Labview Instrumentation*, OPTIROB Proceedings, Romania, 2007.
- [8] **Oprean Aurel, Olaru Serban, Olaru Adrian.** *Some Contributions Of The Modeling And Simulation Of The Magnetorheological Dampers*, OPTIROB Proceedings, Romania, 2007.
- [9] **Adrian Olaru, Paune Danut, Adrian Ghionea, Serban Olaru, Peli Alexandru** *Research with LabVIEW instrumentation of the robot trajectory errors*, OPTIROB Proceedings, Romania, 2007.
- [10] **Adrian Olaru, Serban Olaru,** *Assisted optimization of the electro-hydraulic servo driving with LabVIEW instrumentation*, The 6th Iranian Aerospace Society Conference- Feb. 2007- K.N.Toosi University of Technology, Teheran, Iran, 2007.
- [11] **Olaru Adrian, Olaru Serban,** *Assisted dynamic behavior optimization of the robots elements and systems with the virtual instrumentation*, 15th Annual (International) Mechanical Engineering Conference May 2007, Amirkabir University of Technology, Tehran, Iran, 2007.
- [12] **Oprean Aurel, Olaru Serban, Olaru Adrian,** *Some contributions on the magnetorheological damper assisted research* , OPROTEH2007, Bacau, Romania, 2007.
- [13] **Serban Olaru, Adrian Olaru,** *Assisted research of the Bouc-Wen damper new mathematical model with LabVIEW instrumentation*, AERO2008, Teheran, Iran, 2008.
- [14] **Olaru, A. & Olaru, S.** *-Research of the global dynamic compliance and the viscose global dynamic damper coefficient of the industrial robot-* The 17th INTERNATIONAL DAAAM SYMPOSIUM "Intelligent Manufacturing & Automation: Focus on Mechatronics & Robotics" 08-11th November 2006, Viena, Austria.
- [15] **Olaru Adrian, Olaru Serban-** *Research of the industrial robot fourier spectrum with LabVIEW instrumentation* - First Regional Conference of Mechanical Engineering Islamic Azad University, Majlessi New Town Branch December 13th, 2006.
- [16] **Adrian Olaru** *-Assisted research of the industrial robots global dynamic compliance with LabVIEW instrumentation-* Proceedings of the 15th International Conference on Manufacturing Systems – ICMA S Published by Editura Academiei Romane, University POLITEHNICA of Bucharest, Machine and Manufacturing Systems Department Bucharest, Romania, 26- 27 October, 2006.
- [17] **Olaru, A.** *Assisted research with virtual LabVIEW instrumentation of the industrial robots vibration behavior*, Acta Mechannica Slovaca, Vishe Ruzbachy, Slovakia 2004.
- [18] **Olaru A., Olaru S., Peli Al., Paune D.** *3D complex trajectory by using the robots and perirobots components*, 9th International Conference on Automation/ Robotics in Theory and Practice, Slovakia 2008, p.431-444.
- [19] **Olaru A., Olaru S., Paune D, Ghionea A.** *Assisted research of the Neural Network*, OPTIROB Proceedings, Romania, 2010.
- [20] **Olaru A., Olaru S, Ciupitu, L.** *Research of the Neural Network by Back Propagation Algorithm*, OPTIROB Proceedings, Romania, 2010.

FESTO

www.festo.ro



- Componente, module și sisteme pneumatice: cilindri pneumatice, motoare pneumatice, elemente și sisteme de manipulare și poziționare, senzori și accesorii pentru cilindri și motoare, distribuitoare cu comandă manuală, mecanică, pneumatică, electrică, componente pentru automatizări pneumatice, elemente și accesorii pentru vacuum, elemente proporționale, elemente de filtrare, reglare și ungere aer, racorduri și tuburi
- Senzori de proximitate și fotoelectrici
- Automate programabile
- Calculatoare de proces industriale
- Sisteme de control și vizualizare pentru procese industriale și sisteme energetice
- Elemente de interfațare cu alte sisteme electronice de comandă și control



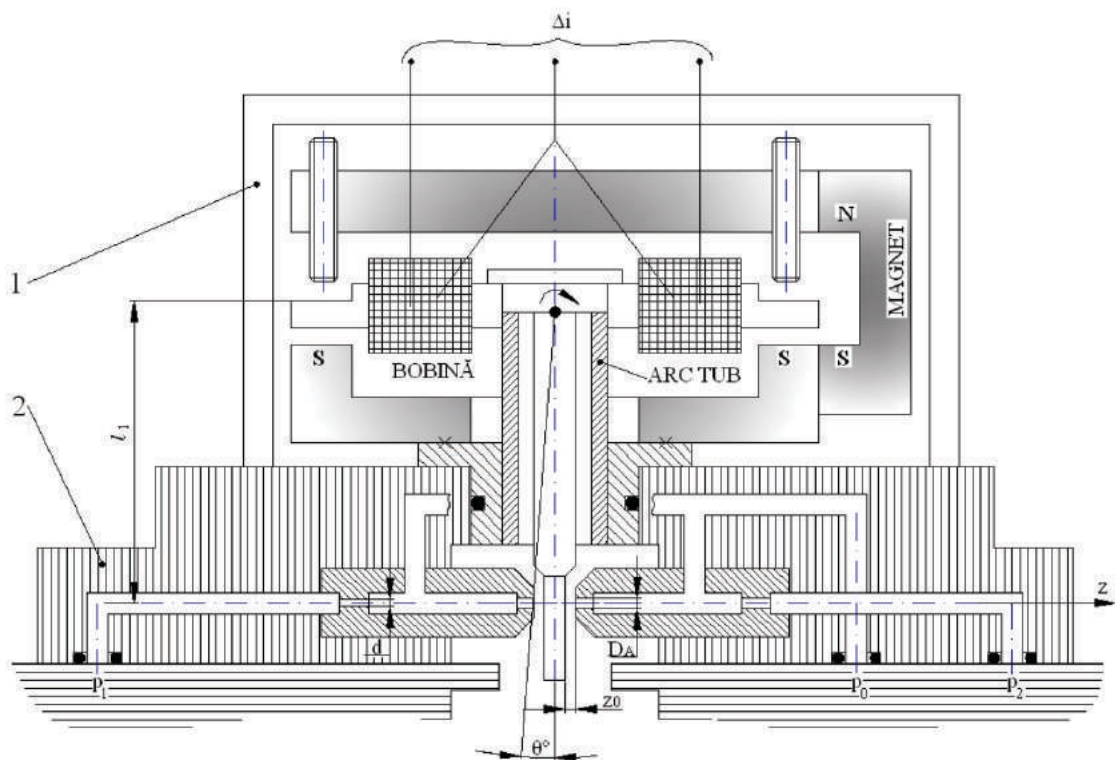
Str. Sf. Constantin, nr. 17,
Sector 1, București
Tel: 021 / 310.31.90; 021 / 314.12.85
Fax: 021 / 310.24.09
E-mail: festo@festo.ro

STATIC DIMENSIONING OF COMPONENT PARTS OF TWO-STAGE SERVO VALVES

Stud.Ph.D.Eng. Dutu I.*, Stud.Ph.D.Eng. Lupu B.*, Stud.Ph.D.Eng. Lepadatu I.*
 * Hydraulics & Pneumatics Research Institute, Bucharest - ROMANIA

1. Knowing of constructive and functional relations between component parts of servo valves' stages can be important beyond merely information as a basis for initiation of research on changes in functional adjustment dedicated to a particular application for which in initial condition is inappropriate, as well as for some routine operations relating to design and functional rehabilitation of used samples which are below the catalogue parameters. Complex structure of servo valves involves elements from the field of electro technique, low pressure fluidics, machine parts and applicative fluid mechanics.

The main structural elements are the **torque motor** electromechanical assembly design to adjust the gap nozzle-flap, driven by a proportional variation current, **pre-amplifying stage** which receives the displacement induced by the mobile fitting and by varying the distance nozzle-flap varies the control pressure; and the **amplifying stage** which actually operates on hydraulic parameters of the system where the servo valve is embedded.



2. Torque motor

Structurally, it consists of a **fixed fitting** (set of permanent magnets) and an iron **oscillating fitting** without remanence, mounted on a tube spring embedded by means of a sealing and attachment system on the preamplifier body.

According to classical theory configuration of the torque motor can be schematically shown as in Fig.2.

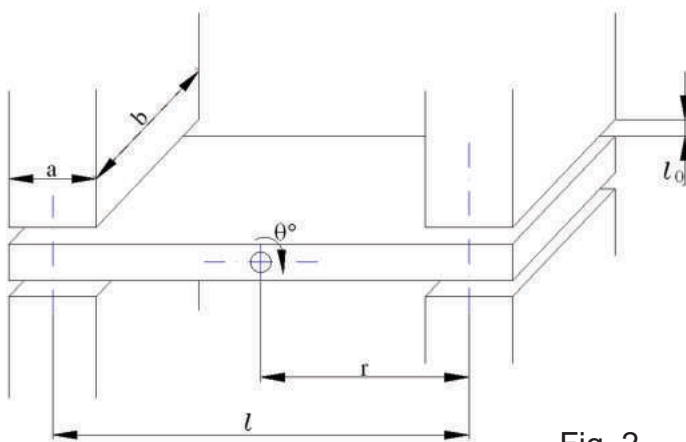


Fig. 2

Notations represent:

- a, b: sizes of magnetic pole;
- r: rotation radius;
- l: distance between poles;
- θ: rotation angle;
- θ₀: maximum rotation angle;
- l₀: between iron and permanent magnets;
- η: magnetic permeability;
- N: number of coil whirls;
- B: magnetic induction;
- i: current

a) Active torque developed by the motor depending on intensities and rotation angle has the expression:

$$M_a(i, \theta) = \frac{4ba}{\left(1 - \frac{\theta^2}{\theta_0^2}\right)^2} \cdot \left(\frac{B \cdot N}{\theta_0} i + \frac{B^2 r}{\mu \theta_0} \theta + \frac{\mu N^2}{r \theta_0^2} i^2 + \frac{BN}{\theta_0^3} i \theta \right) \quad (1)$$

If $\theta \ll \theta_0$ then $\frac{\theta^K}{\theta^{K+1}} \rightarrow 0 \quad \forall K \in N$

and terms 3 and 4 can be neglected, and by noting magnetoelastic constants

$$K_1 = \frac{4abNB}{\theta_0} \quad \text{and} \quad K_2 = \frac{4abrB^2}{\mu \theta_0} \quad (2)$$

$$\text{it results: } M_a = K_1 i + K_2 \theta \quad (3)$$

b) Geometric parameters

Relation angle-displacement is given by $Z \cong \lambda_1 \theta$ where λ_1 length of the blade

- **Elastic constant** of tube spring according to classic theory and Fig. 3 has the expression:

$$K_E = \frac{\pi E (D_T^2 - d_T^2)}{64 l_T} \quad (4)$$

where E is the longitudinal modulus of elasticity.

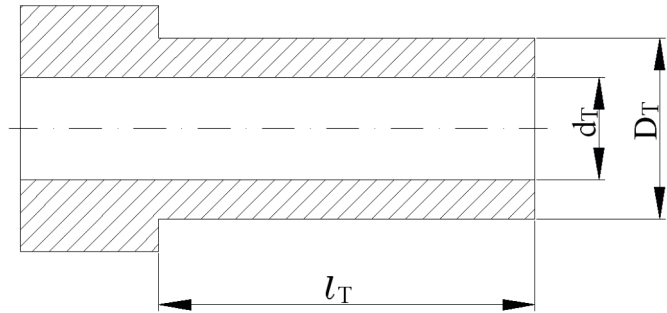


Fig. 3

3. Static dimensioning of the system nozzle-blade

a) Evaluation of parameters is performed according to Fig. 1 where are expressed:

- Area of the nozzle $A_{aj} = \frac{\pi D_A^2}{4}$

D_A diameter of the nozzle

- Connection: $Z \rightarrow \theta \quad Z = \lambda_1 \theta$

- Other necessary information:

d : diameter of control nozzles;

C_D : coefficient of flow through control nozzles ($C_D \cong 0.61$)

ρ : density of fluid

C_{DA} : coefficient of flow through nipples

In stationary regime flows Q_1 and Q_2 through nozzles and nipples are:

$$Q_1 = \pi C_{DA} \cdot D_A (Z_0 - Z) \sqrt{\frac{2p_1}{\rho}} = C_D \frac{\pi d^2}{4} \sqrt{\frac{2(p_0 - p_1)}{\rho}} \quad (5)$$

$$Q_2 = \pi C_{DA} \cdot D_A (Z_0 + Z) \sqrt{\frac{2p_2}{\rho}} = C_D \frac{\pi d^2}{4} \sqrt{\frac{2(p_0 - p_1)}{\rho}} \quad (6)$$

$$p_1 = \frac{p_0}{1 + \left(\frac{C_{DA}}{C_D} \cdot \frac{4D_A}{d^2} \right)^2 (Z_0 - Z)^2} \quad (7)$$

$$p_2 = \frac{p_0}{1 + \left(\frac{C_{DA}}{C_D} \cdot \frac{4D_A}{d^2} \right)^2 (Z_0 + Z)^2}$$

Difference between pressures gives the **control pressure**

$$\Delta p_C = p_1 - p_2 = p_0 \left[\frac{1}{1 + K(Z_0 - Z)^2} - \frac{1}{1 + K(Z_0 + Z)^2} \right] \quad (8)$$

$$K = \left(\frac{C_{DA}}{C_D} \cdot \frac{4D_A}{d^2} \right)^2 \quad (9)$$

From condition of continuity of flowing sections in order to avoid saturation of holes is necessary that:

$$\frac{C_{DA}}{C_D} \cdot \frac{4D_A}{d^2} Z_0 = 1 \quad \text{it results: } Z_0 \sqrt{K} = 1 \quad (10)$$

Equality between geometric sections of flowing nozzle-flap and nozzle

$$\pi D_A Z_0 \leq \frac{1}{2} \cdot \frac{\pi D_A^2}{4} \quad \text{it results: } Z_0 \leq \frac{D_A}{8} \quad (11)$$

- Linearized equation of **control flow** of the preamplifier

$$Q_C = K_Q^I Z - K_C^I \Delta p_C \quad \text{where:}$$

$$\begin{cases} K_Q^I = \pi C_{DA} D_A \sqrt{\frac{2p_0}{\rho}} \\ K_C^I = 2\pi C_{DA} D_A \frac{Z_0}{\sqrt{2\rho p_0}} \end{cases} \quad (12)$$

4. Evaluation of dynamic parameters

- natural pulsation

$$\omega_N = \sqrt{\frac{K_a - K_{e2}}{J}} \quad \begin{cases} K_a : \text{constant of the tube spring} \\ K_{e2} : \text{constant of the spring of amplifier} \\ J : \text{reduced inertial torque of the fitting} \end{cases} \quad (13)$$

$$\text{- frequency } f_n = \frac{\omega_N}{2\pi} \quad \left[\frac{1}{s} \right] \quad (14)$$

- damping factor

$$\xi = \frac{(T_3 - T_A)\omega_N}{2} \quad \text{where: } \begin{cases} T_3 = \frac{K_E L + K_V R}{R K_E} \quad \text{where: } \begin{cases} L : \text{inductance of the coil} \\ R : \text{resistance of the coil} \\ K_V = \eta \frac{D_f l}{Z_0} : \text{coefficient of dynamic viscosity} \end{cases} \\ T_A = \frac{L}{R} \end{cases} \quad (15)$$

Replacing at the end

$$\xi = \frac{1}{2} \cdot \frac{K_V}{K_E} \sqrt{\frac{K_a - K_{e2}}{J}} \quad [0] \quad (16)$$

- Pulsation of the system:

$$\omega_p = \omega_N \sqrt{1 - \xi^2} \quad \left[\frac{1}{s} \right] \quad (17)$$

- Overadjustment

$$-\xi \frac{\pi}{\sqrt{1 - \xi^2}} \quad \sigma = 1 \quad (18)$$

5. Evaluation of the sizes of the amplifying stage of servo valves

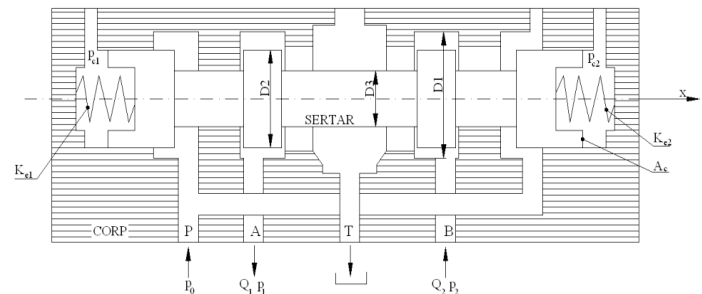
5.1. **Initial data** before structural dimensioning
 p_0 supply pressure of servo valve; Q_n supply flow; Δp_n pressure drop in servo valve; type of $(a^-; a^+)$ coverage p_i threshold of insensibility

5.2. Possible numerical values

$$p_0 \cong 3 \dots 15 \text{ MPa}; Q_n \cong 25 \dots 125 \text{ l/min};$$

$$\Delta p_n = 7 \text{ MPa}; a^-, a^+ \approx 3 \dots 6 \mu\text{m}; p_i \cong 1\%$$

5.3. Diagram of calculus is shown in Fig. 4



a) Diameter of the slide valve

$$D_2 = \frac{Q_n}{\pi C_D C_{\max}} \sqrt{\frac{\rho}{2\Delta p_n}} \quad \begin{cases} C_D = 0,61 \quad \text{flowing coefficient} \\ C_{\max} \approx 10^{-4} \text{ m} \quad \text{maximum stroke} \end{cases} \quad (19)$$

$$A_C = \frac{\pi D_2^2}{4} \quad (20)$$

a) **Deviation** from the rated size of coverages

It is considered that the deviation which brings about negative coverage $a^{(-)}$ causes a lost flow of 1% from Q_n and deviation is taken into consideration only for edges P-A and P-B.

- Expression of negative deviation is:

$$a^{(-)} = \frac{Q_p}{\pi C_D D_2 \sqrt{\frac{2\Delta p}{\rho}}} \quad \text{where:}$$

$$\begin{cases} Q_p \cong 0,01 Q_n \\ \Delta p \cong 2\Delta p_n \end{cases} \quad a^{(-)} \approx 10^{-6} m \quad (21)$$

- Positive deviation is related to the threshold of insensibility

$$a^{(+)} = p_i \cdot C_{\max} \approx 10^{-2} \cdot 10^{-4} \approx 10^{-6} (m) \quad (22)$$

c) Radial clearance

$$J_R = \sqrt[3]{\frac{12\eta Q a^{(+)}}{\pi D_2 \Delta p}} \quad (23)$$

d) Diameter of the ring slot

$$D_1 = \sqrt{\frac{4}{\pi} \cdot \frac{Q_n}{C_D} \sqrt{\frac{\rho}{2\Delta p}}} + D_2^2 \quad (24)$$

e) Diameter of the rod of slide valve

$$D_3 = \sqrt{D_2^2 - \frac{4}{\pi} \cdot \frac{Q_n}{C_D} \sqrt{\frac{\rho}{2\Delta p}}} \quad (25)$$

Methods that can be developed based on the above data may represent a basis for structural and functional development, taking into consideration the characteristics of an appliance in order to know certain information:

- Rated flow which determines rated span
- Supply voltage
- Type of coverage which determines sensibility

Group of information about mechanical parameters of the actuated machine part

- Stroke and respectively rotation angle
- Speed and respectively rotational speed
- Force and respectively torque

Group of information about electronic control:

- Adjustment technique
- Type of regulator
- Measurement technique.

References

Ju.Ciuprakov – “*Commande hydraulique et automatismes hydrauliques*”, MIR Publishing House, 1979

W. Backe – *Hydraulic systems with valves and adjustment curves*, Krausskopf Publishing House, 1974

K. Himler – *Electro hydraulic systems*

FLUIDAS



**NATIONAL PROFESSIONAL ASSOCIATION OF
HYDRAULICS AND PNEUMATICS IN ROMANIA**



www.fluidas.ro

fluidas@fluidas.ro